

PRICES SUBJECT TO CHANGE



(NASA-CR-120400) THE DEVELOPMENT OF A SOLAR POWERED RESIDENTIAL HEATING AND COOLING SYSTEM Final Report (Lockheed Missiles and Space Co.) 95 p HC \$7.75

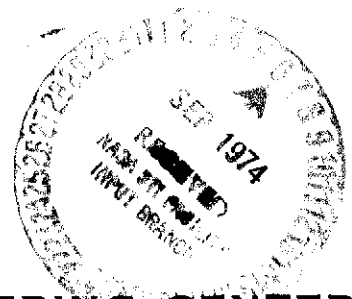
N74-31532

Unclas
47095

CSCL 10A G3/03

Reproduced by
**NATIONAL TECHNICAL
INFORMATION SERVICE**
US Department of Commerce
Springfield, VA. 22151

Lockheed



HUNTSVILLE RESEARCH & ENGINEERING CENTER

LOCKHEED MISSILES & SPACE COMPANY, INC.
A SUBSIDIARY OF LOCKHEED AIRCRAFT CORPORATION

HUNTSVILLE, ALABAMA

LOCKHEED MISSILES & SPACE COMPANY, INC.
HUNTSVILLE RESEARCH & ENGINEERING CENTER
HUNTSVILLE RESEARCH PARK
4800 BRADFORD DRIVE, HUNTSVILLE, ALABAMA

N74-31532

THE DEVELOPMENT OF A SOLAR-
POWERED RESIDENTIAL HEATING
AND COOLING SYSTEM

FINAL REPORT

Contract NAS8-25986

July 1974

PRICES SUBJECT TO CHANGE

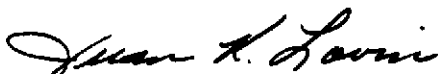
Prepared for National Aeronautics and Space Administration
Marshall Space Flight Center, Alabama 35812

by

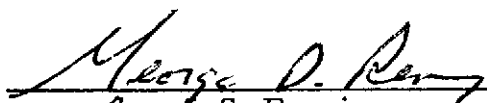
Mark J. O'Neill
Paul O. McCormick
William R. Kruse

Reproduced by
NATIONAL TECHNICAL
INFORMATION SERVICE
US Department of Commerce
Springfield, VA. 22151

APPROVED:



Juan K. Lovin, Supervisor
Thermodynamics & Structures Section



for J. S. Farrior
Resident Director

FOREWORD

This report represents the results of work performed by the Lockheed-Huntsville Research & Engineering Center for the NASA-Marshall Space Flight Center, Alabama, under Exhibit A of Contract NAS8-25986.

The NASA contract monitor for this study was Mr. R. L. Middleton of the MSFC Astronautics Laboratory.

SUMMARY

Lockheed-Huntsville's contractual efforts during the last 15 months are documented in this report. These analytical efforts are in support of a full-scale demonstration system which is currently under construction at the National Aeronautics and Space Administration, Marshall Space Flight Center, Huntsville, Alabama. The previous contract report was Ref. 1*, published in November 1972.

The basic solar heating and cooling system utilizes a flat plate solar energy collector, a large water tank for thermal energy storage, heat exchangers for space heating and water heating, and an absorption cycle air conditioner for space cooling. A complete description of the system is presented in Section 2.

Using previously developed computer tools, a wide range of solar energy collector studies have been conducted. The effects of collector design and operating conditions upon collector performance have been explored extensively, as described in Section 3.

Thermal analyses of the energy storage system have been conducted, as reported in Section 4.

Numerous parametric studies of the total system performance have been conducted using a sophisticated system simulation computer program. This program uses measured meteorological data and mathematical models of all system components to perform a transient energy transfer analysis through an entire year. Section 5 contains details and results of such simulations.

Pressure distribution studies also have been completed, as discussed in Section 6.

* Cited references are listed in Section 12. Additional sources of information not directly cited in this report are listed in Section 13, Bibliography.

A novel approach to economic comparisons between solar and conventional heating and cooling is described in Section 7. The current state of the art in solar air conditioning is reviewed in Section 8. A variety of small studies and their results are presented in Section 9.

Section 10 presents the conclusions which have been reached based upon studies to date. Among these, the most important are the following:

- Solar-powered heating and cooling systems are technically feasible and will be economically competitive with conventional systems.
- There are a tremendous number of benefits offered by the exploitation of solar energy to heat and cooling buildings, including fuel shortage alleviation, pollution reduction, natural resource preservation, environmental protection, and national energy independence.

Finally, recommended future activities to expedite the widespread utilization of solar energy for heating and cooling are delineated in Section 11.

CONTENTS

<u>Section</u>		<u>Page</u>
	FOREWORD	ii
	SUMMARY	iii
	NOMENCLATURE	x
1	INTRODUCTION	1
2	DESCRIPTION OF THE SOLAR-POWERED RESIDENTIAL HEATING AND COOLING SYSTEM	2
3	SOLAR ENERGY COLLECTOR STUDIES	8
	3.1 Collector Absorber Plate	8
	3.2 Flow Passage Geometry Definition	9
	3.3 Backside Insulation	11
	3.4 No-Flow Temperature Extremes	14
	3.5 Radiation Properties of Selective Coating	14
	3.6 Wire/Tedlar Composite	23
	3.7 Comparison of Experimental Collector Performance with Analytical Predictions	23
	3.8 Solar Flux and Incidence Angle Effects	27
	3.9 Further Tilt Angle Studies	32
4	ENERGY STORAGE SYSTEM STUDIES	34
	4.1 Tank Selection	34
	4.2 Tank Insulation Selection	34
	4.3 Thermal Analysis of Tank	38
5	PARAMETRIC TOTAL SYSTEM PERFORMANCE STUDIES	43
	5.1 Modeling Techniques	43
	5.2 Simulation Results	47

CONTENTS (Continued)

<u>Section</u>		<u>Page</u>
6	PRESSURE DISTRIBUTION STUDIES	58
	6.1 Storage Tank Pressure	58
	6.2 Supply Lines	58
	6.3 Collector Roof Manifolds	58
	6.4 Main Pump Requirement	60
7	A NEW APPROACH TO COMPARING THE ECONOMICS OF SOLAR-POWERED VERSUS CONVENTIONAL HEATING AND COOLING	62
8	A BRIEF REVIEW OF ALTERNATIVE SOLAR COOLING CONCEPTS	68
9	MISCELLANEOUS SMALL STUDIES	70
	9.1 Effect of Blower Speed on Heating Coil Performance	70
	9.2 Transient Thermal Analysis of Water Lines	70
10	CONCLUSIONS	73
11	RECOMMENDATIONS	75
12	REFERENCES	76
13	BIBLIOGRAPHY	78
Appendix	Solar Collector Model	80

LIST OF ILLUSTRATIONS

<u>Figure</u>		<u>Page</u>
1	Schematic of the Solar-Powered Heating and Cooling System	3
2	Artist's Concept of Conventional Home with Solar Heating and Cooling	5
3	Schematic of NASA-MSFC Collector	6
4	Drawing of Energy Storage Tank	7
5	Roll-Bond Panel Design	10
6	Predicted Thermal Performance of Roll-Bond Panel Design	12

LIST OF ILLUSTRATIONS (Continued)

<u>Figure</u>		<u>Page</u>
7	Heat Transfer from Collector to Collector Insulation for a Step Jump in Roll-Bond Plate Temperature	13
8	Collector Performance under "Best Possible Conditions" to Determine Maximum Temperature Extremes	15
9	Collector Performance under "Best Possible Conditions" to Determine Maximum Temperature Extremes	16
10	Solar Energy Collection Efficiency for a "Typical Clear Summer Day" (One Tedlar Cover)	17
11	Solar Energy Collection Efficiency for a "Typical Clear Winter Day" (One Tedlar Cover)	18
12	Solar Energy Collection Efficiency for a "Typical Clear Summer Day" (Two Tedlar Covers)	19
13	Solar Energy Collection Efficiency for a "Typical Clear Winter Day" (Two Tedlar Covers)	20
14	Effect of Number of Covers on Collector Efficiency for "Typical Clear Summer Day"	21
15	Effect of Number of Covers on Collector Efficiency for "Typical Clear Winter Day"	22
16	Wire Equilibrium Temperature	24
17	Analytical/Experimental Comparison for Solar Collector Tests	25
18	Analytical/Experimental Comparison for 280°F Solar Collector Test	26
19	Energy Flows for 160°F Collector Test	28
20	Energy Flows for 280°F Collector Test	29
21	Effect of Solar Flux on Collector Performance	30
22	Effect of Incidence Angle on Collector Performance	31
23	Seasonal Variation in Ideal Solar Irradiation for Various Tilt Angles (measured from horizontal)	33

LIST OF ILLUSTRATIONS (Concluded)

<u>Figure</u>		<u>Page</u>
24	Auxiliary Heat Required for Different Collector Areas and Energy Storage System Capacities ($T_{\max} = 220^{\circ}\text{F}$)	35
25	Auxiliary Heat Required for Different Collector Areas and Energy Storage System Capacities ($T_{\max} = 250^{\circ}\text{F}$)	36
26	Auxiliary Heat Required for Different Collector Areas and Energy Storage System Capacities ($T_{\max} = 280^{\circ}\text{F}$)	37
27	Energy Storage Tank	40
28	Heat Loss Through Tank Insulation	41
29	Heat Loss Through Tank Support Structure and Supply Lines	42
30	Basic Components of the Simulation Program	44
31	Effect of Cover Design on System Performance	48
32	Effect of Tilting Collector Twice a Year on Heating/Cooling Performance	49
33	Effect of Degraded Properties on System Performance	51
34	Effect of Collector Covers on System Performance for June and July Operation Only	52
35	Effect of Maximum Tank Operating Pressure on System Performance for June and July Operation Only	53
36	Effect of Tedlar Transmittance on System Performance for One-Tedlar Cover Collector	54
37	Effect of Tedlar Transmittance on System Performance for Two-Tedlar Cover Collector	55
38	Pressure Drop in Supply Lines for Various Pipe Diameters	59
39	Comparison of Solar-Powered vs Conventional Heating and Cooling with a 10% Yearly Increase in Energy Cost	65
40	Comparison of Total Cumulative Costs for the Solar-Powered and Conventional Heating and Cooling Systems	67
41	Effect of Blower Speed on Heating Coil Performance ($UA = 2000 \text{ Btu/Hr } ^{\circ}\text{F}$)	71
42	Temperature of Water in Insulated Pipe as a Function of Time	72
43	Energy Exchange Mechanisms in Flat-Plate Solar Collector	81
44	Daily Transient Solar Collector Performance	82

LIST OF TABLES

<u>Number</u>		<u>Page</u>
1	Tank Insulation	39
2	Cost Comparison for Conventional Versus Solar-Powered Heating and Cooling	63

NOMENCLATURE

<u>Symbol</u>	<u>Description</u>
A	area
$A_{\text{collector}}$	solar collector area
Btu	British thermal unit
cfm	cubic feet per minute
cos	cosine function
\cos^{-1}	inverse cosine function
C_p	constant-pressure specific heat
D	diameter
deg	degree
$^{\circ}\text{F}$	degrees Fahrenheit
ft^2	square feet
gal/min, gpm	gallons per minute
hp	horsepower
hr	hour
H_2O	water
i.d.	inner diameter
I_o	incident solar flux (measured on plane of collector)
K	thermal conductivity
L	length
lbm, lb	pound mass
m_{water}	mass of water in the thermal energy storage tank
\dot{m}	mass flow rate
mph	miles per hour
o.d.	outer diameter

NOMENCLATURE (Continued)

<u>Symbol</u>	<u>Description</u>
P	pressure
psi	pounds per square inch
psia	pounds per square inch absolute
psig	pounds per square inch gage
Q	heat
\dot{Q}	heat transfer rate
\dot{Q}/A	heat transfer rate per unit area
$Q_{aux}, Q_{auxiliary}$	auxiliary heat requirement
Q_{tot}, Q_{total}	total energy required to provide heating and cooling
$^{\circ}R$	degrees Rankine
T	temperature
t	thickness or time
ton (of air conditioning)	12,000 Btu/hr
$T_{ambient}, T_{amb}$	ambient temperature
$T_{collector}, T_{coll}, T_c$	average plate temperature of solar collector
T_{max}	maximum allowable water temperature in thermal storage tank
$T_{min\ htg}$	minimum allowable water temperature for space heating
$T_{min\ cooling}$	minimum allowable water temperature for space cooling
UA	overall heat transfer coefficient
VM	Vuilleumier cycle

NOMENCLATURE (Concluded)

<u>Symbol</u>	<u>Description</u>
<u>Greek</u>	
α_s	solar absorptance
Δ	difference
ϵ, ϵ_{ir}	infrared emittance
λ	wavelength
ϕ	tilt angle of collector
ρ	mass density
σ	ratio of auxiliary to total heat requirements (Q_{aux}/Q_{tot}) for June and July
$\frac{\partial \sigma}{\partial A}$	partial derivative of σ with respect to collector area (A)
$\frac{\partial \sigma}{\partial \alpha_s}$	partial derivative of σ with respect to solar absorptance (α_s) of collector plate
$\frac{\partial \sigma}{\partial \epsilon}$	partial derivative of σ with respect to emittance (ϵ) of collector plate
$\frac{\partial \sigma}{\partial \tau}$	partial derivative of σ with respect to solar transmittance (τ) of outermost collector cover
θ	incidence angle of solar radiation measured from collector normal
τ	solar transmittance of collector covers
τ_{eff}	effective solar transmittance
$\tau_{inner}, \tau_{in}, \tau_i$	solar transmittance of inner cover of collector
$\tau_{outer}, \tau_{out}, \tau_o$	solar transmittance of outer cover of collector

Section 1 INTRODUCTION

The current worldwide shortage of petroleum dramatically emphasizes the need for alternative energy sources. Among the possible alternative energy sources, the most pollution-free, non-depletable, boundless source of all is solar energy. One may reasonably expect that the sun will ultimately be harnessed to produce electricity, synthetic liquid and gaseous fuels, and high temperature thermal energy for industrial processes. However, the first major application of solar energy will be to heat and cool buildings since this application will require the fewest technological advances and the least expenditures of time and money. During 1972, Lockheed-Huntsville conducted a study of the technical and economic feasibility of a residential heating and cooling system to be located in Huntsville, Alabama. This study was funded by NASA-MSFC and was fully documented in Ref. 1. During 1973 and 1974, Lockheed-Huntsville has been providing design analyses in support of the NASA solar heating and cooling demonstration system, currently being fabricated at MSFC.

The objectives of the work documented in this report include the following:

- To determine a solar energy collector design which would be efficient for both energy transfer and fluid flow, based upon extensive parametric analyses
- To generate the thermal design requirements for the energy storage system, which utilizes sensible heat storage in water
- To properly size system components (including the collector and storage) and to determine a practical, efficient total system configuration, by means of computer simulation of system performance.

This report contains the results of all contractual efforts conducted from January 1973 through March 1974.

Section 2

DESCRIPTION OF THE SOLAR-POWERED RESIDENTIAL
HEATING AND COOLING SYSTEM

The solar-powered residential space heating, air conditioning and hot water heating system considered in this study is shown schematically in Fig. 1. The major components of the system are the flat-plate solar energy collector, the large hot water tank for energy storage, an auxiliary furnace to provide needed thermal energy when storage is depleted, and the output units: air heater, water heater, and absorption cycle air conditioner.

The system operation is simple. Water from the storage tank is pumped through the collector where it is heated by absorbed solar radiation. The heated water in the storage tank is used as the primary energy source for water heating, space heating, and air conditioning. For water heating, cold city water is passed through the heat exchanger shown submerged in the storage tank. In general, this will heat the city water to a temperature level sufficient for domestic hot water. When storage is depleted, though, the city water will be passed through the auxiliary furnace to boost its temperature to the required level. For space heating, water from the storage tank is passed through the air heater, which is a simple water-to-air heat exchanger located in the inlet air duct of the residence. For cooling, water from the storage tank is passed through the absorption cycle air conditioner, which uses this input heat to power the conventional lithium bromide/water absorption refrigeration cycle for cooling and dehumidifying the house air. The cooling coil (evaporator) of the absorption refrigeration cycle machine is also located in the inlet air duct of the residence. Whenever space heating or cooling is needed but the stored water temperature is below the level required by the output heater or absorption air conditioner, the auxiliary furnace will be used to provide the required thermal energy. Whenever auxiliary heat is being used for space heating or cooling, the water flow will go through the bypass shown in Fig. 1,

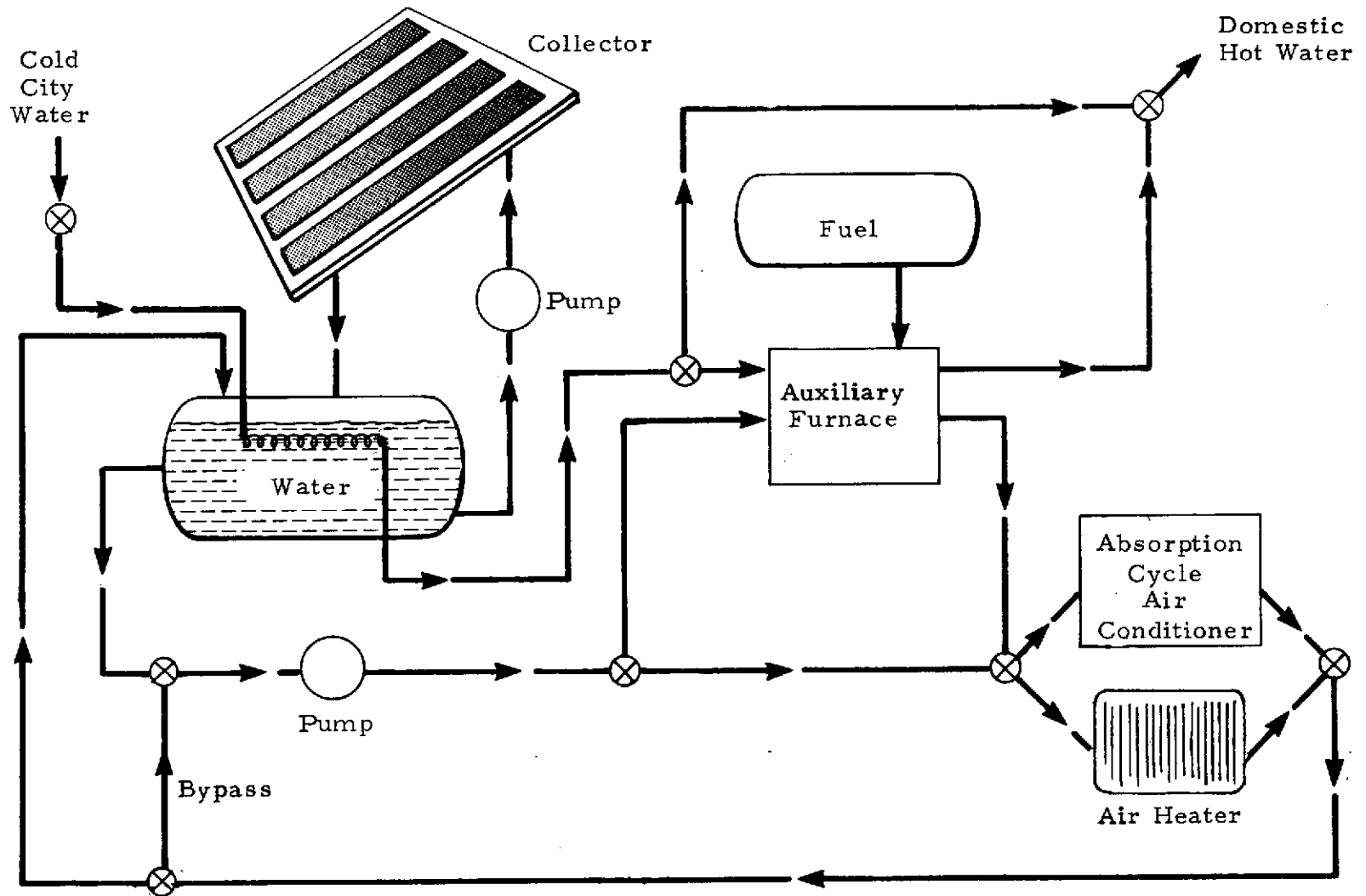


Fig. 1 - Schematic of the Solar-Powered Heating and Cooling System

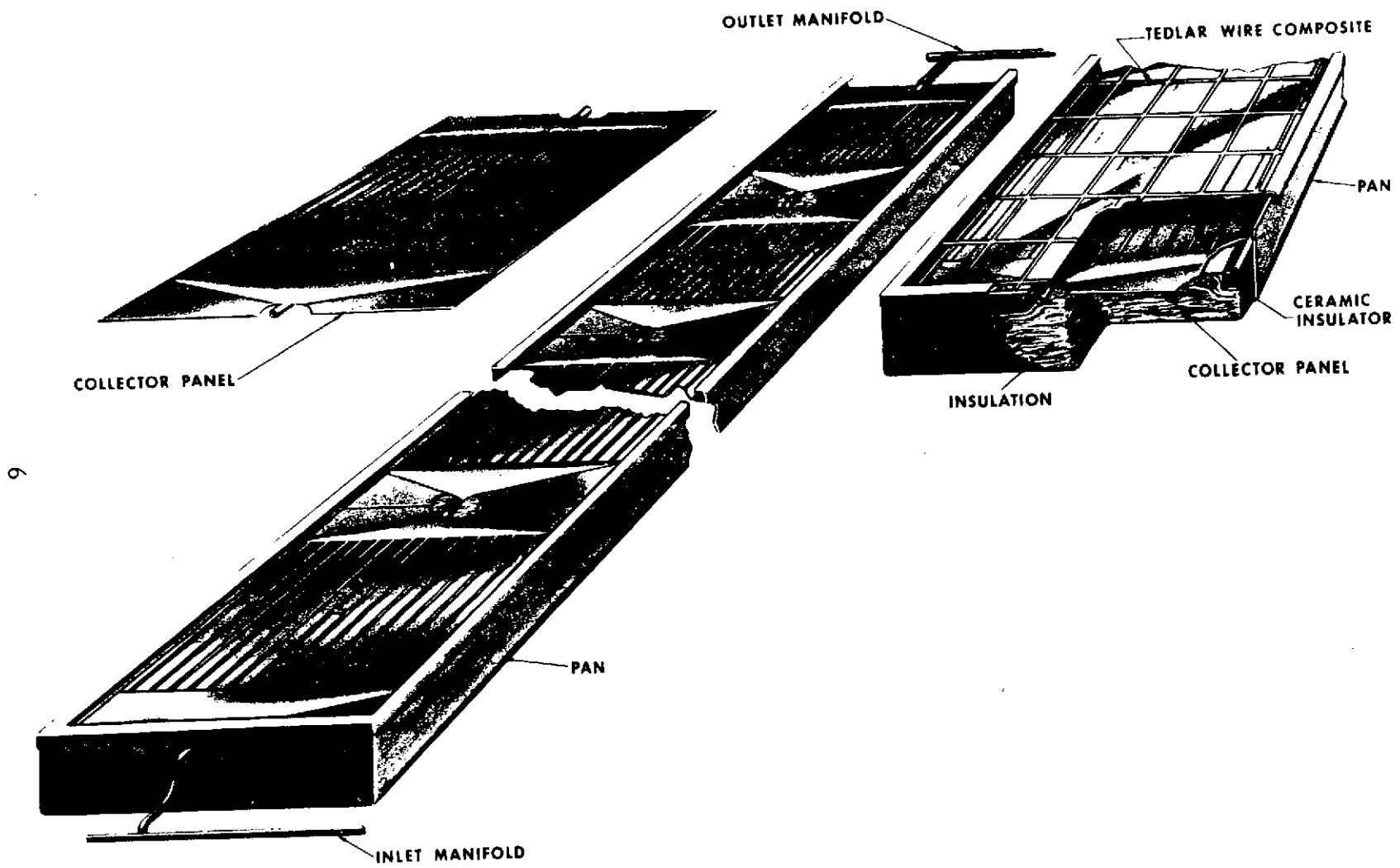
rather than returning to the large storage tank. This is to prevent the use of auxiliary heat to raise the temperature of the stored water, which would lower collector efficiency.

Figure 2 presents an artist's concept of the visual appearance of a home with an installed solar collector on its south-facing roof. The flat-plate collector can be integrated with the structure in an aesthetically pleasing manner. Figure 3 is a schematic of the flat-plate solar collector which will be used in the NASA-MSFC demonstration system. Further details of the collector design are discussed in Section 3. Figure 4 presents a drawing of the energy storage tank, which can be located in the basement of the house or below the ground.

The following sections of this report contain the results of studies of the major components of the solar-powered system, and of the total system as a whole.



Fig. 2 - Artist's Concept of Conventional Home with Solar Heating and Cooling



9

Fig. 3 - Schematic of NASA-MSFC Collector

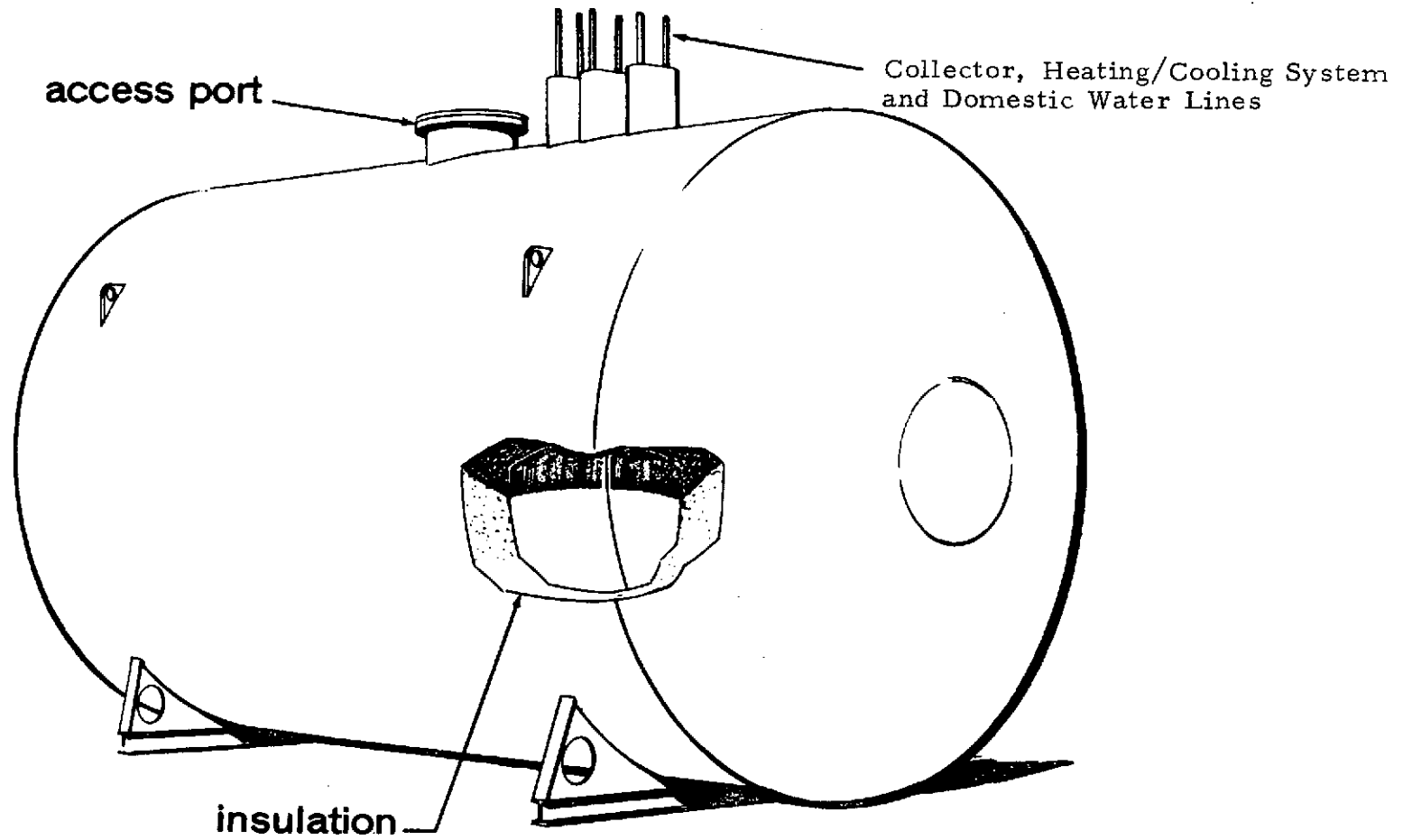


Fig. 4 - Drawing of Energy Storage Tank

Section 3

SOLAR ENERGY COLLECTOR STUDIES

During the past 15 months, numerous studies of flat-plate solar collectors were conducted under this contract. These studies and results are discussed in the following subsections.

3.1 COLLECTOR ABSORBER PLATE

Several large metal companies were contacted regarding the absorber plate of the flat-plate solar energy collector to determine the commercial availability of integral tube-in-sheet material. The major result of this survey was the identification of Olin Brass Roll-Bond material. This material is in the form of flat sheets with integral flow passages and appears ideal for solar collector applications. The material is available in aluminum alloys and copper alloys, and virtually any flow passage/manifold design can be fabricated with the silk screen/hot roll process used in manufacturing the Roll-Bond panels. Material cost is the major cost element, such that a cost of about 60 to 70 cents per square foot can be achieved for 0.060-inch thick aluminum Roll-Bond panels. Thinner sheets could be manufactured for less, although current tooling is set up for a minimum thickness of about 0.040 to 0.045 inch, depending on material. Connectors can be attached during sheet manufacture, and sheets up to 36 by 110 inches are currently available. MSFC is currently using the aluminum Roll-Bond material.

Unfortunately, NASA-MSFC plating facilities would allow application of the MSFC shiny nickel/nickel black selective coating only on panels of small size. Therefore, a 2-foot wide by 3-foot long nominal panel size was adopted as a design constraint for the MSFC demonstration system. However, larger panels would be used in downstream, mass-production applications.

3.2 FLOW PASSAGE GEOMETRY DEFINITION

After selecting the Roll-Bond material and setting the 2 x 3 foot size limitation on the panels, the flow passage geometry had to be defined. There are three basic considerations involved in designing the flow passages and manifolding for the panels:

- Uniform flow distribution throughout the panel is required for good thermal and fluid flow performance.
- A small overall pressure drop through the panel is required to minimize pump power for fluid circulation.
- Passage spacing and sizing must be selected for high fin efficiency and high film coefficient to achieve good thermal performance.

Parametric fluid flow analyses and thermal analyses were conducted to define a design that would have favorable characteristics with respect to each of the three considerations cited above. For design purposes, a flow rate of 0.80 gpm was assumed to flow through the panel; this was calculated based upon stacking seven small panels in series to yield about 42 ft² of collector. Under excellent operating conditions, 0.80 gpm flowing through 42 ft² of collector would allow about a 20°F rise in water temperature from inlet to outlet. This was taken to be a reasonable value for the maximum temperature rise.

The results of the parametric analyses indicated that the design shown in Fig. 5 would be excellent from fluid distribution, pressure drop, and heat transfer viewpoints. This design utilizes 16 identical flow passages arranged in parallel. The passages are 0.375-inch wide as shown in the detail of Fig. 5, and are spaced on 1.500-inch centers. The manifold is a simple triangular passage designed to feed each of the 16 passages with an equal flow of water. Although not shown in the figure, the manifold flow passage is twice the height of the 16 separate flow passages, i.e., the manifold outside height is 0.250-inch rather than the 0.125 inch used for the individual flow passages. This extra flow area minimizes pressure variations in the manifold.

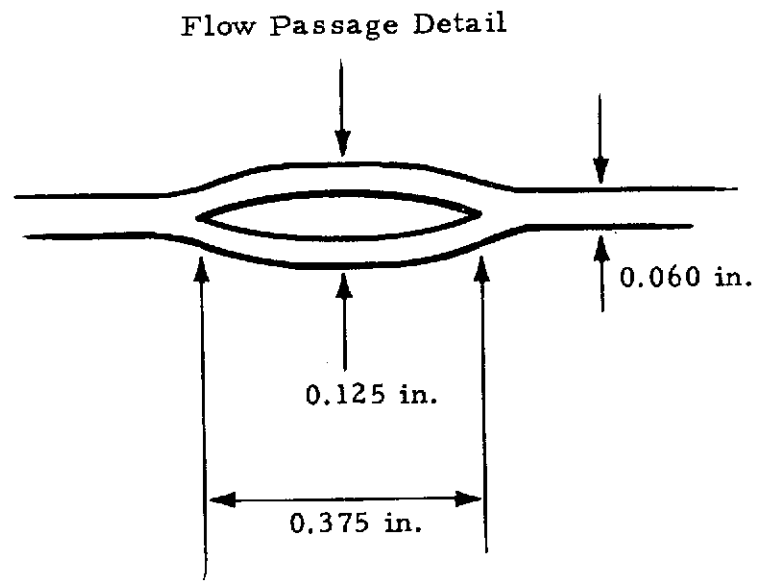
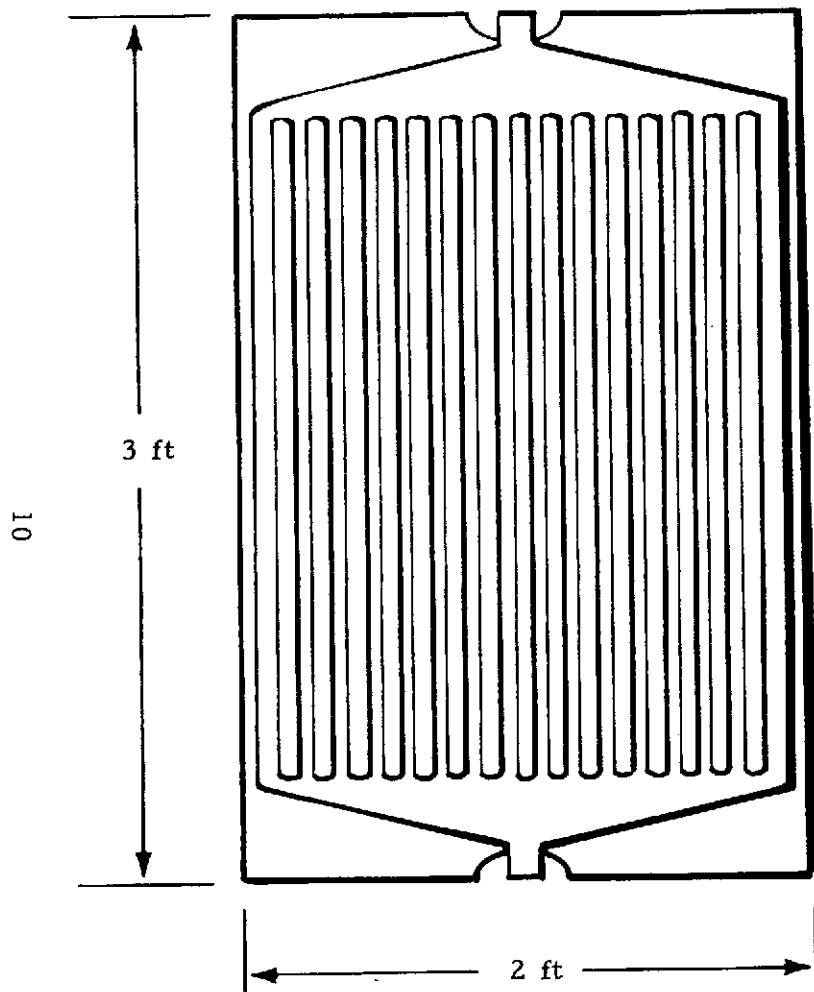


Fig. 5 - Roll-Bond Panel Design

The predicted thermal performance of the panel for typical operating conditions is shown in Fig. 6. As shown in the figure, the temperature difference between plate and water is less than 1.5°F from inlet to outlet; this small temperature differential signifies excellent conductive and convective heat transfer. Also shown in Fig. 6, the ΔP through the panel for the given conditions is only 0.04 psi, a totally acceptable value. Regarding flow uniformity, NASA-MSFC fabricated a test panel of plexiglass using this design and conducted a flow visualization test, using dye in water. The results verified a uniformly distributed flow through all the passages.

One slight design modification was required prior to fabricating all of the panels for the MSFC collector. Since only a soft aluminum alloy was available as the material for the panels, some spot weld points were included in the manifolds to reduce the unsupported spans in the manifold. These were required to maintain structural integrity under the slightly pressurized conditions under which the collector will operate.

3.3 BACKSIDE INSULATION

The backside of the collector must be insulated to minimize downward heat losses. A transient thermal analysis of this backside insulation was conducted to determine its heat transfer characteristics. Six inches of fiberglass were assumed to be subject to a 200°F step jump in Roll-Bond plate temperature. The resultant heat transfer into the insulation is presented in Fig. 7, for the given insulation properties. As shown in the figure, the steady-state heat flux of about $8 \text{ Btu/ft}^2\text{-hr}$ is reached in a few hours. This value was considered acceptable and six inches of fiberglass insulation were incorporated into the collector design. However, the fact that the heat loss from the plate is more than twice the steady-state value for about one hour should be remembered, especially in collector testing where data points are often obtained in quick succession at progressively higher temperatures.

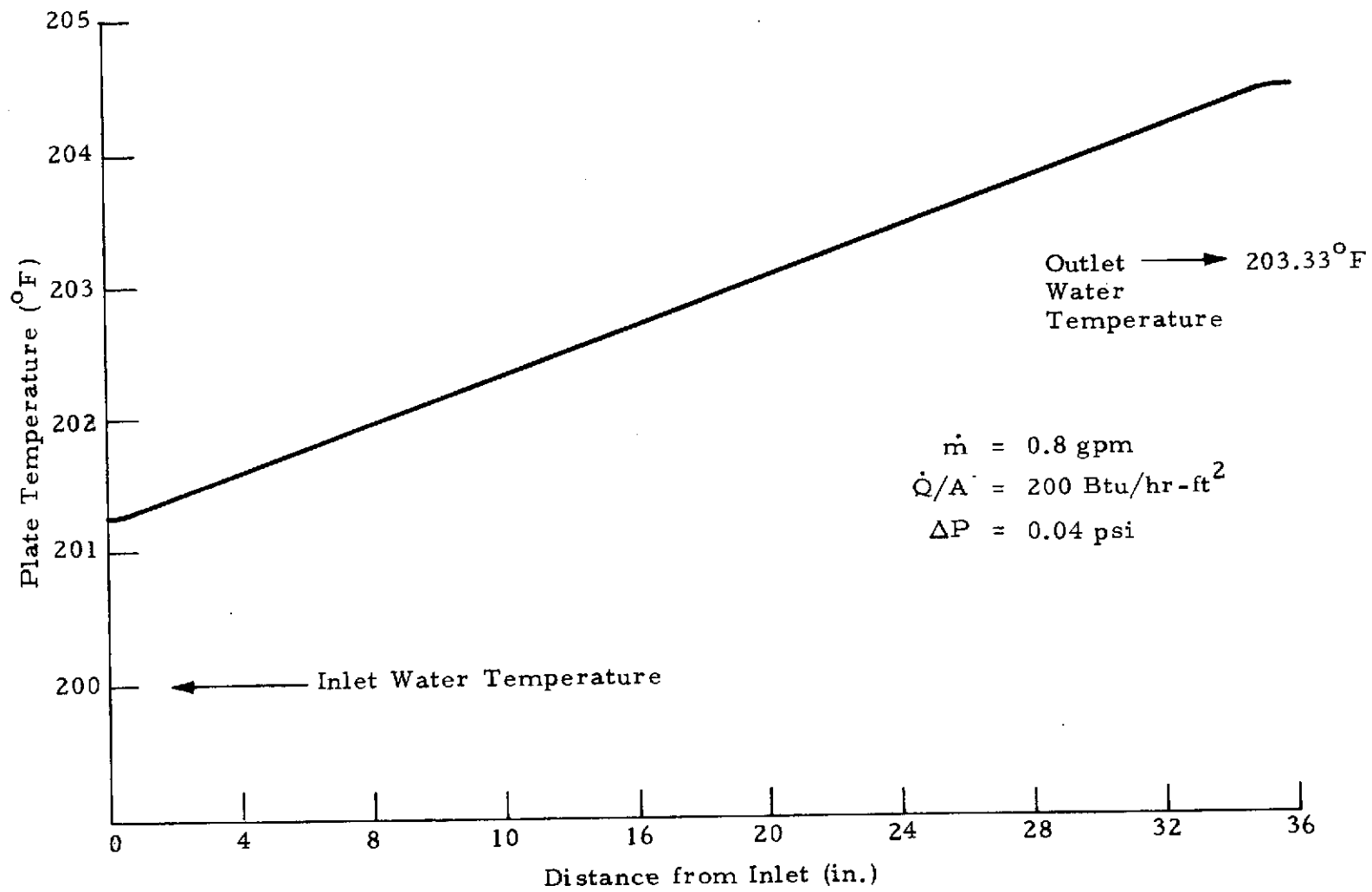


Fig. 6 - Predicted Thermal Performance of Roll-Bond Panel Design

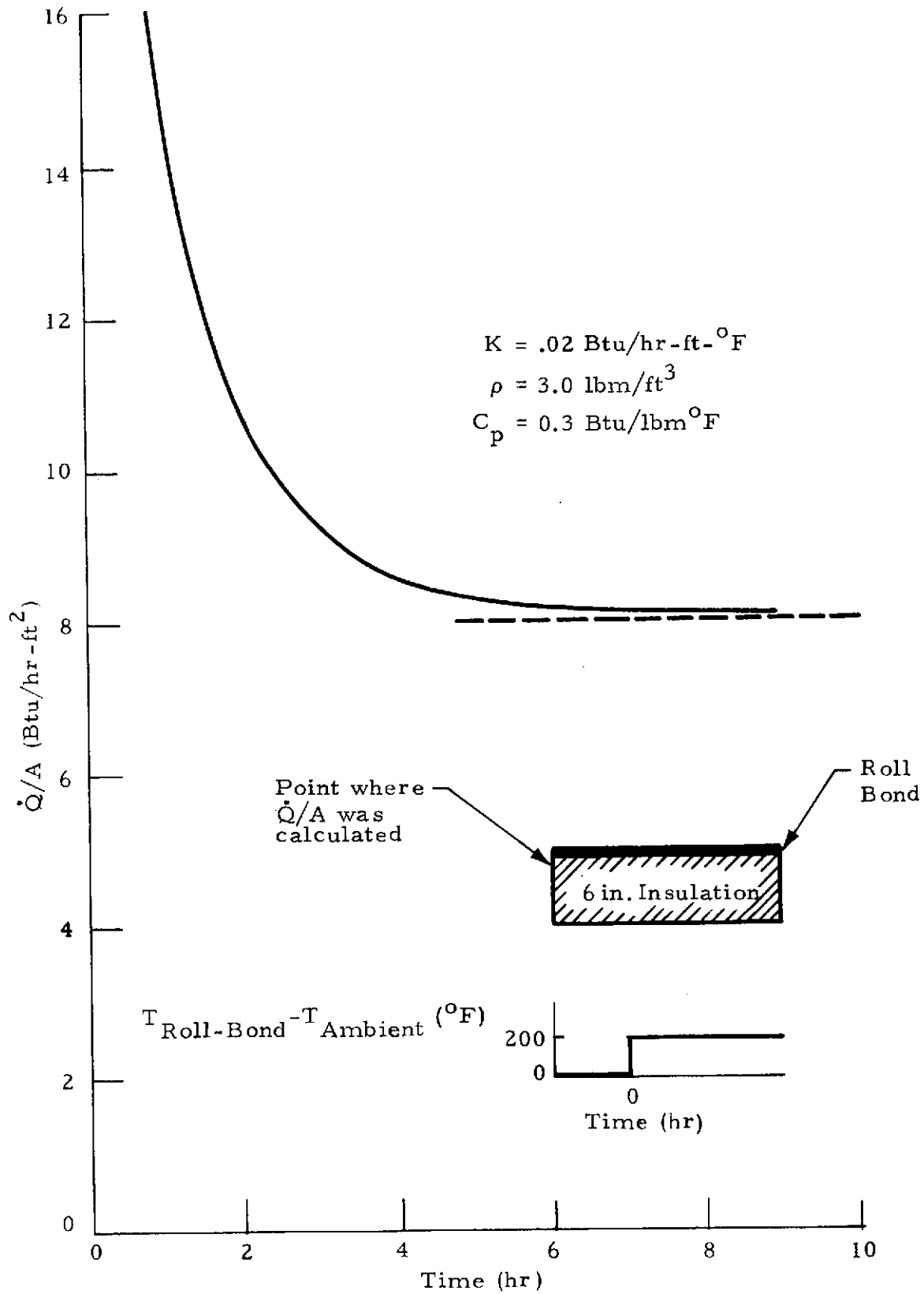


Fig. 7 - Heat Transfer from Collector to Collector Insulation for a Step Jump in Roll-Bond Plate Temperature

3.4 NO-FLOW TEMPERATURE EXTREMES

To determine the maximum temperature levels which the collector components could experience, an analysis was conducted for the collector operating under the best possible set of circumstances. The results are presented in Figs. 8 and 9 for single-glazed and double-glazed collectors, respectively. For the one-Tedlar cover collector, the maximum plate temperature which could be reached under no-flow circumstances would be 485°F , corresponding to zero efficiency as shown in Fig. 8. The Tedlar cover would reach about 220°F . For the two-Tedlar cover collector, the maximum plate temperature achievable would be about 580°F , with the inner Tedlar approaching 300°F . Clearly, such temperatures must be avoided in case of flow failure coupled with excellent collection conditions. The recommended method of preventing such overheating is to flow cold city water through the collector in the event of plate temperature rise above a safe level, e.g., 300°F .

3.5 RADIATION PROPERTIES OF SELECTIVE COATING

Parametric studies were conducted to determine the effect of selective coating properties on collector performance under typical operating conditions. Figures 10 through 13 present the results of these studies for typical clear summer and winter days for both single-glazed and double-glazed collector designs. The operating conditions are specified on the figures, and the solar absorptance and infrared emittance are parameterized. The great benefits of high solar absorptance and low infrared emittance are clearly demonstrated in these figures.

Figures 14 and 15 present comparisons of performance for the single- and double-glazed collectors. The large benefits offered by the double-glazing are apparent in these figures, especially for higher emittance values and lower solar absorptance values.

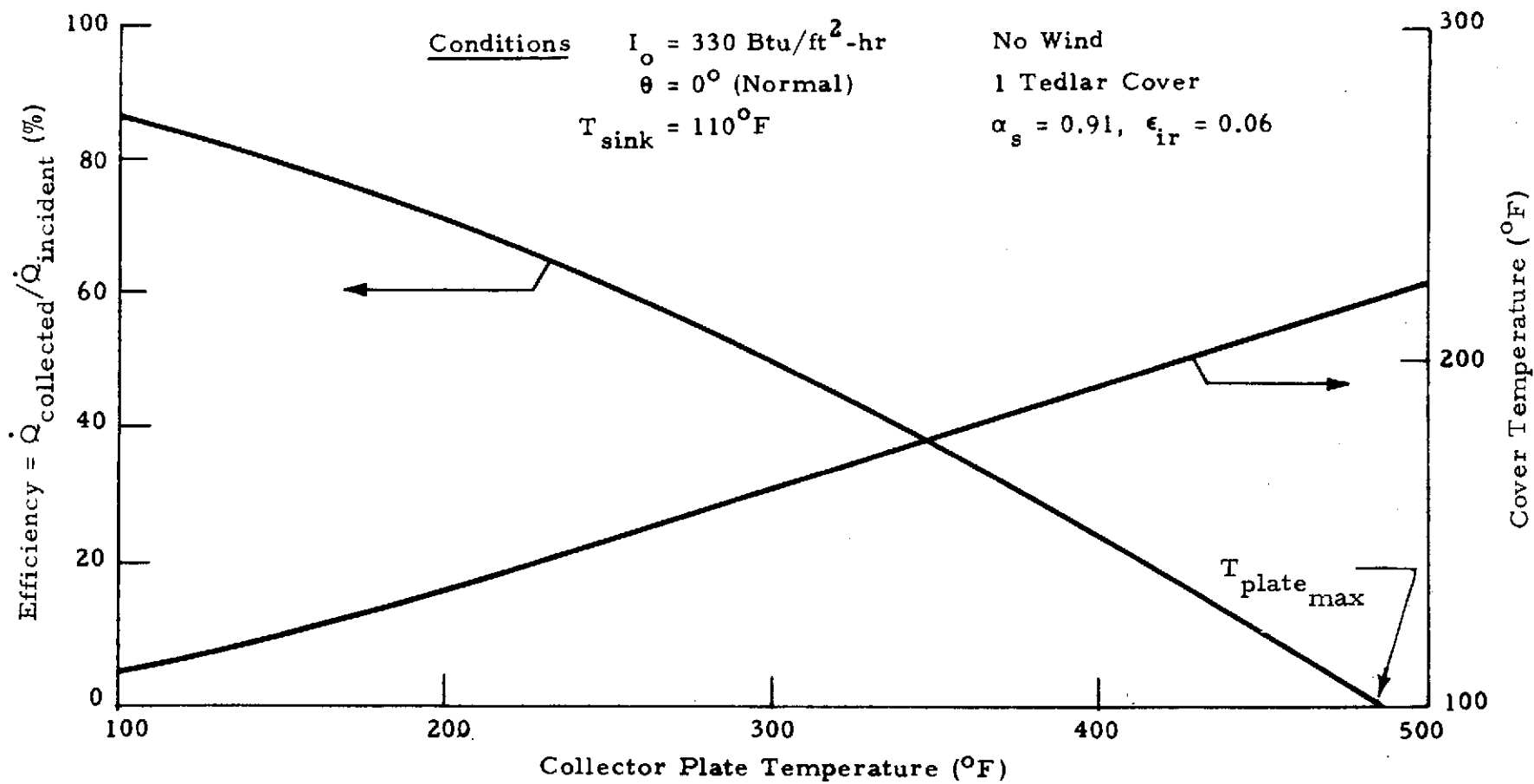


Fig. 8 - Collector Performance under "Best Possible Conditions" to Determine Maximum Temperature Extremes

Conditions:

$$I_o = 330 \text{ Btu/hr-ft}^2$$

$$\theta = 0^\circ \text{ (normal)}$$

$$T_{\text{sink}} = 110^\circ \text{F}$$

No wind

Two Tedlar Covers

$$\alpha_s = .91 \quad \epsilon_{\text{ir}} = .06$$

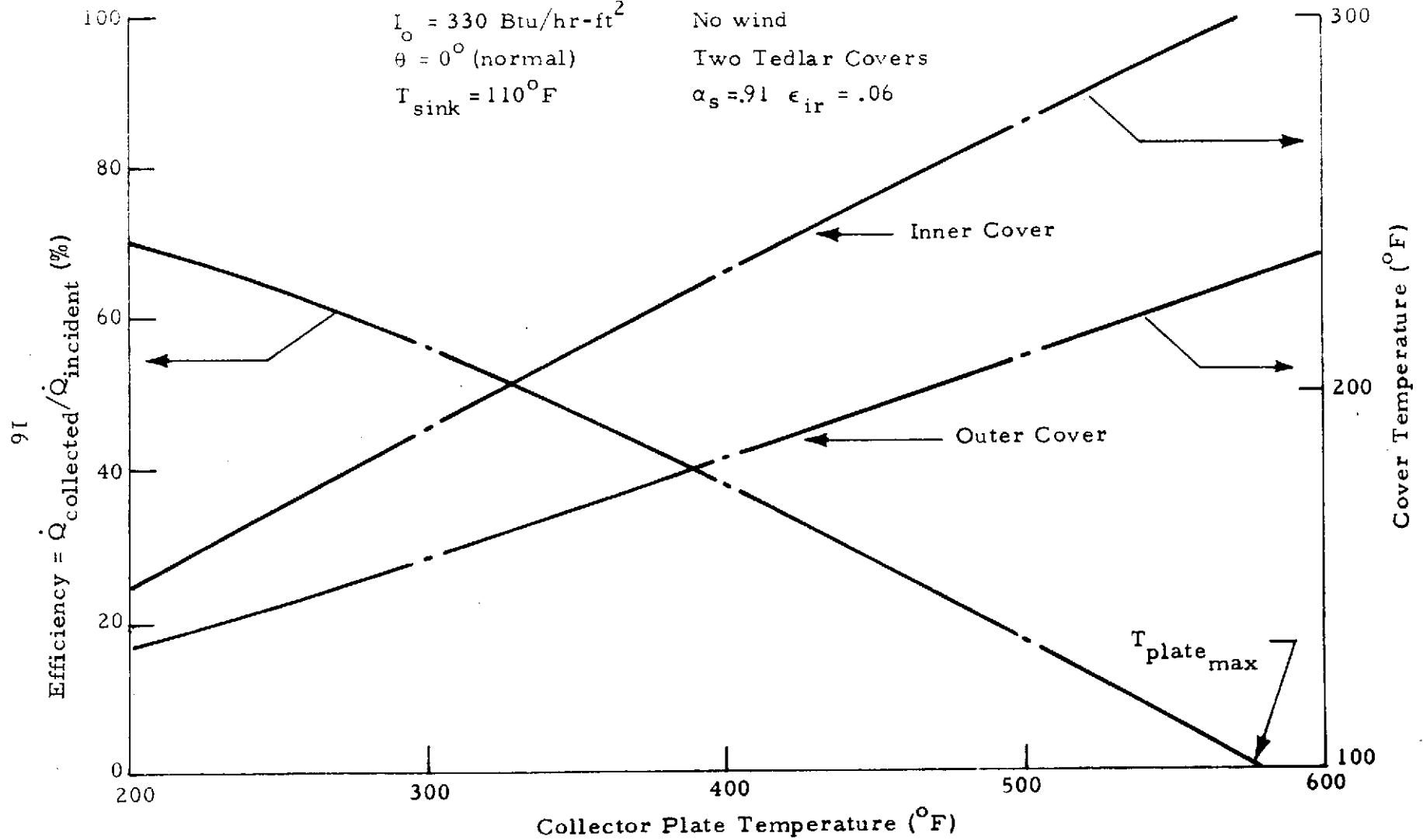


Fig. 9 - Collector Performance under "Best Possible Conditions" to Determine Maximum Temperature Extremes

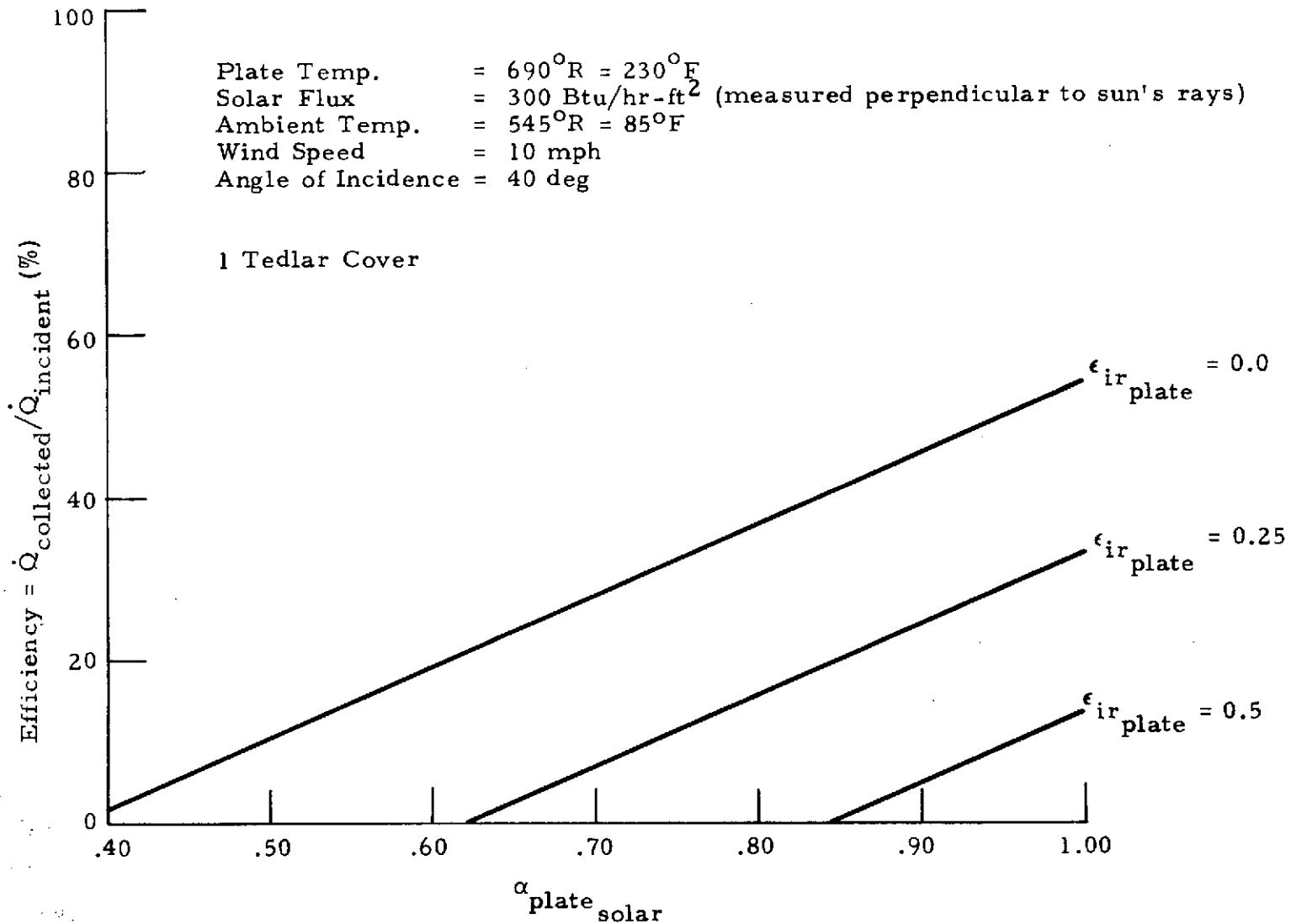


Fig. 10 - Solar Energy Collection Efficiency for a "Typical Clear Summer Day"
 (One Tedlar Cover)

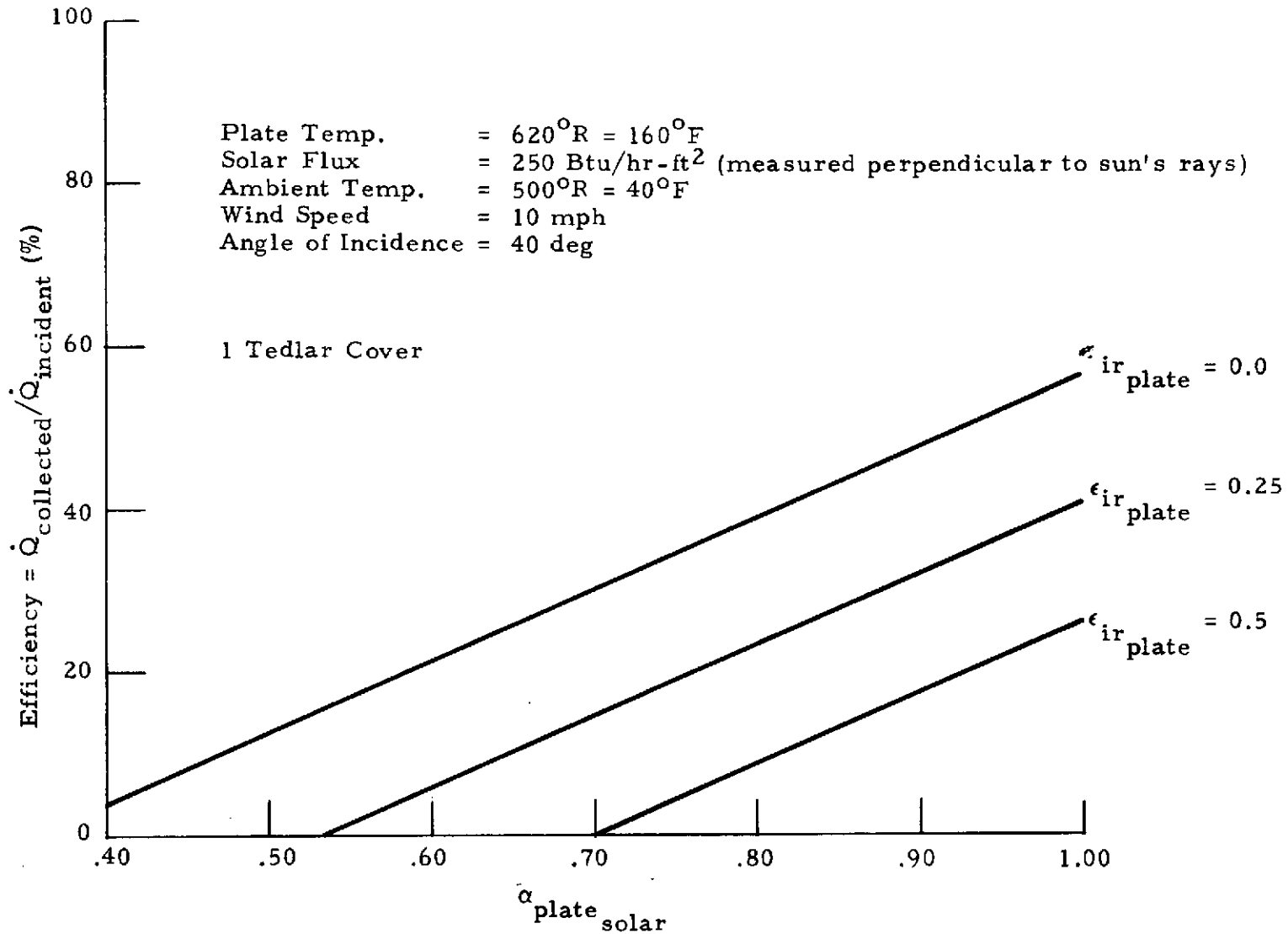


Fig. 11 - Solar Energy Collection Efficiency for a "Typical Clear Winter Day"
(One Tedlar Cover)

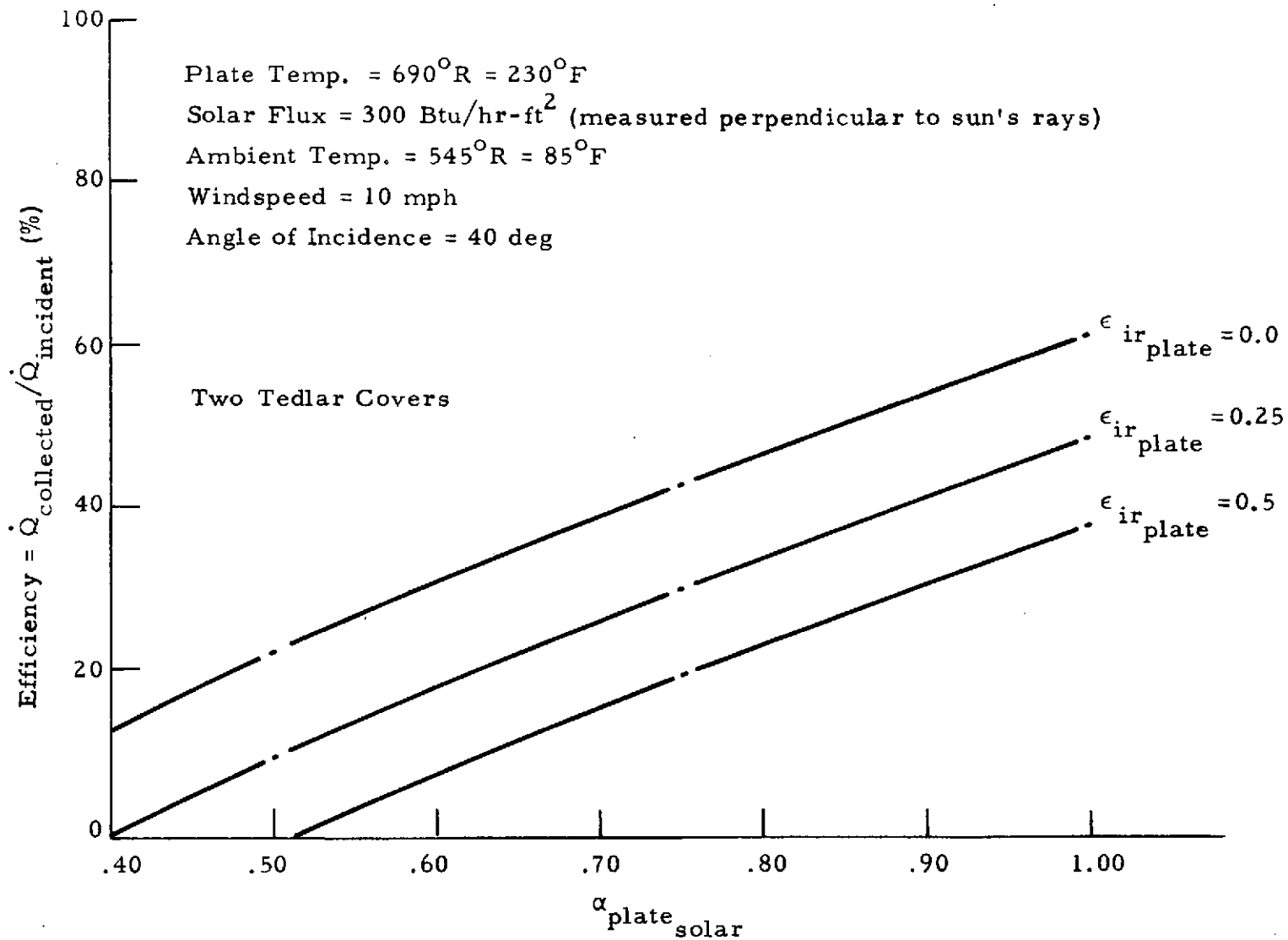


Fig. 12 - Solar Energy Collection Efficiency for a "Typical Clear Summer Day"
 (Two Tedlar Covers)

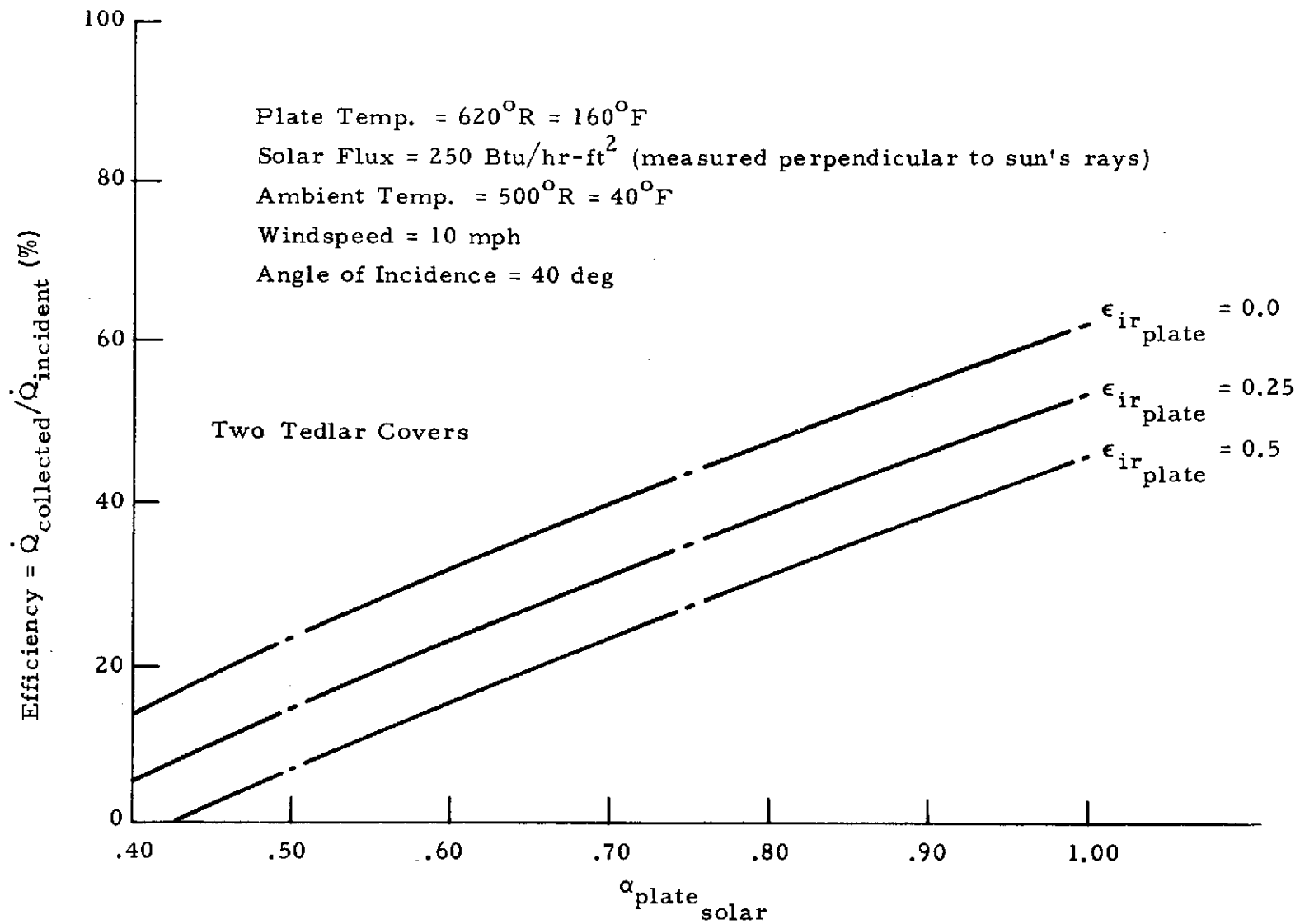


Fig. 13 - Solar Energy Collection Efficiency for a "Typical Clear Winter Day"
(Two Tedlar Covers)

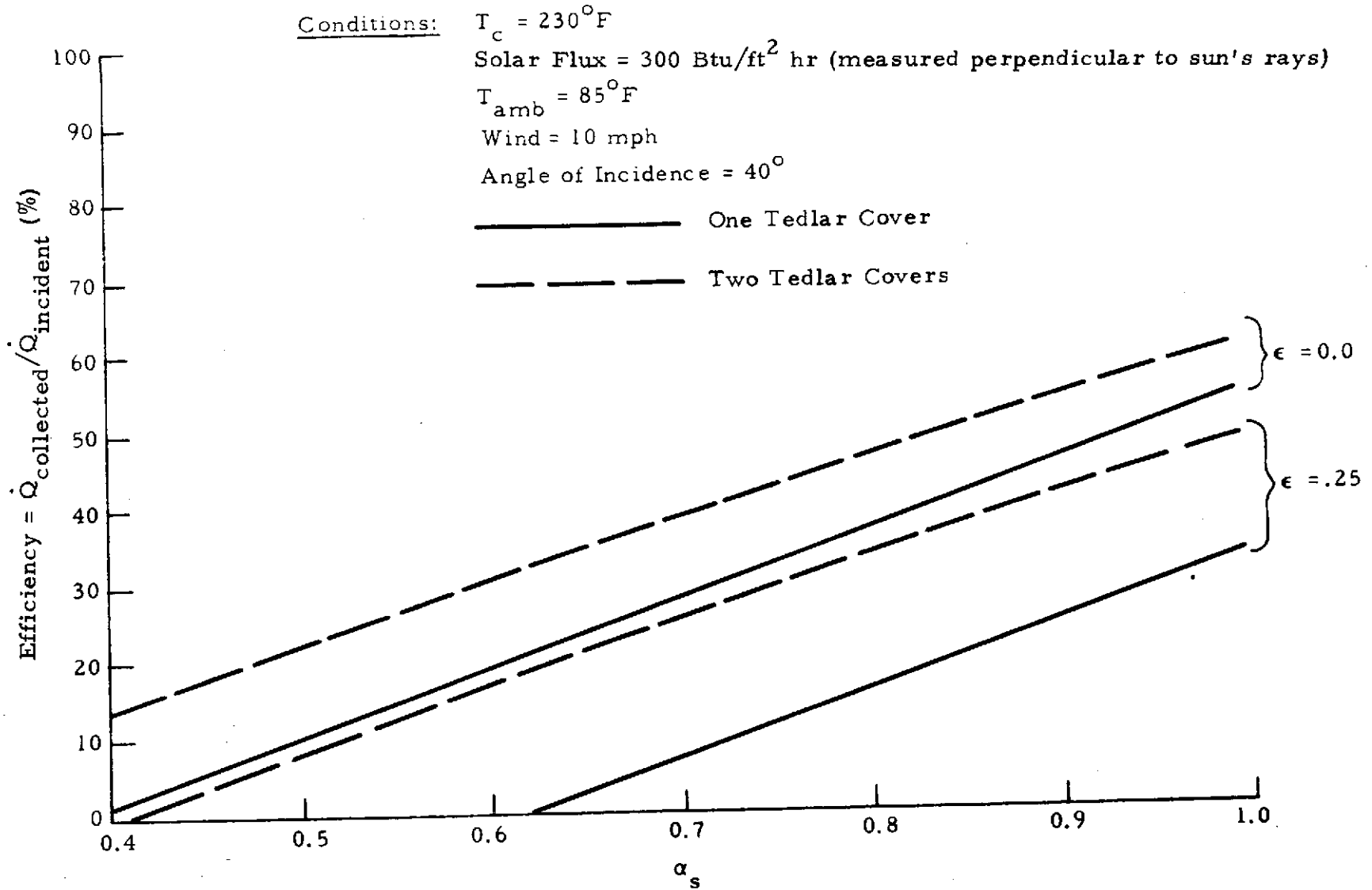


Fig. 14 - Effect of Number of Covers on Collection Efficiency for "Typical Clear Summer Day"

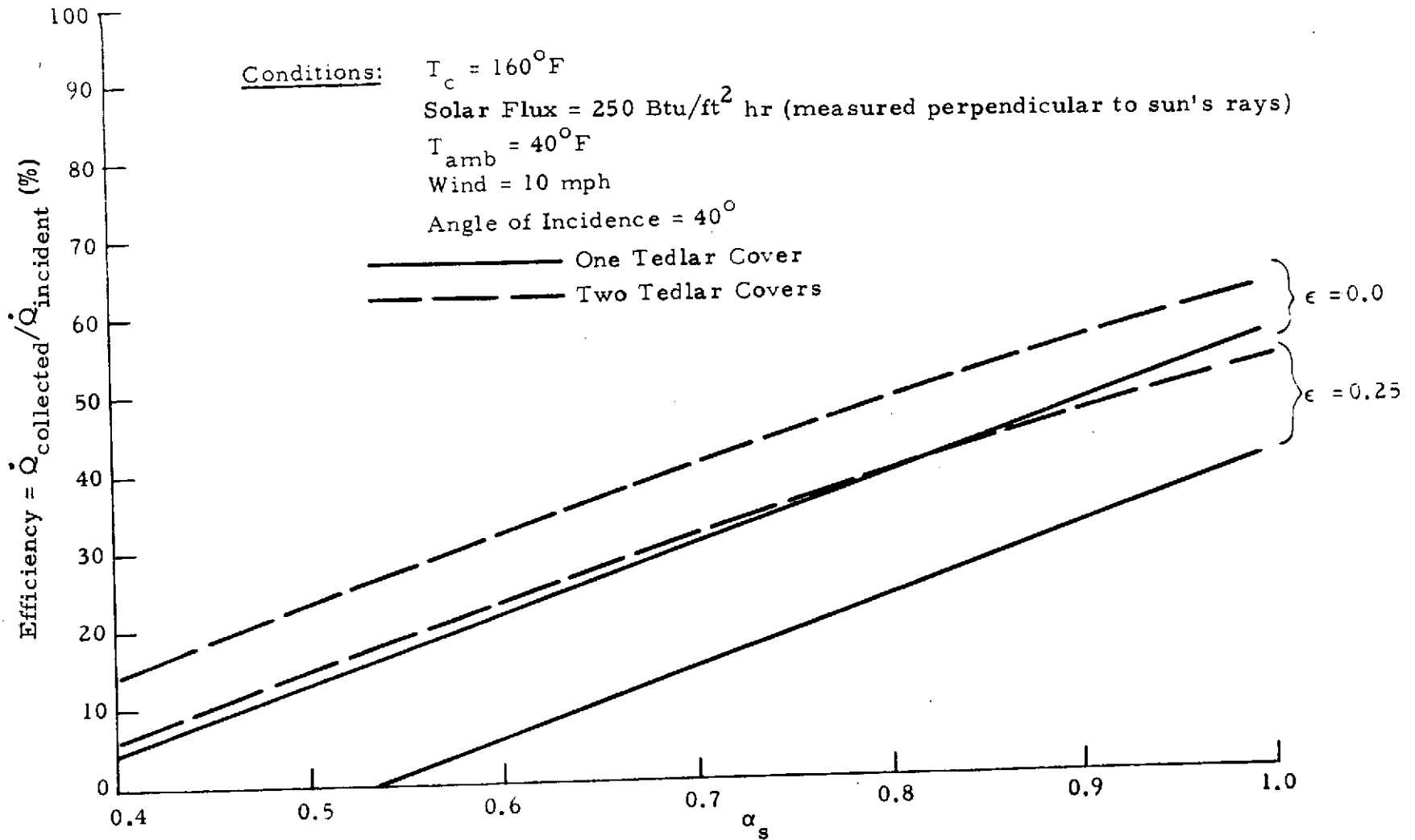


Fig. 15 - Effect of Number of Covers on Collection Efficiency for "Typical Clear Winter Day"

3.6 WIRE/TEDLAR COMPOSITE

The MSFC collector design will utilize Tedlar bonded to a rectangular wire mesh for strength and rigidity. The wire mesh is a 2 by 4-inch welded steel mesh fencing material.

The wire mesh has one significant effect on the collector performance. It blocks about 7% of the solar radiation incident upon the Tedlar, resulting in an effective perpendicular transmittance of 0.85 rather than the 0.92 quoted for plain Tedlar.

During preliminary testing, the wire in the Tedlar/wire composite transparent cover was observed to reach a much warmer temperature than the Tedlar. To explain this effect and determine its magnitude and its dependence on wire surface properties, a thermal analysis was conducted. The results are shown in Fig. 16. Note that the higher the emittance and the lower the absorptance, the cooler the wire. However, the temperature rise of the wire above the Tedlar temperature will have no noticeable effect on collector efficiency, and the flexible nature of the adhesive between the wire and Tedlar should prevent any thermal stress problems.

3.7 COMPARISON OF EXPERIMENTAL COLLECTOR PERFORMANCE WITH ANALYTICAL PREDICTIONS

During the first quarter of 1974, MSFC initiated testing of a solar collector module of approximately 40 ft², oriented southward with a 45-degree tilt off horizontal. The results of three quasi-steady-state tests are presented in Figs. 17 and 18. Also presented in the figures are the Lockheed predictions of collector performance for the measured meteorological conditions (solid curves). The experimental points are below the solid, prediction curves for all three tests. To investigate these relatively small discrepancies between theory and test, a rough thermal analysis of the edge losses was conducted. When the calculated edge losses are included in the collector analysis, the dashed-line efficiency curves of Figs. 17 and 18 are obtained. Clearly, the comparison between the dashed-line curves and the test points shows excellent correlation, within about 1% in each case.

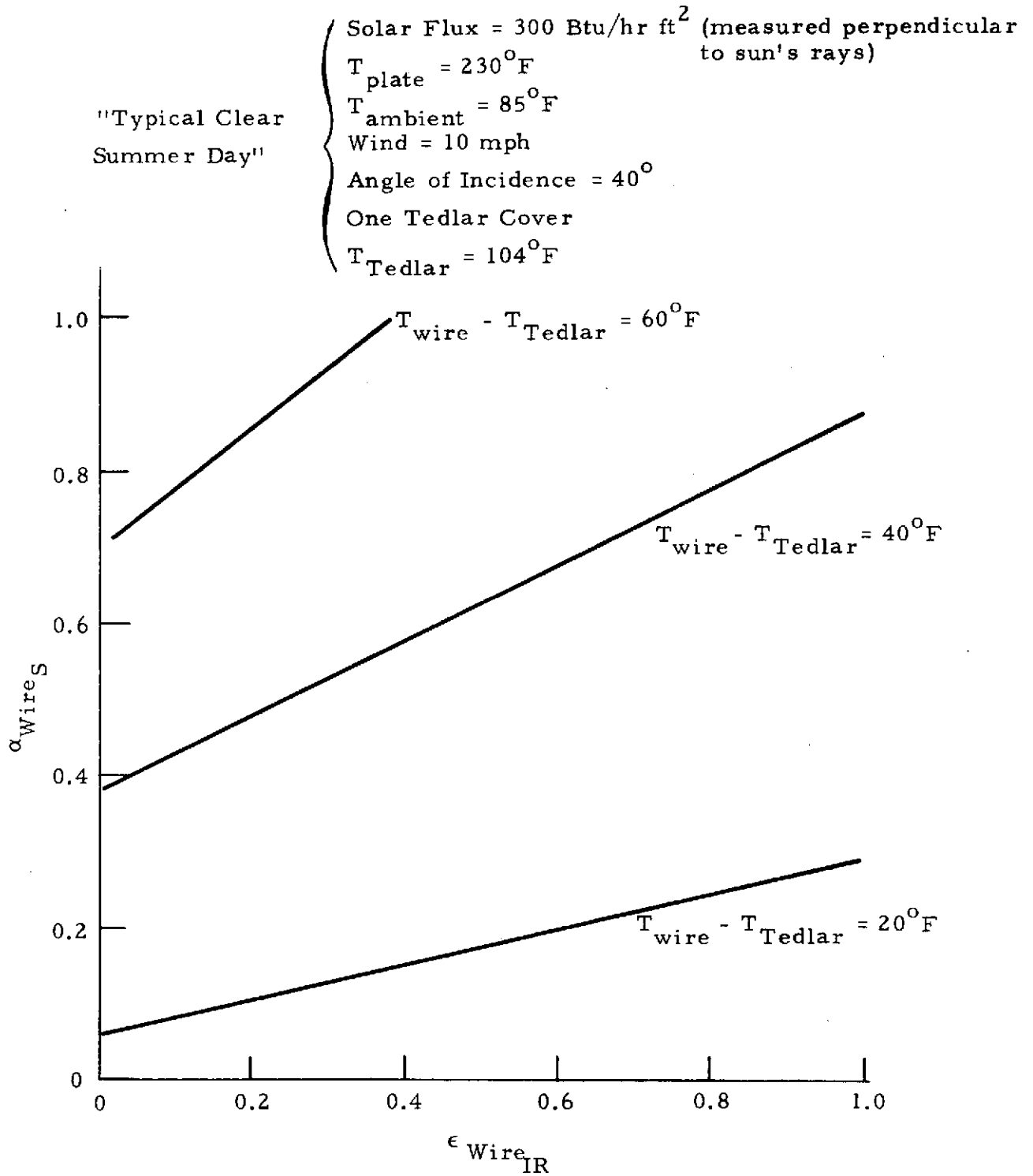


Fig. 16 - Wire Equilibrium Temperature

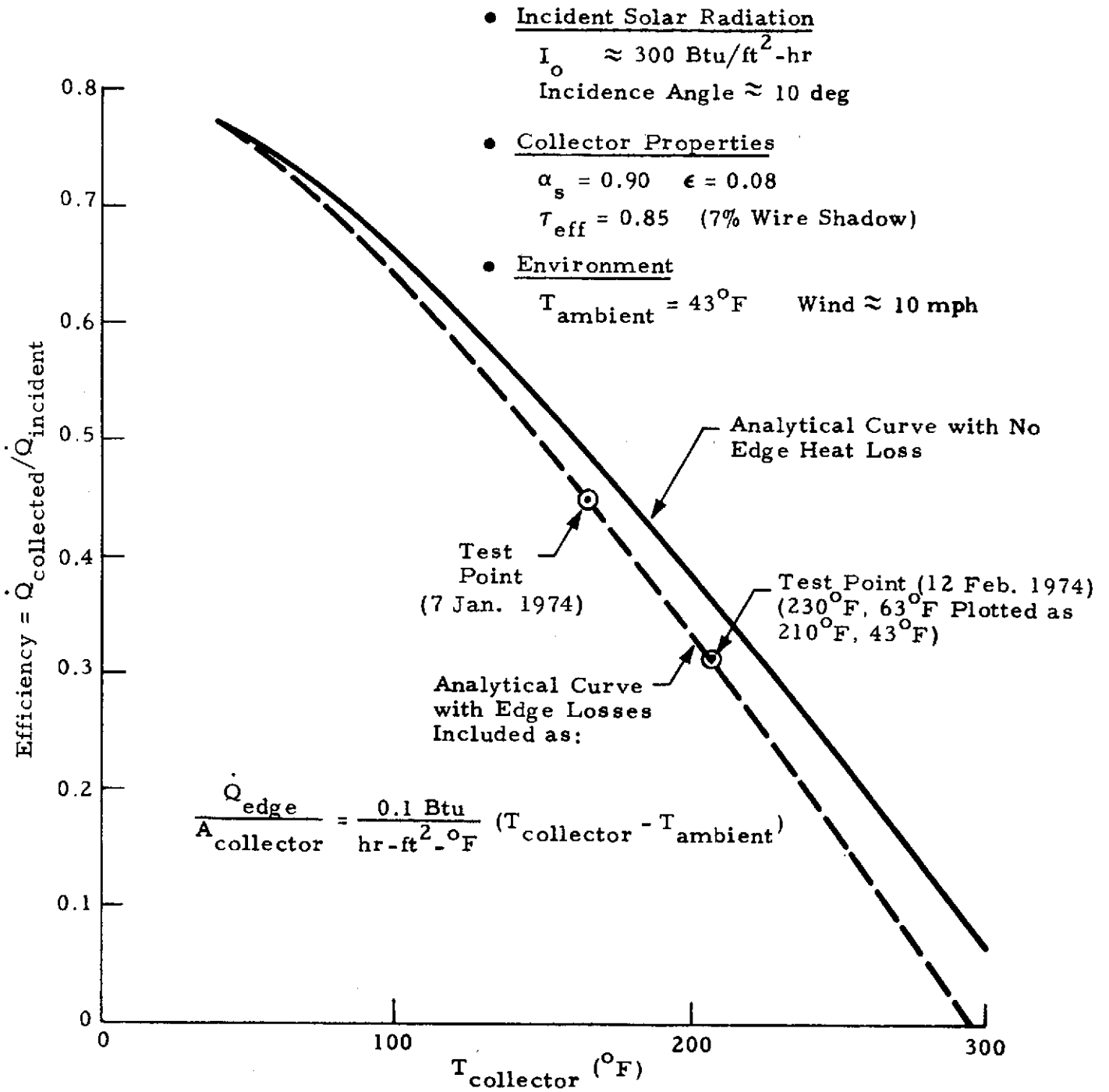


Fig. 17 - Analytical/Experimental Comparison for Solar Collector Test

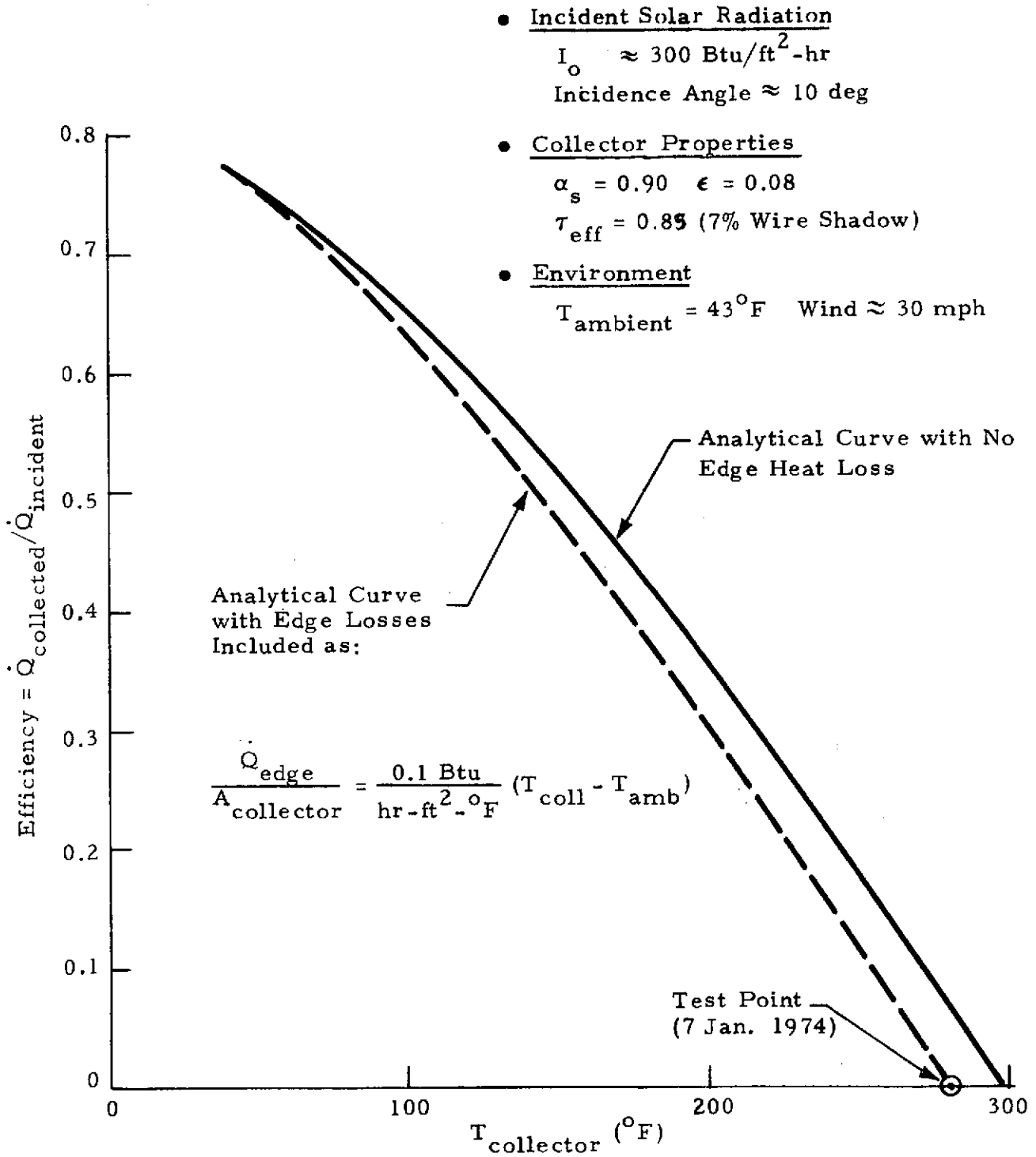


Fig. 18 - Analytical/Experimental Comparison for 280°F Solar Collector Test

Based upon these calculations, MSFC engineers have modified the design of the full-scale, 1300 ft² collector to reduce or eliminate the edge losses. Figures 19 and 20 present schematics of all of the energy flows about the collector for two of the test points. These figures point out the relative magnitudes of the different energy exchange mechanisms involved.

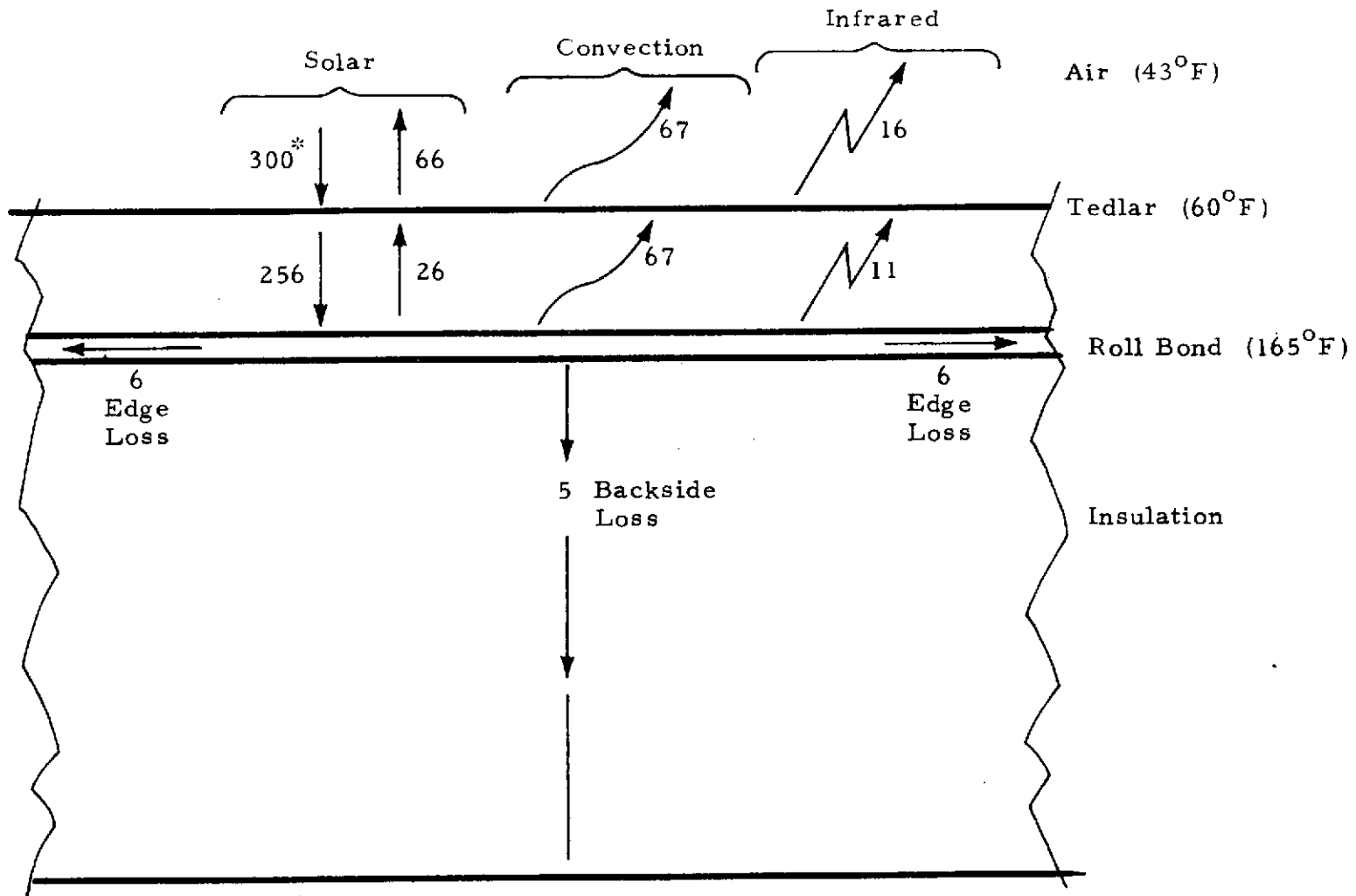
3.8 SOLAR FLUX AND INCIDENCE ANGLE EFFECTS

To extrapolate the findings discussed above to summer operation of the collector, analytical studies were conducted assuming typical summer conditions. Figure 21 presents the results of a study of the effect of solar flux on collector efficiency. The three curves show the performance of three collector designs as labeled. The effect of edge loss is seen to be greater at lower fluxes than at higher fluxes. Also, the performance of a two-cover collector is seen to be far superior to a one-cover collector at lower solar flux levels.

Figure 22 presents the results of a study of the effects of incidence angle on collector performance. The incidence angle is measured between the sun's rays and a vector normal to the collector. Again, both the performance degradation due to edge loss and the performance improvement offered by two covers are seen to be of greatest importance at large incidence angles. Interestingly, the daily average incidence angle during the cooling season, when defined as

$$\theta_{\text{average}} = \cos^{-1} \left[\frac{\int_{\text{Sunrise}}^{\text{Sunset}} \cos \theta \, dt}{t_{\text{sunset}} - t_{\text{sunrise}}} \right],$$

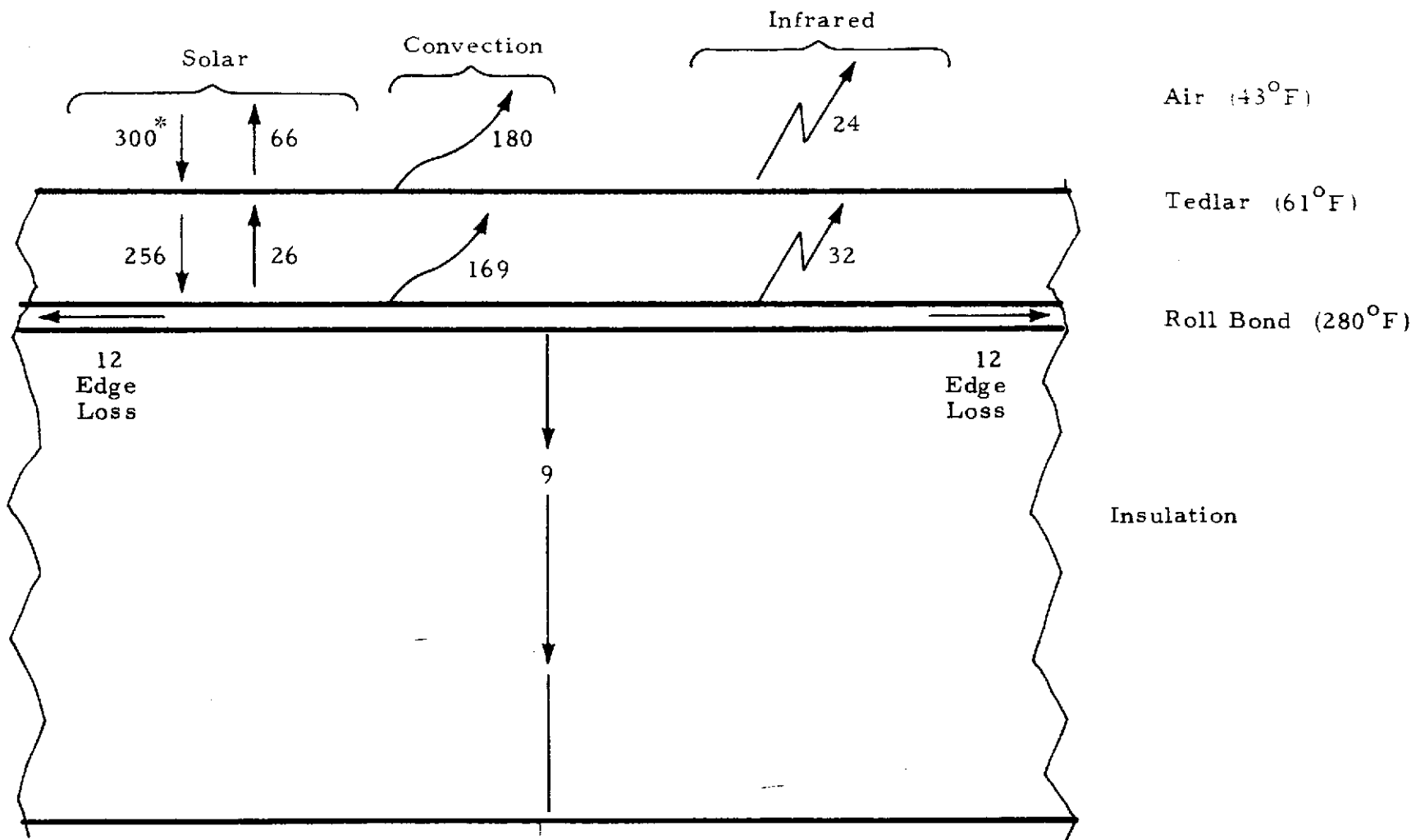
varies from about 55° in early summer to about 50° in early fall for the MSFC collector with its 45° tilt.



*NOTE: All energy flows are Btu per hr per ft² of collector area.

$$\text{Efficiency} = \frac{256 - 26 - 67 - 11 - 5 - 6 - 6}{300} = 45\%$$

Fig.19 - Energy Flows for 165°F Collector Test



* NOTE: All energy flows are Btu per hr per ft² of collector area.

$$\text{Efficiency} = \frac{256 - 26 - 169 - 32 - 9 - 12 - 12}{300} = -1\% \approx 0\%$$

Fig.20 - Energy Flows for 280°F Collector Test

Typical Summer Day

$T_{\text{collector}} = 230^{\circ}\text{F}$

$T_{\text{ambient}} = 80^{\circ}\text{F}$

Wind = 10 mph

Incidence Angle = 0

$\epsilon = .08$

$\alpha_s = .90$

$\tau_{\text{eff}} = .85$

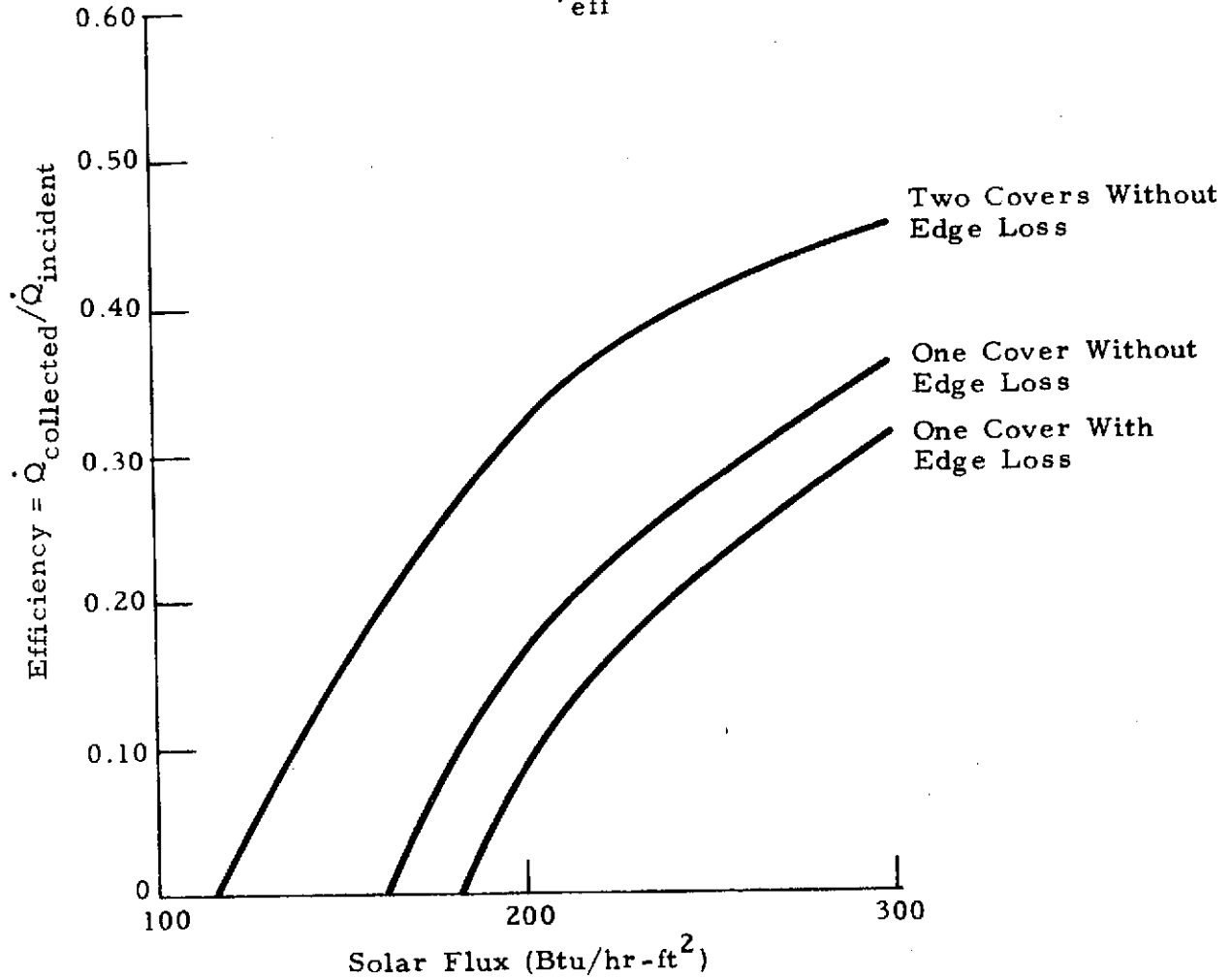


Fig.21 - Effect of Solar Flux on Collector Performance

Typical Clear Summer Day

$T_{\text{collector}} = 230^{\circ}\text{F}$

$T_{\text{ambient}} = 80^{\circ}\text{F}$

Wind = 10 mph

Solar Flux = 300 Btu/hr ft² (measured perpendicular to sun's rays)

$\epsilon = .08$

$\alpha_s = .90$

$\tau_{\text{eff}} = .85$

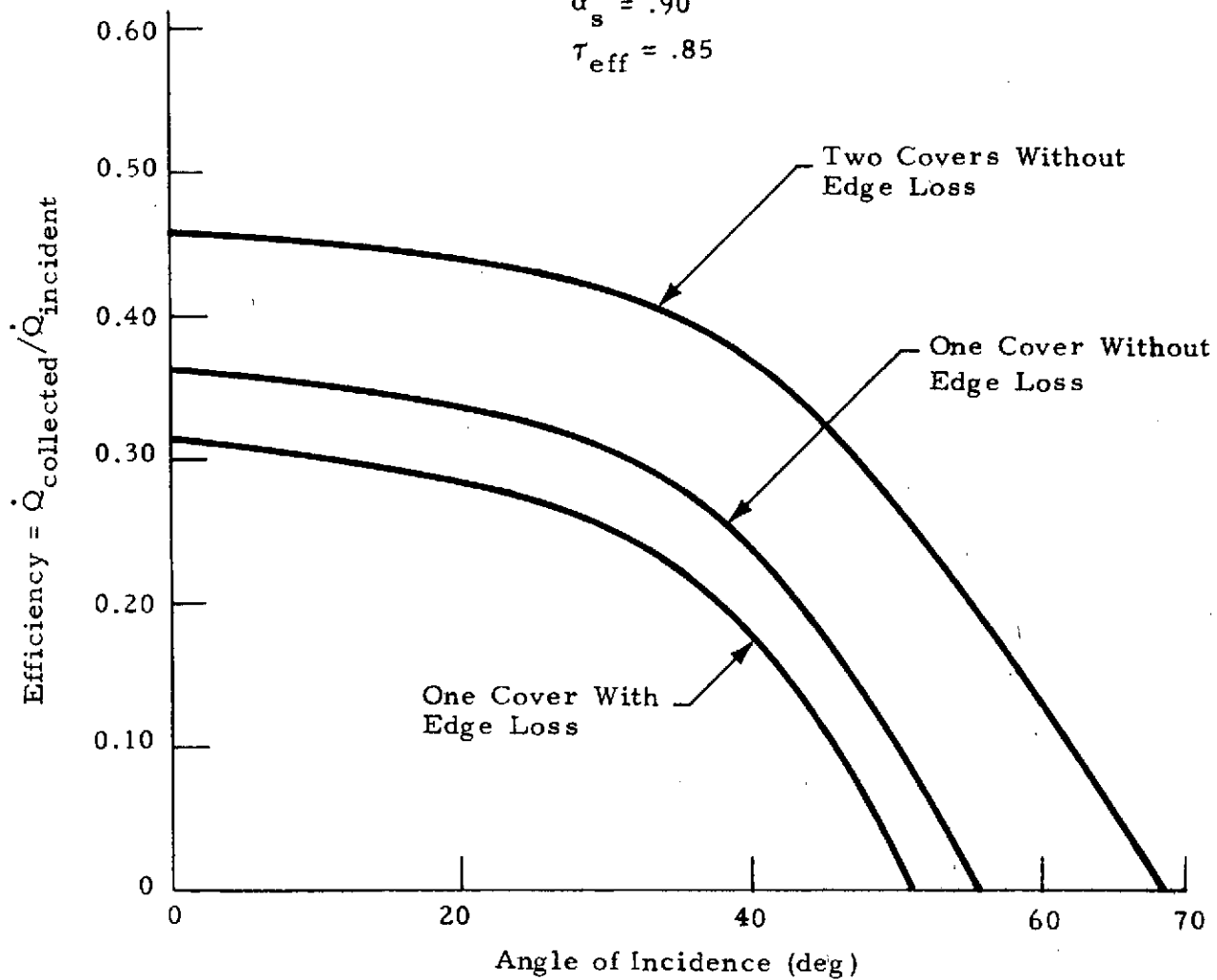


Fig. 22 - Effect of Incidence Angle on Collector Performance

3.9 FURTHER TILT ANGLE STUDIES

Figure 23 presents an interesting comparison of the total daily insolation on surfaces tilted toward the equator at different tilt angles. These curves were calculated for Huntsville's latitude. No atmospheric effects were treated — just the geometrical effects of the sun-earth astronomy. Clearly, the 45-degree angle chosen for the MSFC test system is a reasonable choice. It is biased in favor of winter operation, but not so much as to greatly degrade summer operation. Section 5 presents results of some total system performance studies of tilt angle effects which further substantiate the 45-degree tilt angle as being a good year-round choice for Huntsville.

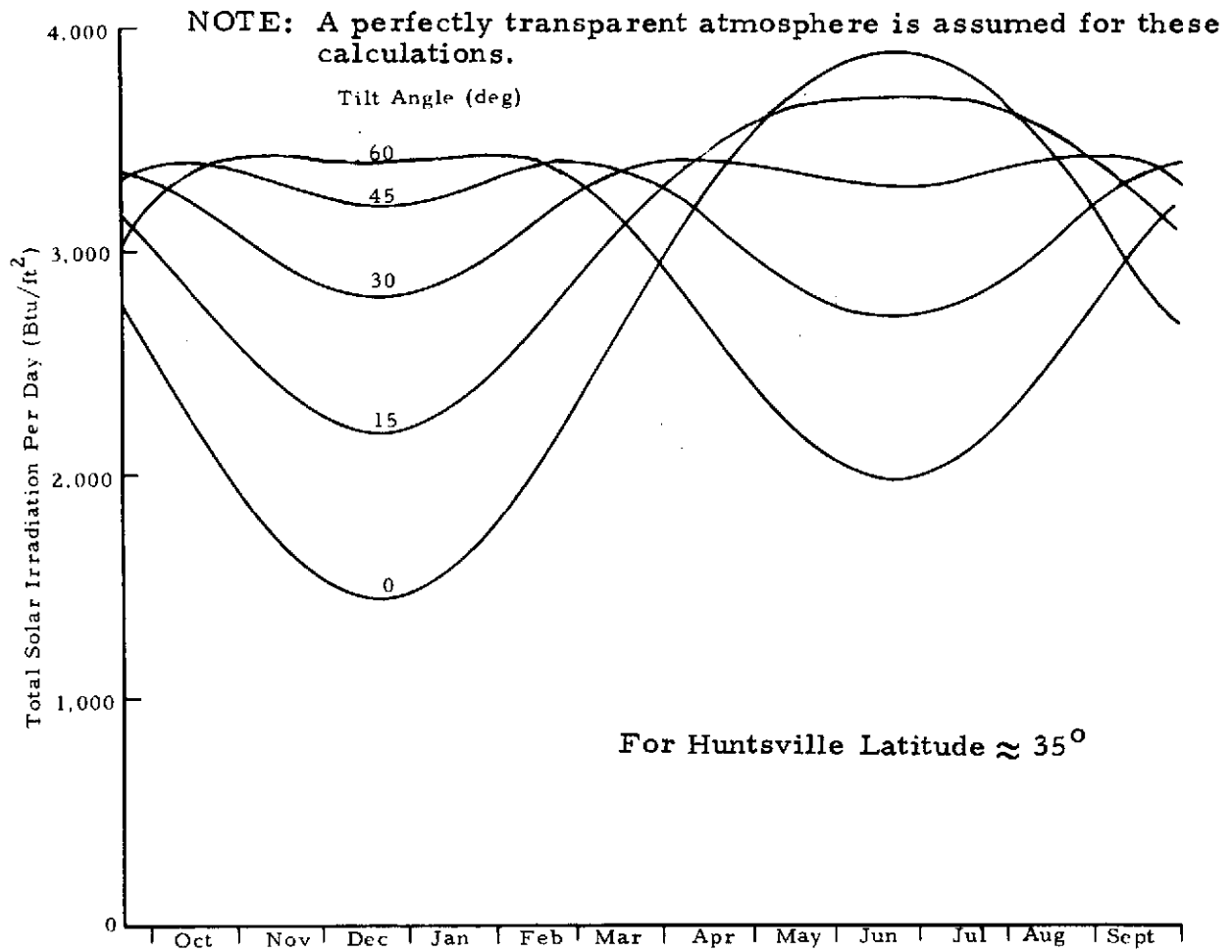


Fig. 23 - Seasonal Variation in Ideal Solar Irradiation for Various Tilt Angles (measured from horizontal)

Section 4 ENERGY STORAGE SYSTEM STUDIES

Storage system studies were concentrated in the three areas discussed below.

4.1 TANK SELECTION

Several potential water storage tanks were available at MSFC as surplus material. These tanks varied in size and condition. The tank in best condition was a 4200 gallon aluminum tank. This tank would correspond to about 34,000 lbm of energy storage mass. Figures 24 through 26 can be used to determine how this tank would work in the total system under consideration*. These figures show the effect of varying maximum temperature (which sets the maximum tank pressure), collector area, and storage tank capacity with regard to auxiliary energy requirements. NASA-MSFC is currently planning to use a collector area of more than 1200 ft². Accordingly, the figures show that the 34,000 lbm tank will result in a reasonably small auxiliary energy requirement for any reasonable maximum temperature. Therefore, this tank was selected as fully adequate for the demonstration program.

4.2 TANK INSULATION SELECTION

Several materials were considered as insulation candidates, but selection was quickly narrowed to a loose fill Fiberglas insulation. The primary criterion

*The data presented in these figures were generated early in the study and do not include the effects of building thermal inertia, a finite allowable temperature band within the building, and other beneficial features included in the later total system performance analyses discussed in Section 5. Also, NASA-MSFC decided after choosing the tank to utilize a single-glazed collector rather than the double-glazed collector used to generate these figures. Therefore, please refer to Section 5 for more accurate total system performance predictions.

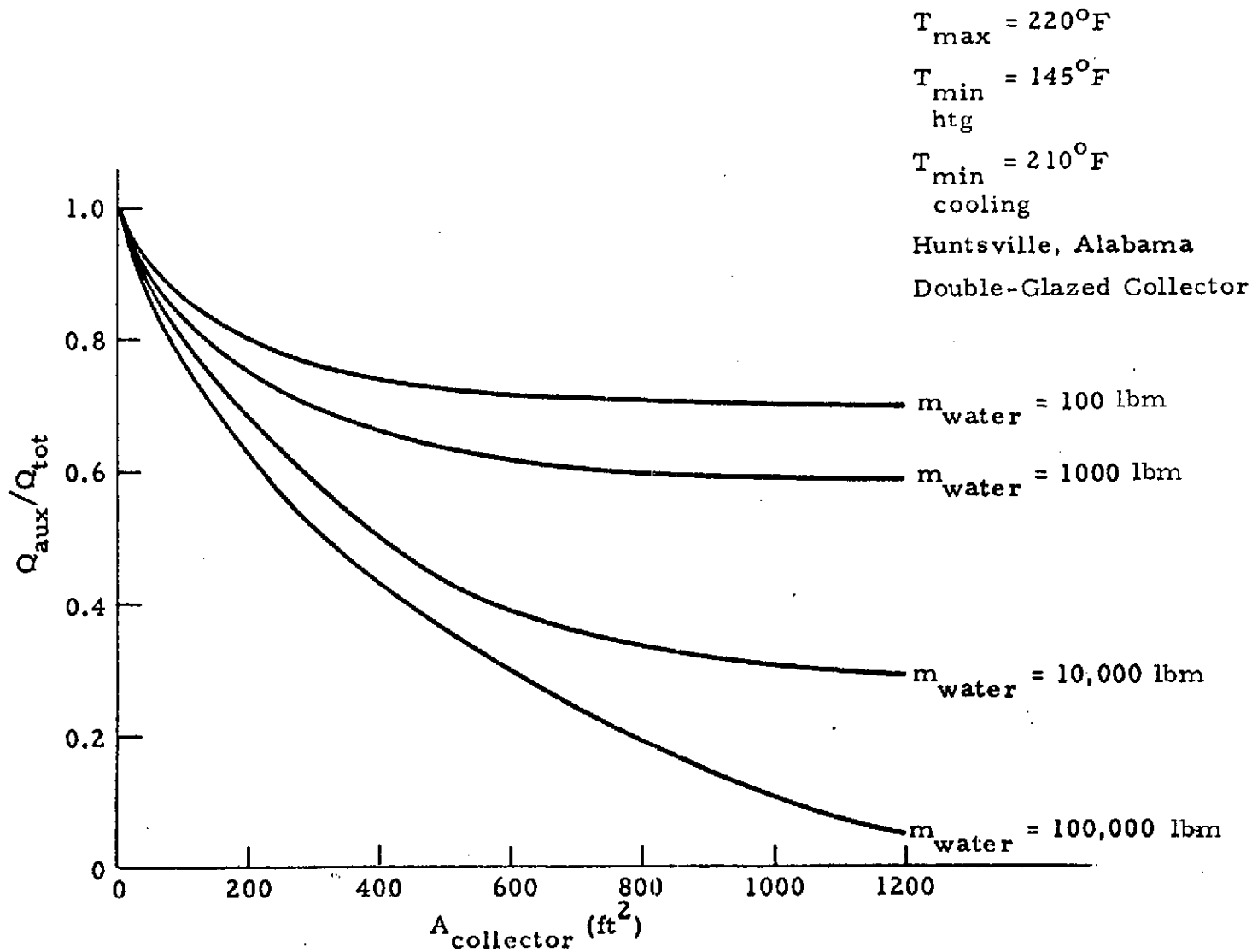


Fig. 24 - Auxiliary Heat Required for Different Collector Areas and Energy Storage System Capacities ($T_{\max} = 220^{\circ}\text{F}$)

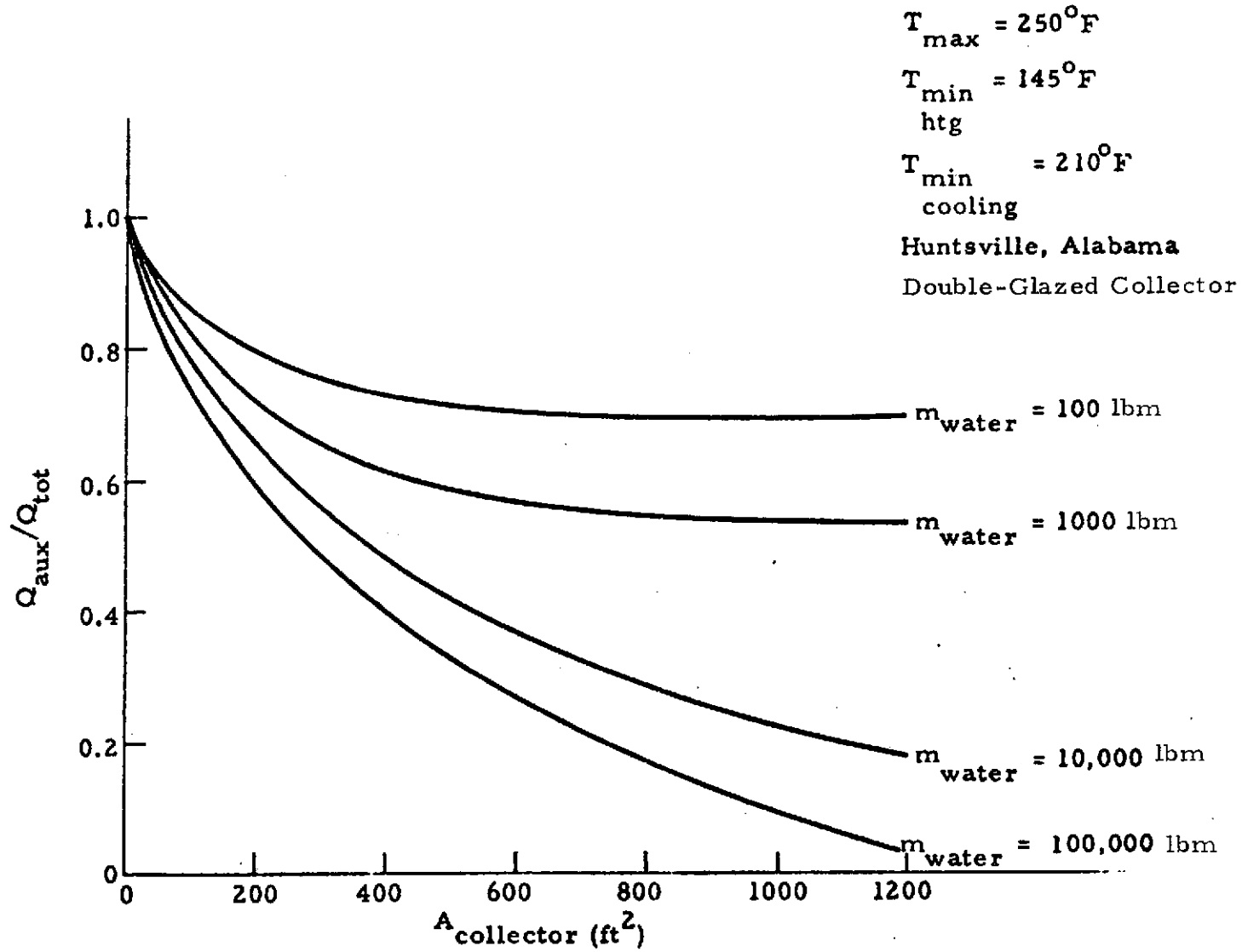


Fig. 25 - Auxiliary Heat Required for Different Collector Areas and Energy Storage System Capacities ($T_{\max} = 250^{\circ}\text{F}$)

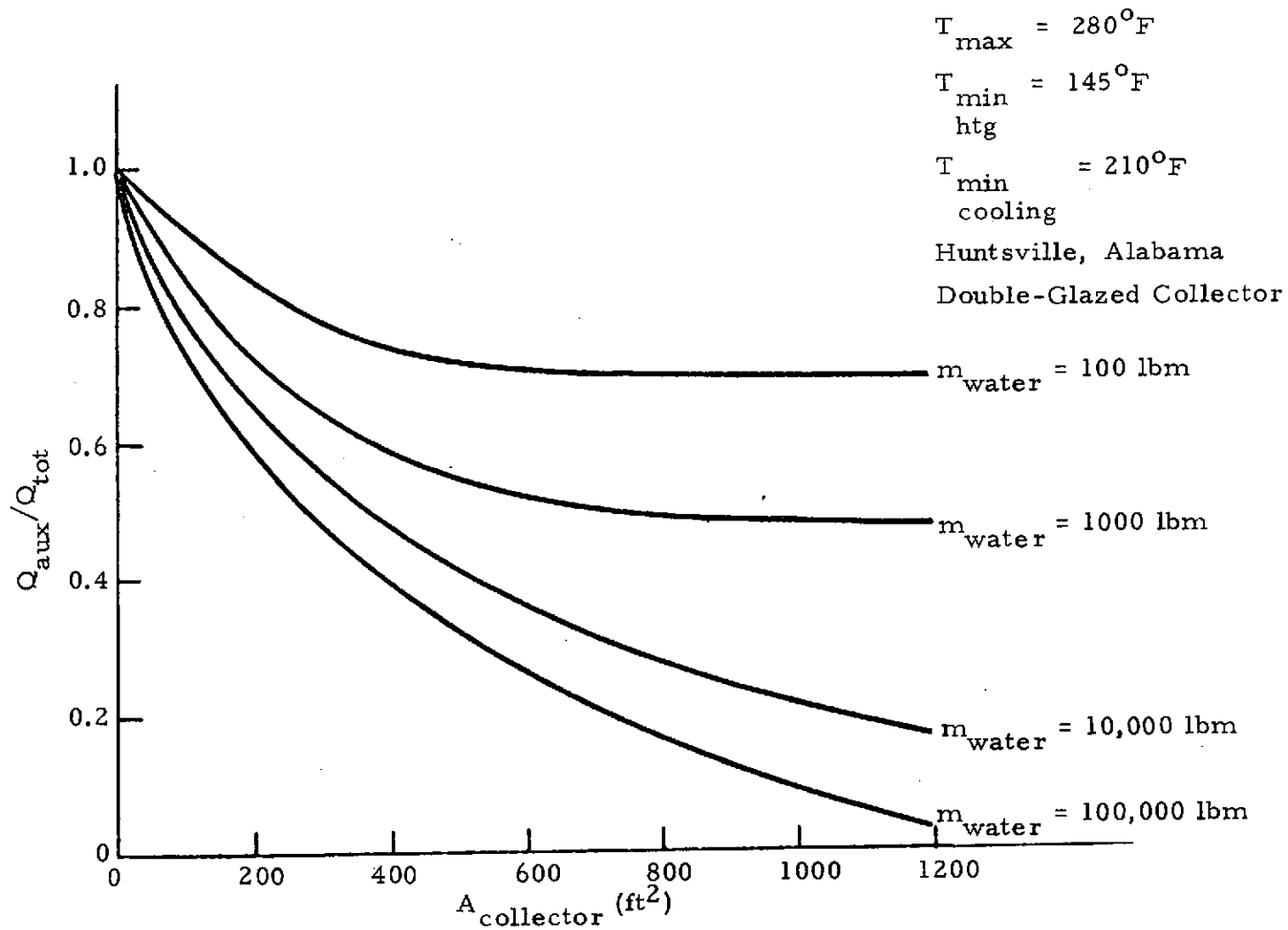


Fig.26 - Auxiliary Heat Required for Different Collector Areas and Energy Storage System Capacities ($T_{\max} = 280^{\circ}\text{F}$)

used in selecting Fiberglas was cost. A properties table (Table 1) was compiled for the selected material. As the table shows, this material is reasonably cheap. It takes about \$450 to fill the box illustrated in Fig.27, even at a density of 3 lb/ft³. No conductivity data could be obtained at a mean temperature of 150°F, but it should be around 0.025 Btu/hr-ft-°F, based upon extrapolation from reported values.

4.3 THERMAL ANALYSIS OF TANK

Thermal analyses were performed on the water storage tank to be used in the solar home prototype heating and cooling system. These studies were used to determine the heat loss from the storage tank as a function of insulation thickness (as shown in Fig.27). The heat loss as a function of insulation thickness is shown in Fig.28. Figure 29 is the heat loss through the support structures and the water supply lines. This heat loss is independent of the insulation thickness.

Table 1
TANK INSULATION

<u>Type:</u> Loose Fill Fiberglas		
<u>Manufacturer:</u> Johns-Manville and Others		
<u>Maximum Service Temperature:</u> > 300°F		
<u>Conductivity:</u>	At 75°F	$\rho \approx .8 \text{ lb/ft}^3$ $K \approx .030 \text{ Btu/hr-ft-}^\circ\text{F}$
		$\rho \approx 3 \text{ lb/ft}^3$ $K \approx .018 \text{ Btu/hr-ft-}^\circ\text{F}$
<u>Cost:</u> \approx \$.14/lb		
	Box Minimum Wall Clearance	Cost*
	1 ft	\$450.
	2	700.
	3	1000.
<u>Recommended:</u>	$\rho \approx 3 \text{ lb/ft}^3$	
	K (estimated) \approx 0.025 Btu/hr-ft-°F	

* At $\rho = 3 \text{ lb/ft}^3$

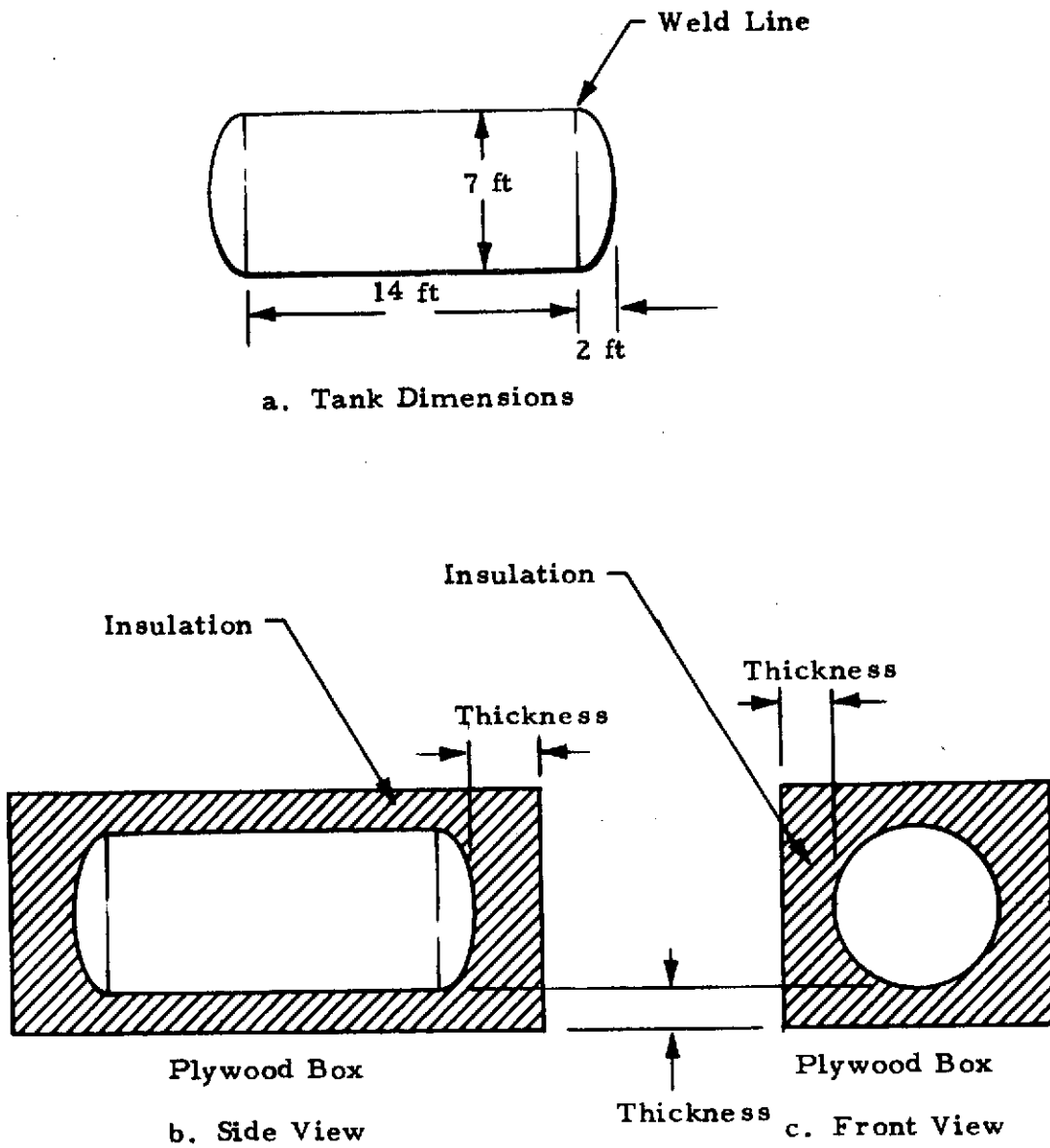


Fig.27 - Energy Storage Tank

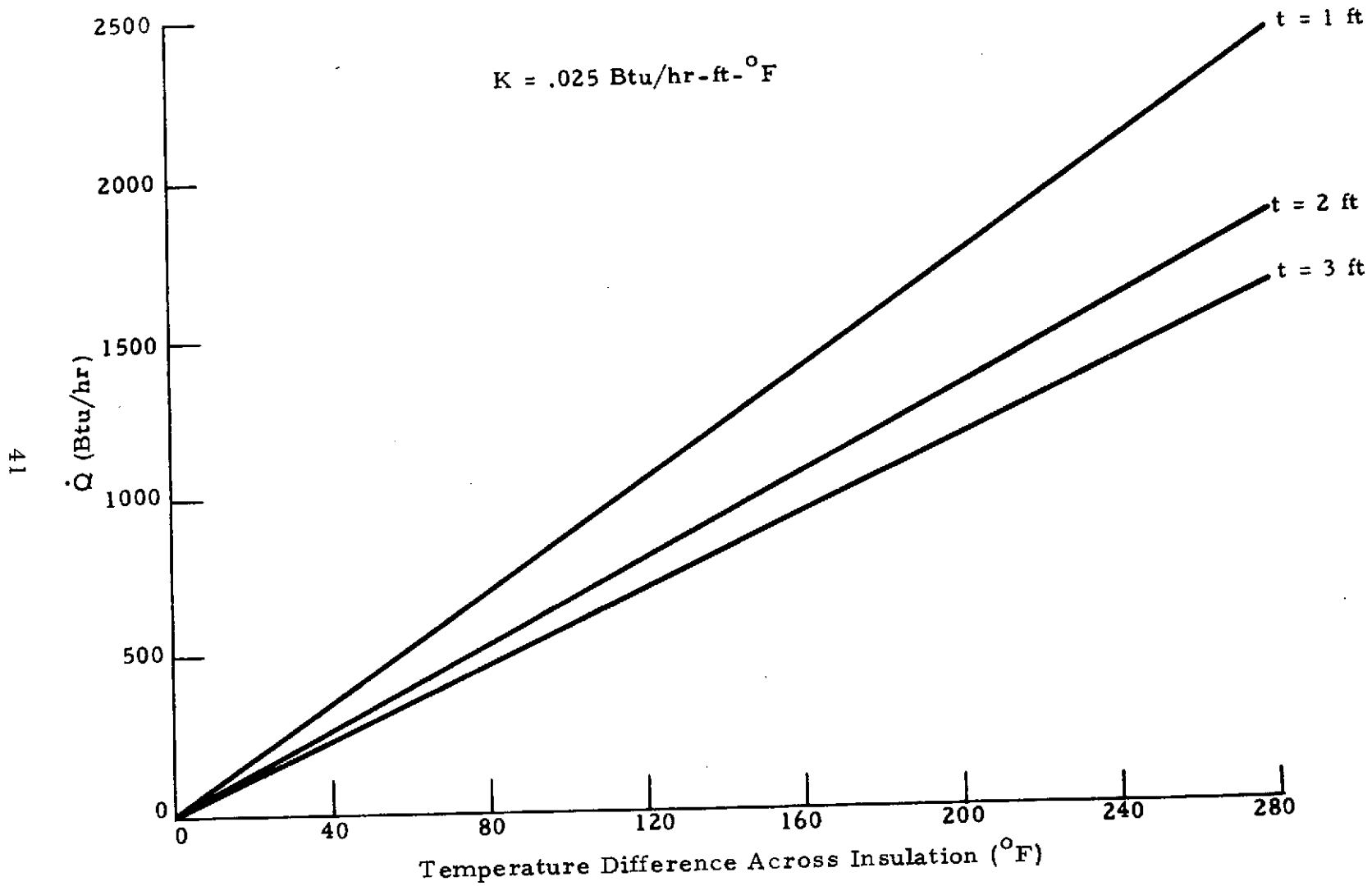


Fig. 28 - Heat Loss Through Tank Insulation

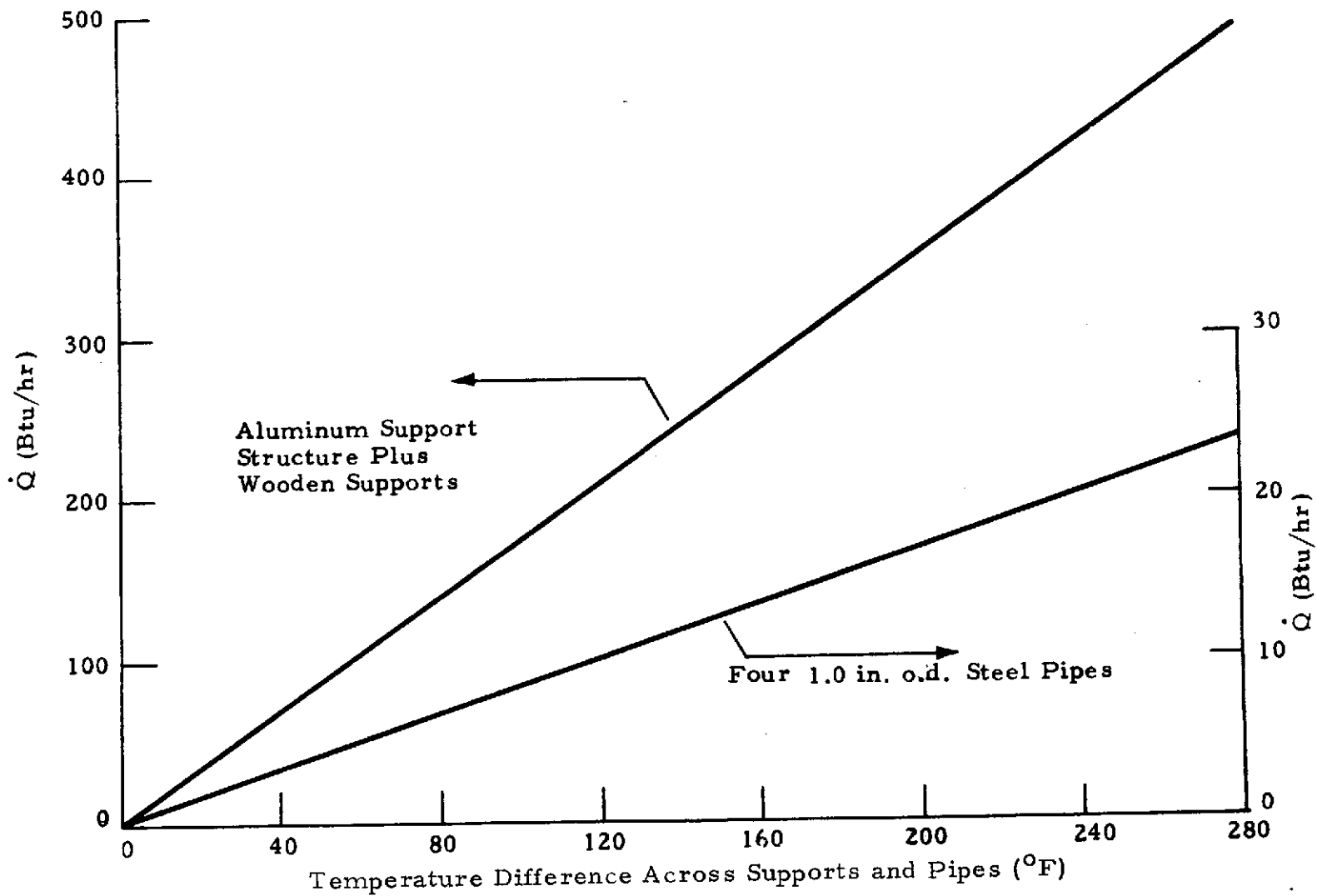


Fig.29 - Heat Loss Through Tank Support Structure and Supply Lines

Section 5

PARAMETRIC TOTAL SYSTEM PERFORMANCE STUDIES

To evaluate the effect of different design options upon the performance of the total solar-powered system, a computer program has been developed and refined over the last two and one-half years to simulate the transient behavior of the system over an entire year. A brief description of modeling techniques and results of simulations are presented in the following paragraphs.

5.1 MODELING TECHNIQUES

Figure 30 shows the basic components which make up the simulation program. The six subsystems which comprise the total system are each separately modeled. Environmental data in the form of time-varying ambient temperature, wind speed, and direct and diffuse solar fluxes are required inputs. These environmental data are required for an entire year to allow transient analysis over the entire year. When time-varying solar data are not available, as is usually the case, techniques for calculating these data from available whole day total insolation values have been developed. The method which is currently used to recorrelate the whole day flux totals into time-varying fluxes is to simply determine the average atmospheric attenuation of the solar constant for each day, and apply this attenuation factor to the solar constant throughout the day while conducting the system analysis. Thus the solar flux intensity is held constant through the day, while the relative position of the sun to the collector (the incidence angle) is calculated instantaneously throughout the day, based upon input values of latitude and collector tilt angle.

A control system logic routine allows for choices in such parameters as thermostat settings, energy exchanges between components, flow rates, switches, etc.

The six subsystem models used in the computer program to simulate the MSFC solar-powered facility are described below. These models pertain

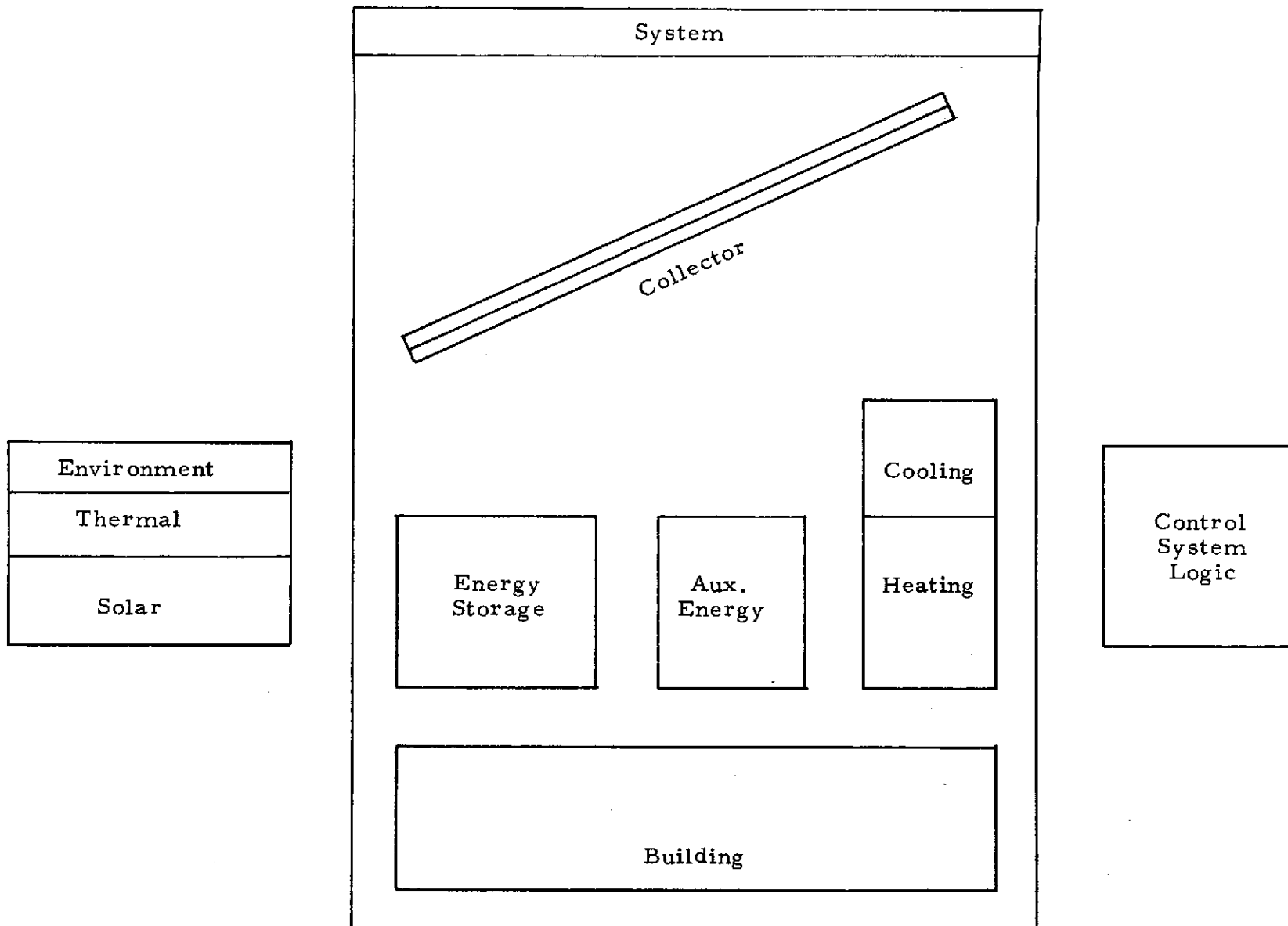


Fig. 30 - Basic Components of the Simulation Program

only to the residential solar-powered system being developed at MSFC. Other systems for other buildings in other regions would require different models, although the same simulation approach should prove valuable for analyzing these other systems.

The six subsystem models are very simple, with the exception of the solar collector model, which is a sophisticated mathematical model that allows accurate determination of the transient thermal performance of the collector. Each of the six models is discussed below.

● Building Model

The building is treated as a fixed thermal capacitance connected to the outside environment through a variable thermal resistance. The capacitance is assumed to be 10,000 Btu/°F. This capacitance value represents the effective thermal inertia (mass times specific heat) of the building and its contents, which serve to dampen the effect of external temperature variations on the inside air temperature. The resistance value is different for hot weather than for cold weather. When the ambient temperature is above 70°F, the resistance value is set at 0.0007°F-hr/Btu, which corresponds to a 3-ton (36,000 Btu/hr) cooling load at 95°F ambient temperature. When the ambient temperature is below 70°F, the resistance value is set at 0.00117°F-hr/Btu, which corresponds to a 60,000 Btu/hr heating load at 0°F ambient temperature. The reduced resistance value for cooling is used to include latent loads which are important during the cooling season. These resistance values were based upon MSFC load calculations, and represent the overall heat transfer path between the inside air and the outside air.

● Energy Storage Model

The energy storage system is treated as a fixed thermal capacitance for the MSFC simulations. The capacitance value is an input quantity which represents the mass times specific heat product of the water in the energy storage tank. The storage system heat losses are treated as a fixed thermal resistance, and heat flows through this resistance to the outside environment. A maximum temperature is also a required input.

- Auxiliary Energy Model

The auxiliary energy system is a zero capacitance thermal energy source. Several options are available concerning the control of the auxiliary energy system, including whether the heat is added to storage or used directly to power the heating, cooling, and water heating components. The output heating rate of the auxiliary heater is 60,000 Btu/hr for heating and 55,000 Btu/hr for cooling.

- Heating Model

The space heating model is a zero capacitance input/output unit which utilizes heat from either the collector, energy storage, or the auxiliary energy system, depending on control logic selection and instantaneous conditions. The efficiency of the unit is an input variable, being defined as heat output divided by heat input. The heating rate output as a function of water temperature and air temperature as these fluids enter the heat exchanger is also input to simulate the actual heat exchanger performance.

- Cooling Model

The space cooling model is a zero capacitance heat-driven air-conditioner, with its performance defined by an input coefficient of performance (0.65). This input/output unit may be driven with heat from either the collector, storage or auxiliary, depending on prevailing conditions and control logic selection. The cooling rate is considered constant at 36,000 Btu/hr.

- Solar Collector Model

The solar collector model is a flexible energy transfer model which allows considerable variation in collector design. Input design variables include collector area, tilt angle, number of transparent covers, characteristic dimensions and spacings, and thermophysical properties of absorber plate, transparent covers, and backside insulation. Water is assumed as the energy transport fluid and its flow rate is an input parameter. The thermal capacitances of the plate, covers, insulation, and water are all used in the transient numerical treatment of the collector. Further details of the solar collector model are presented in the Appendix. The accuracy of the collector model is well verified by test data, as discussed in Section 3.

(At NASA-MSFC's request, water heating for domestic usage was left out of the MSFC simulation program, although it can be and has been included in other Lockheed studies.)

5.2 SIMULATION RESULTS

The computer program takes the inputs and models described above and conducts a transient energy transfer analysis through the year, obtaining all pertinent energy flows including energy used for heating and cooling, energy collected, auxiliary energy used, and energy wasted for lack of storage capacity. Daily totals and cumulative totals throughout the year are determined for all of these energy flows.

This simulation computer program has been widely used to compare different system designs. The major parameter of comparison has been taken as the dimensionless ratio, Q_{aux}/Q_{tot} , which represents the fraction of the total energy requirements for heating and cooling which must be met with conventional, auxiliary energy. Obviously, the smaller this value, the better the system performance.

One comparison is presented in Fig. 31. This comparison is between two collector designs and two tank sizes, all as a function of collector area. The benefits of using two Tedlar covers and large storage are apparent.

The effect of tilting the collector was investigated to some extent as shown in Fig. 32. The roof was assumed to be tilted 60 degrees from the horizontal during the winter and 30 degrees during the remainder of the year. This results in a significant savings in collector area but adds to the initial cost due to having a pivot mechanism. Another point made by this figure is that the fixed-tilt-angle collector at 45 degrees with respect to the horizontal performs almost as well as the more complicated double-tilt-angle system, again verifying this selected tilt angle as a good choice for whole-year operation (as previously discussed in Section 3).

The radiation properties of the selective coating and the transparent covers are extremely important to the overall performance of the solar-powered

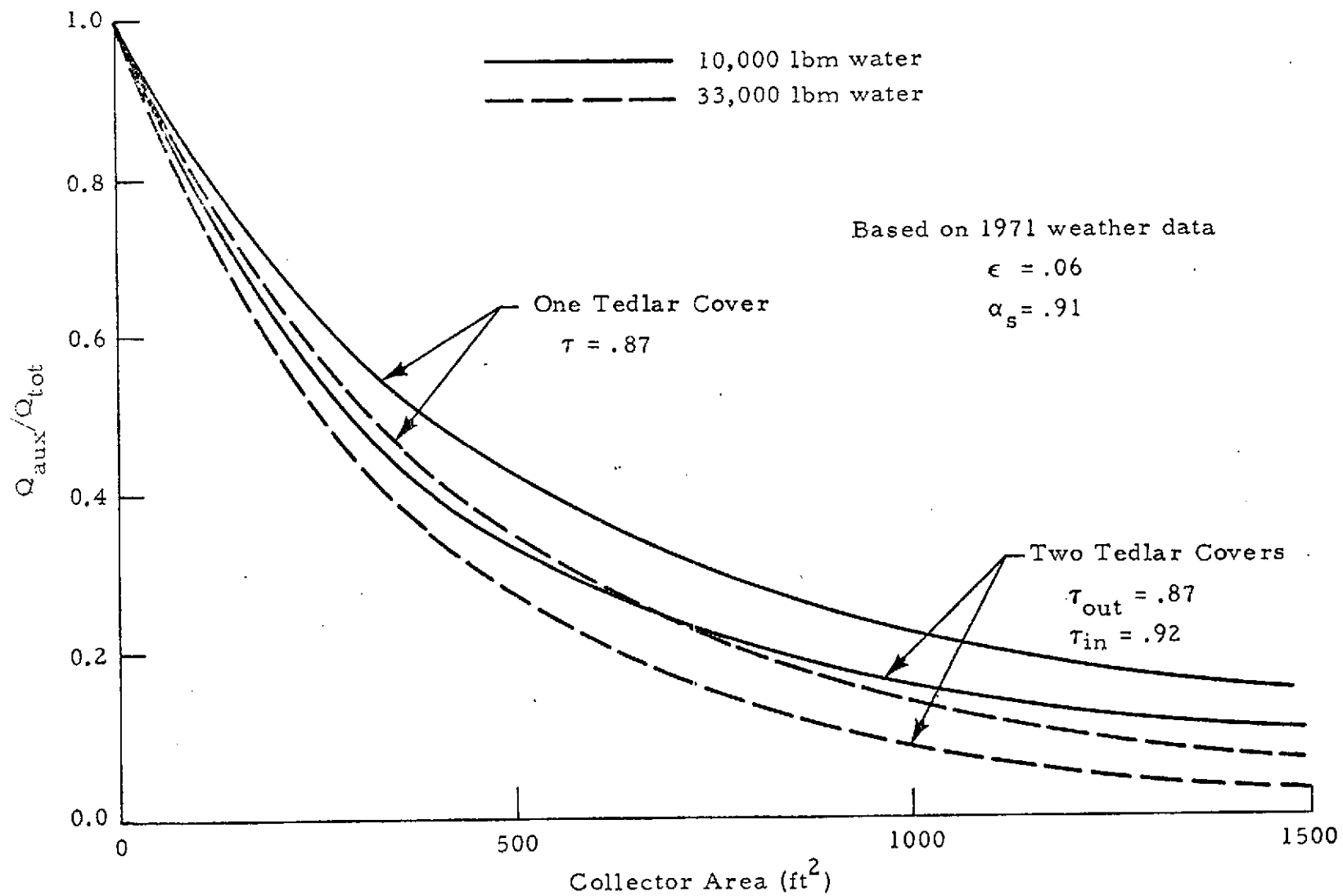


Fig. 31 - Effect of Cover Design on System Performance

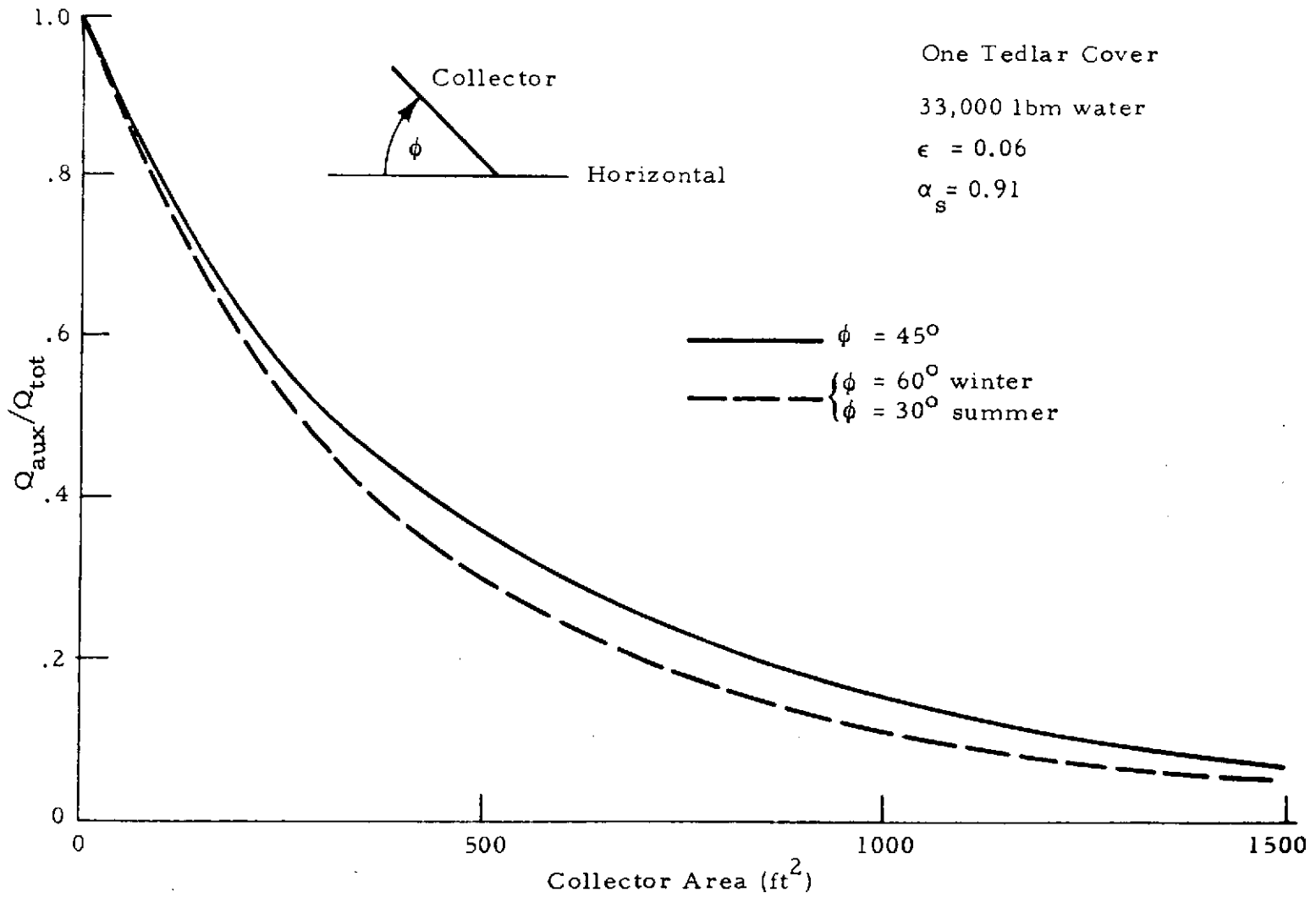


Fig. 32 - Effect of Tilting Collector Twice a Year on Heating/Cooling Performance

system. The transmittance of the Tedlar film currently being manufactured and its possible degradation with age have not been clearly defined. Also, the changes in solar absorptance and infrared emittance of the selective coating with age are currently unknown. Therefore, a sensitivity study was conducted to determine the effect of property degradation on overall performance. The results are presented in Fig. 33 for undegraded (good) and degraded properties. The degraded property values were set at levels which might be reached if degradation were to occur.

Figure 34 presents the results of a study to determine the effect of the number of transparent covers on early summer operation. The curves show the auxiliary energy requirements for the two-month period as a function of collector area for one and two Tedlar covers. Clearly, the performance of the two-cover system is superior to the performance of the one-cover system. For example, the auxiliary energy required for the one-cover system with an area of 1500 ft^2 is identical to that required for the two-cover system with an area of 950 ft^2 .

Figure 35 presents the results of a study to determine the effect of maximum tank operating pressure on early summer operation. The maximum pressure corresponds to the water vapor pressure plus 15 psi to allow for the 30-foot rise in elevation from the tank to the collector, plus another ΔP to allow 20°F temperature rise through the collector without boiling. The maximum temperatures corresponding to the pressures are shown below the pressure axis. The curve shows the auxiliary energy required for June and July operation. For the large tank under consideration, the improvement in performance with increasing pressure reaches the point of diminishing returns at about 45 psia. For a smaller tank, the curve would probably flatten out at a somewhat higher pressure.

The results of a study to determine the effect of effective transmittance of the Tedlar covers on system performance are presented in Figs. 36 and 37. The curves show the degradation of performance with decreasing transmittance for both good selective coating properties (solid curves) and for degraded selective coating properties (dashed curves). Again, the superiority of the two cover system is clearly demonstrated.

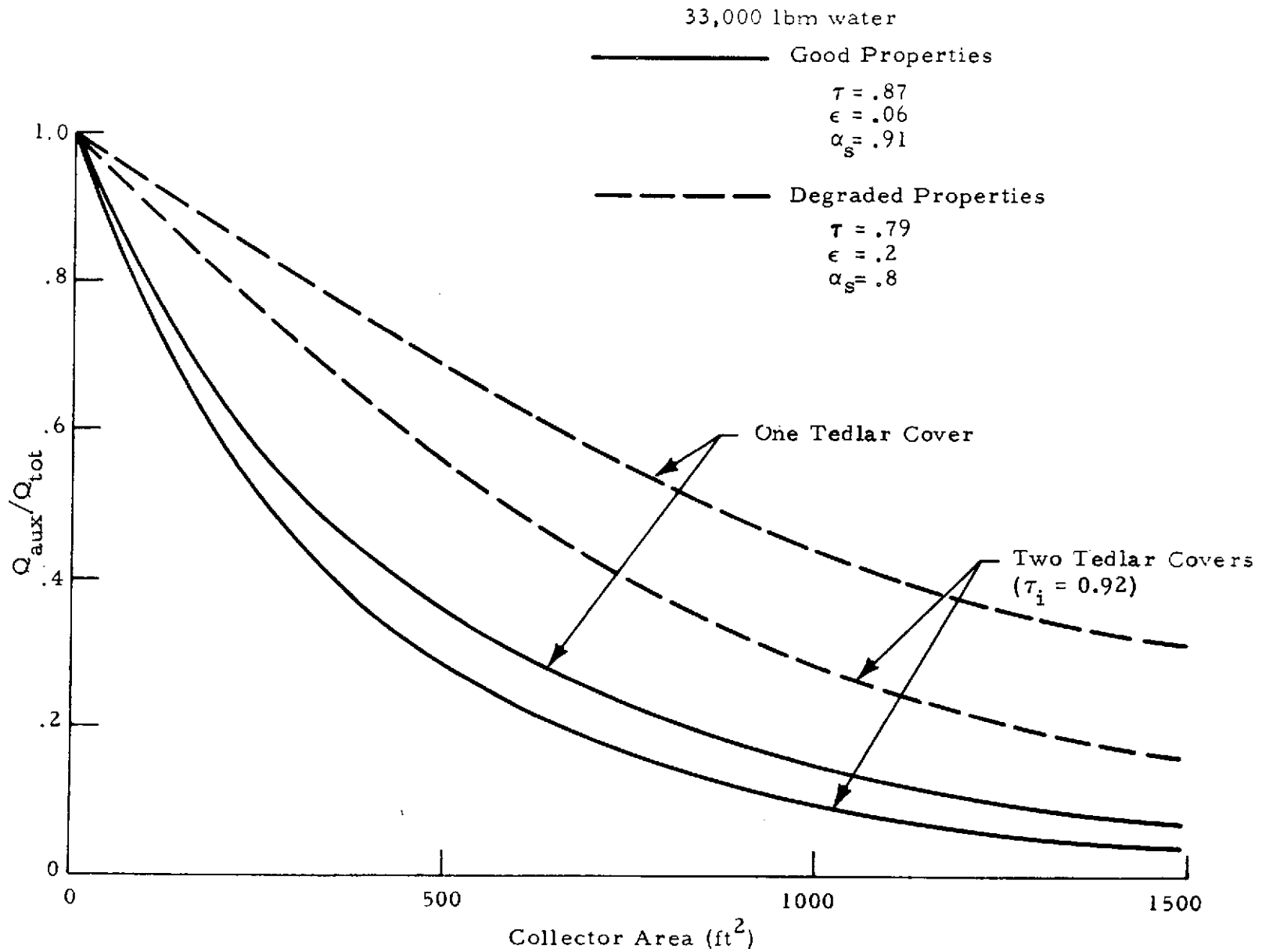


Fig. 33 - Effect of Degraded Properties on System Performance

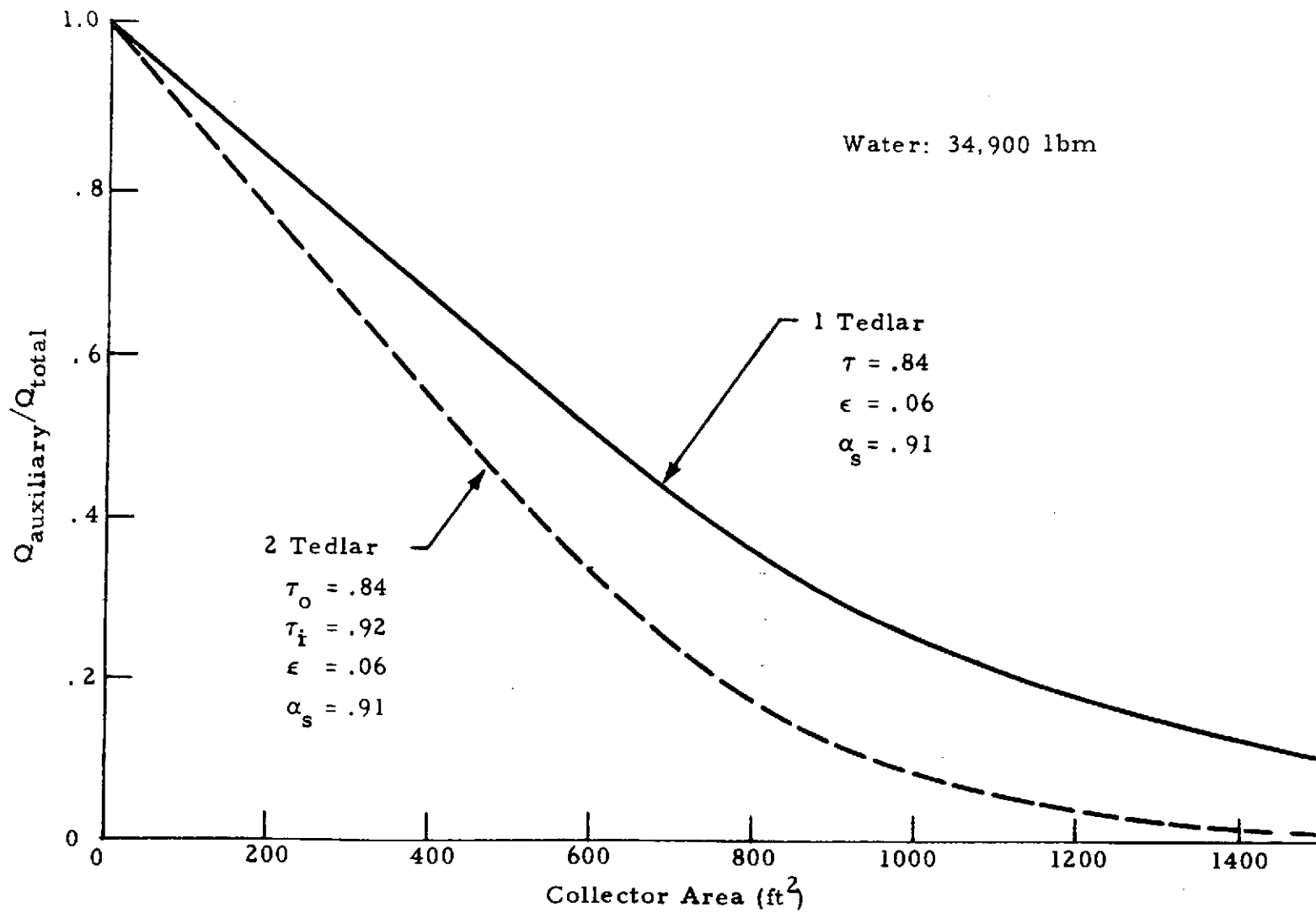


Fig. 34 - Effect of Collector Covers on System Performance for June and July Operation Only

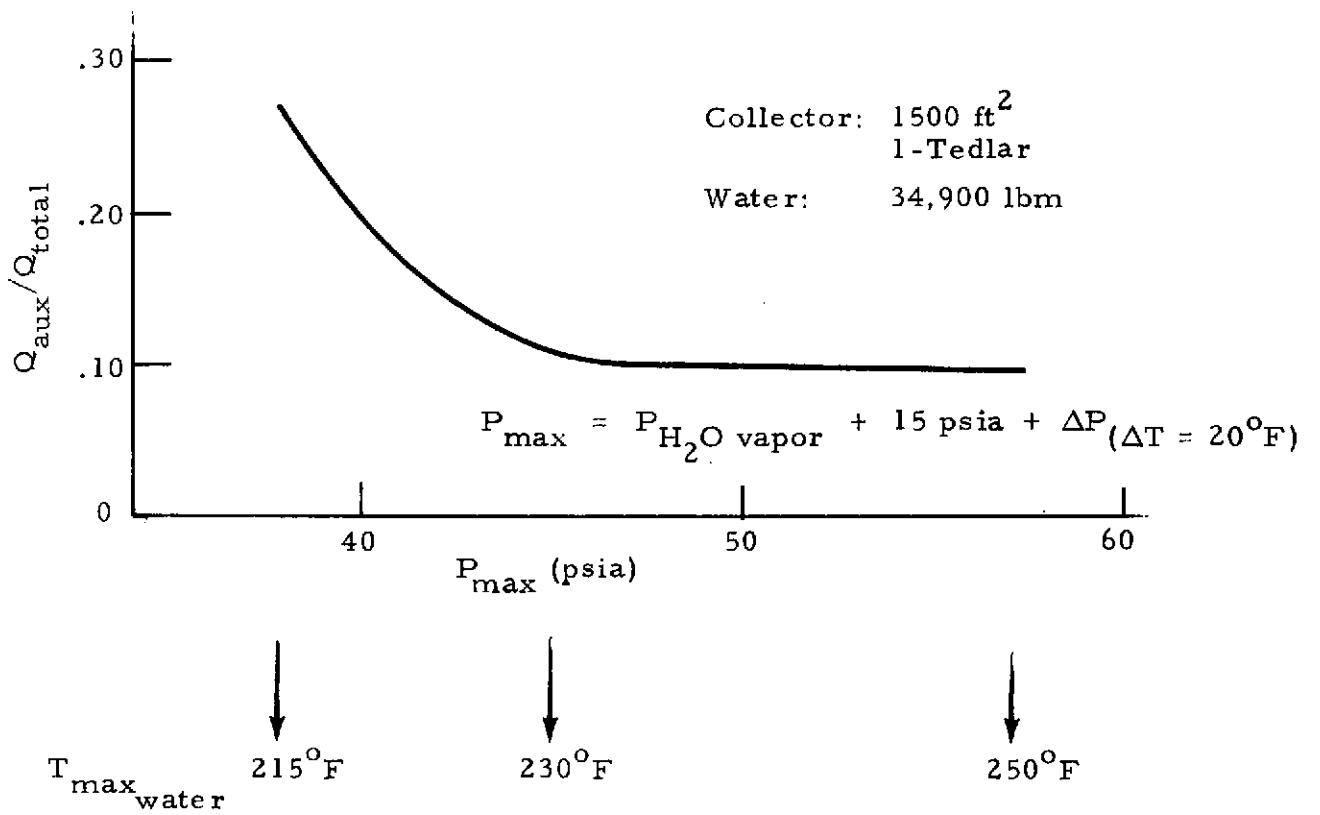


Fig. 35 - Effect of Maximum Tank Operating Pressure on System Performance for June and July Operation Only

- $m_{\text{water}} = 33,000 \text{ lb}_m$
- $A_{\text{collector}} = 1500 \text{ ft}^2$
- 1 Tedlar Cover

- ————— $\epsilon = 0.06, \alpha_s = 0.91$
- - - - - - $\epsilon = 0.10, \alpha_s = 0.75$

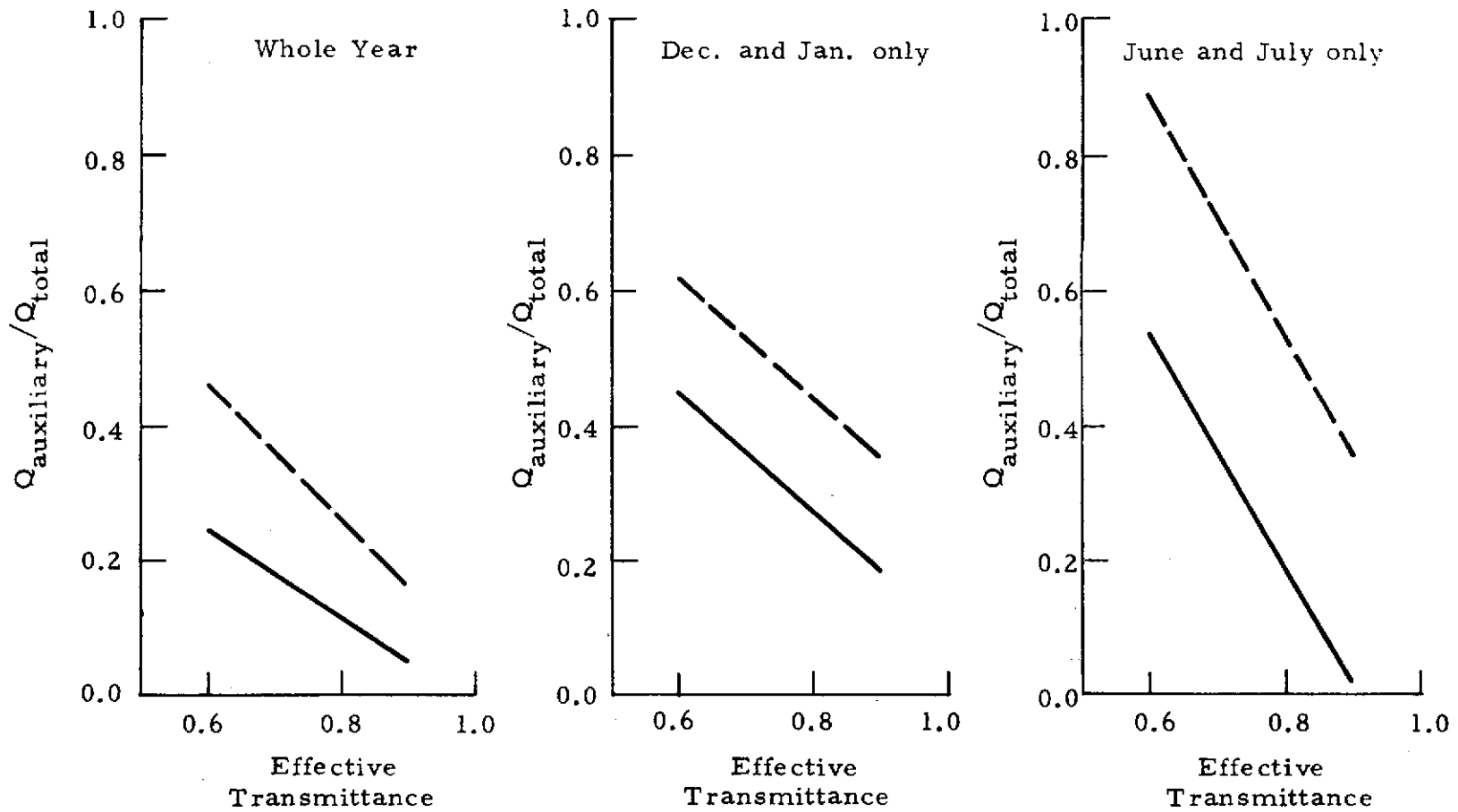


Fig. 36 - Effect of Tedlar Transmittance on System Performance for One-Tedlar Cover Collector

- $m_{\text{water}} = 33,000 \text{ lb}_m$
 - $A_{\text{collector}} = 1500 \text{ ft}^2$
 - 2 Tedlar Covers ($\tau_{\text{inner}} = 0.92$)
- ————— $\epsilon = 0.06, \alpha_s = 0.91$
 - - - - - - $\epsilon = 0.10, \alpha_s = 0.75$

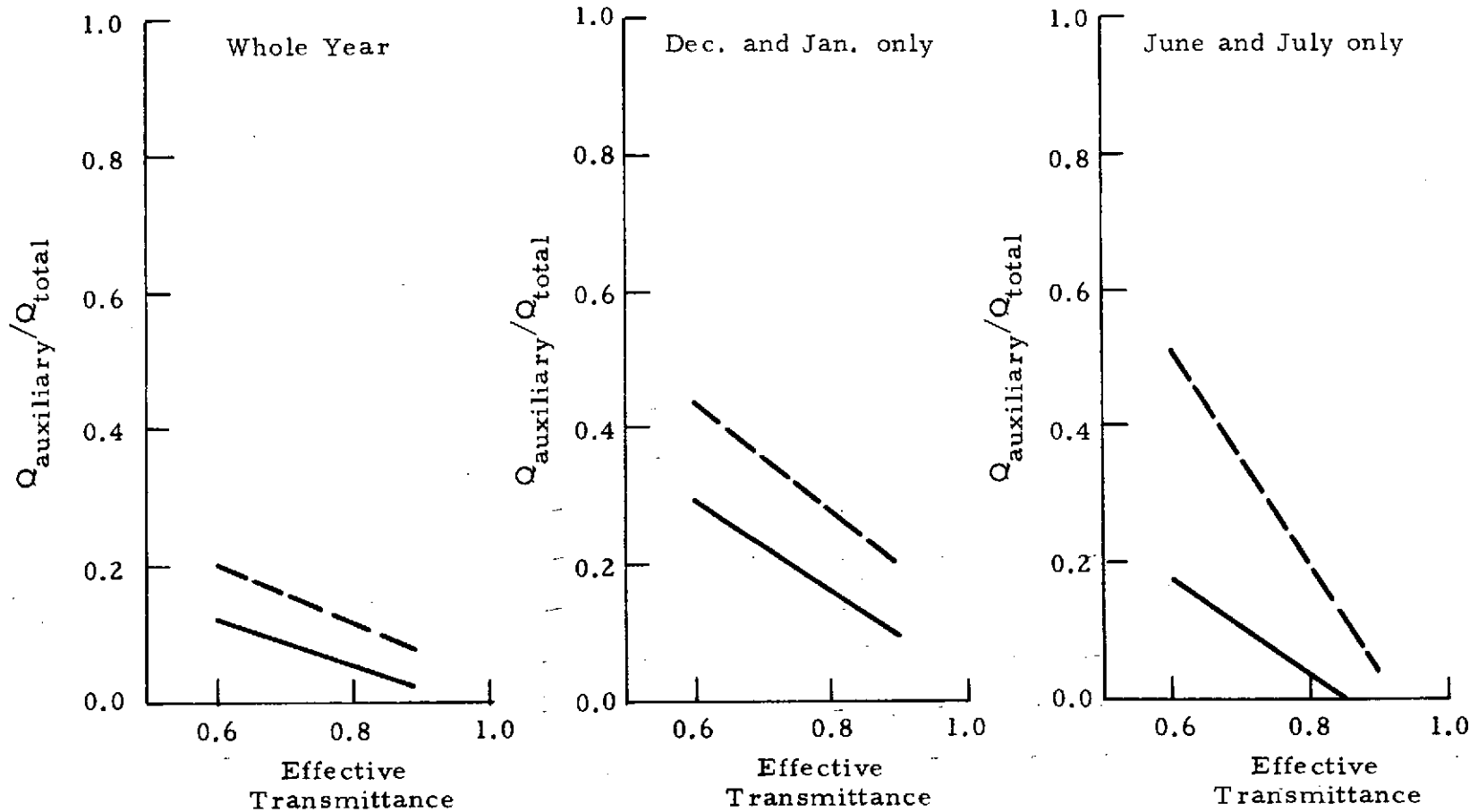


Fig. 37 - Effect of Tedlar Transmittance on System Performance for Two-Tedlar Cover Collector

For rapid calculations without having to run the computer program, a differential approximation of system performance sensitivity to small changes in radiation properties and area of the solar collector was developed. The basic sensitivity correlation was developed as shown below.

$$\text{Let } \sigma = \left(\frac{Q_{\text{auxiliary}}}{Q_{\text{total}}} \right) \text{ June + July}$$

Then:

$$d\sigma = \left(\frac{\partial \sigma}{\partial \alpha_s} \right) d\alpha_s + \left(\frac{\partial \sigma}{\partial \epsilon} \right) d\epsilon + \left(\frac{\partial \sigma}{\partial \tau} \right) d\tau + \left(\frac{\partial \sigma}{\partial A} \right) dA,$$

where α_s = solar absorptance of plate
 ϵ = infrared emittance of plate
 τ = effective transmittance of Tedlar
 A = collector area (ft²).

Then:

$$\sigma = \sigma_{\text{nominal}} + d\sigma.$$

The nominal values of the variables were:

$$\begin{aligned} \alpha_s &= 0.91 \\ \epsilon &= 0.06 \\ \tau &= 0.84 \\ A &= 1500 \text{ ft}^2 \end{aligned}$$

The computer simulation program was used to evaluate the partial derivatives at the nominal point for both one-Tedlar and two-Tedlar collector designs. The resulting correlations are given below.

$$\sigma_{1 \text{ cover}} = 0.0954 - 1.81 d\alpha_s + 1.92 d\epsilon - 1.74 d\tau - \frac{0.00031}{\text{ft}^2} dA$$

$$\sigma_{2 \text{ cover}} = 0.00392 - 0.786 d\alpha_s + 0.431 d\epsilon - 0.724 d\tau - \frac{0.000147}{\text{ft}^2} dA.$$

Care must be taken with the signs of the small changes in α_s , ϵ , τ and A . Positive changes indicate increases above nominal values and negative signs indicate decreases below nominal values. Spot checks indicate that the correlations are surprisingly accurate for small changes in the variables.

Section 6

PRESSURE DISTRIBUTION STUDIES

Various pressure distribution studies were conducted to determine maximum tank pressure requirements, line sizes and pump requirements.

6.1 STORAGE TANK PRESSURE

For summer heat storage the water must, in general, be above 210°F to be useful. This limits the sensible heat storage to the range from 210°F to some upper limit determined by how much pressure is allowed in the system. If the temperature in the tank is desired to be 250°F and the temperature rise in the collector is 20°F, then the maximum temperature of the system will be 270°F at the top of the collector. The minimum pressure in the system will also be at the top of the collector, so to prevent boiling in the collector the pressure in the fluid must be above the vapor pressure of water at 270°F (about 45 psia). The column of water from the top of the collector to the tank will account for about 15 psi so the pressure in the tank must be about 45 psig to allow use of the 250°F water.

6.2 SUPPLY LINES

There will be about 100 feet of supply lines to the collector from the tank. A 1-inch i.d. water pipe would seem adequate for the purpose, but pressure drops (Fig. 38) in the supply lines alone would require a 1.2 hp pump (at 30% efficiency) which is obviously too high. A 2-inch pipe was chosen because it was easily obtainable, cheap, and required only about 0.075 hp to maintain flow through the supply lines.

6.3 COLLECTOR ROOF MANIFOLDS

For ease of installation and to reduce insulation problems it was decided to use 2-inch i.d. pipe for the manifolds at the top and bottom of the roof with

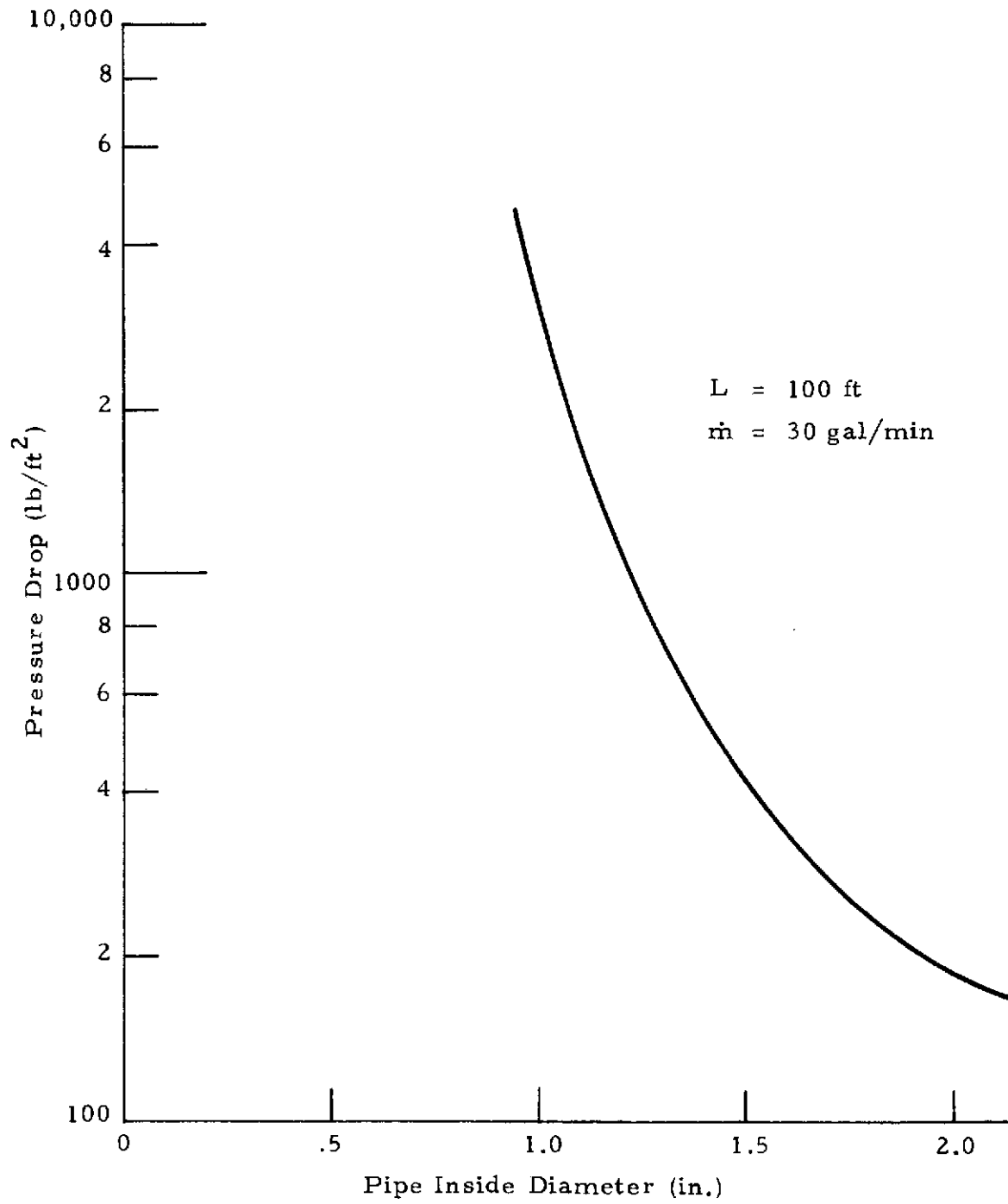
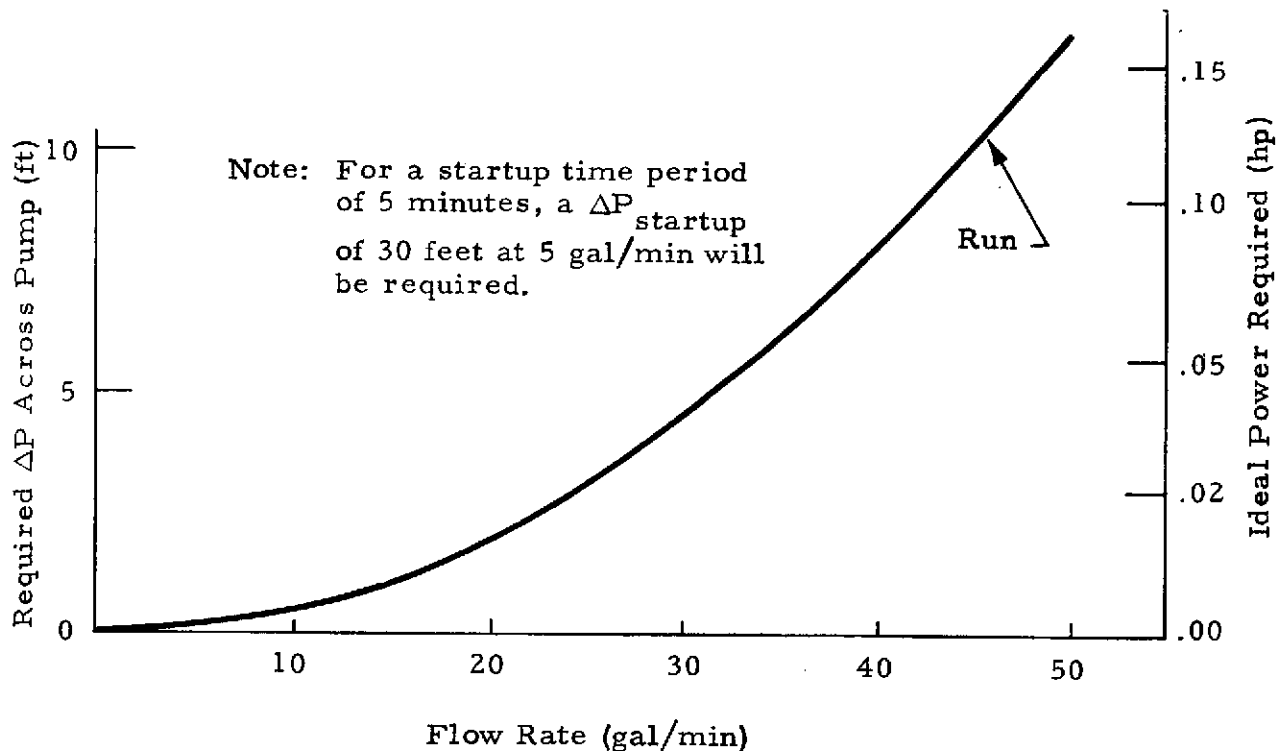


Fig. 38 - Pressure Drop in Supply Lines for Various Pipe Diameters

the supply line entering the middle. The use of this small diameter pipe will cause significant flow rate variation in the panels unless valves are installed on each column of panels to balance the flow. This procedure for balancing the flow causes about a 10% increase in the total pressure drop (not to mention the cost of the valves) and would not be desirable in a commercial application. However, in the MSFC prototype system, such valves were installed since this system is not intended to be an optimized system.

6.4 MAIN PUMP REQUIREMENT

The main collector pump requirements for the system are shown in the sketch below. Only pressure drops through 100 feet of lines and through the panels were treated. A perfect siphon effect was assumed for the return lines. Water properties were evaluated at 200°F.



Pumps available on the market are in general designed for much higher pressures than needed at the 30 gal/min flow rate. This will cause the system to either stabilize at a much higher flow rate or require a valve to artificially reduce the pressure. Both of these fixes would cause unnecessary waste of electrical energy in commercial use, but for the test house a certain amount of excess power in the pump is desirable so that some flow rate variation can be performed, time permitting. The ideal pump requirements are about 0.05 hp but, using 30% efficiency for the pump, the power requirement would be 1/6 hp or about half that available in the pump that will be used. Thermal insulation of the pump requires a wide coupled pump to prevent the motor from getting too hot.

Section 7

A NEW APPROACH TO COMPARING THE ECONOMICS
OF SOLAR-POWERED VERSUS CONVENTIONAL
HEATING AND COOLING

There are many ways of comparing the economics of solar-powered versus conventional heating and cooling. One method (suggested by Peter McCrary of AVCO in Everett, Massachusetts, in telephone conversations during July 1973) presents a positive case for solar energy in a very tangible way for the average person. This method involves comparing a total monthly payment for the solar-powered system to that for a conventional system where this monthly payment includes the regular home loan payment, the monthly taxes and insurance on the home, and the monthly payment for water heating, space heating and air conditioning. A realistic example of this method is presented in the following paragraphs.

Lockheed-Huntsville's studies have indicated that a typical 2000 ft² home in the Huntsville area can be equipped with an 800 ft² solar collector (with double glazing and selective coating) and a 1000 gallon storage tank (like those widely used for propane storage) to provide 80% of the residence's requirements for space heating, water heating and air conditioning with solar energy, while the remaining 20% is met with auxiliary conventional energy. While this system is not necessarily the optimum, a comparison of this solar-powered system with a conventional system leads to interesting results. Table 2 presents some reasonable cost estimates for the two systems. The basic house cost is \$30,000 in both cases. The conventional heating and cooling equipment is estimated to cost \$1500; this includes space heating equipment, air conditioning equipment, and a hot water heater. The solar heating and cooling equipment is estimated to cost \$5000, under mass production conditions. This figure was obtained from the following reasoning.

Table 2
 COST COMPARISON FOR CONVENTIONAL VERSUS
 SOLAR-POWERED HEATING AND COOLING

Consideration	Conventional (dollars)	Solar-Powered (dollars)
Basic House	30,000	30,000
Heating/Cooling System	<u>1,500</u>	<u>5,000****</u>
Total Investment	31,500	35,000
Monthly Loan Payment	244*	271*
Monthly Tax and Insurance	43**	48**
Monthly Heating/Cooling	<u>30***</u>	<u>6***</u>
Total Monthly Payment at the Beginning of Repayment Period	317	325

* At 8.5% interest over 30 year repayment period.

** At Huntsville rates.

*** Estimated for current utility rates in Huntsville.

**** Rough estimate of solar-powered system cost under future mass-production conditions. Prototype systems will cost orders of magnitude more.

- **Solar Collector:** If this component is integrated into the roof, its net cost over and above that for a conventional roof could be about \$2.50 per square foot if mass production techniques are used in its manufacture. Materials would require about \$1.50 per square foot, including 50 cents for two transparent covers, 70 cents for the Roll-Bond plate, 20 cents for insulation, and 10 cents for the selective coating. The other \$1.00 would cover costs for distribution, on-site fabrication, and profits. Thus, for 800 ft², a cost of \$2000 seems reasonable.
- **Storage Tank:** Current 1000 gallon propane vessels cost about \$500. Thus, for an insulated, installed tank, a cost of \$800 seems reasonable.
- **Heating and Cooling Output Units:** These include the heat exchangers for water heating and space heating, the absorption cycle air conditioner, and their associated pumps and controls. Estimated price: \$1500.
- **Auxiliary Furnace:** \$300.
- **Assorted Pumps, Plumbing and Controls:** \$400.

The total capital investment for the conventional home is thus \$31,500, while for the solar home it is \$35,000. With an 8.5%, 30-year homeowner's loan, the monthly loan payments would be \$244 and \$271, as shown in Table 2. At Huntsville rates, taxes and insurance on a monthly basis would be \$43 and \$48 for the two homes. The total cost for conventional space heating, water heating, and air conditioning is estimated to be \$30 per month at current utility rates when averaged over the whole year. For the solar-powered system, 80% of these requirements will be met with solar energy and only \$6 per month will be required for auxiliary energy. Now, as shown in Table 2, the total monthly payments for the conventional and solar-powered homes are \$317 and \$325, respectively, when the heating and cooling costs are included with the loan payment, taxes and insurance. Thus, the conventional system costs the homeowner \$8 less per month at current utility rates. However, these rates have been skyrocketing in recent years and all indications are that this trend will continue in the future. Therefore, consider Fig. 39. This figure shows a comparison of the systems in future years, reflecting the increases in the cost of energy which are anticipated. In recent years in the Tennessee Valley Authority region, rates have been increasing at about 10% per year. Therefore, a yearly

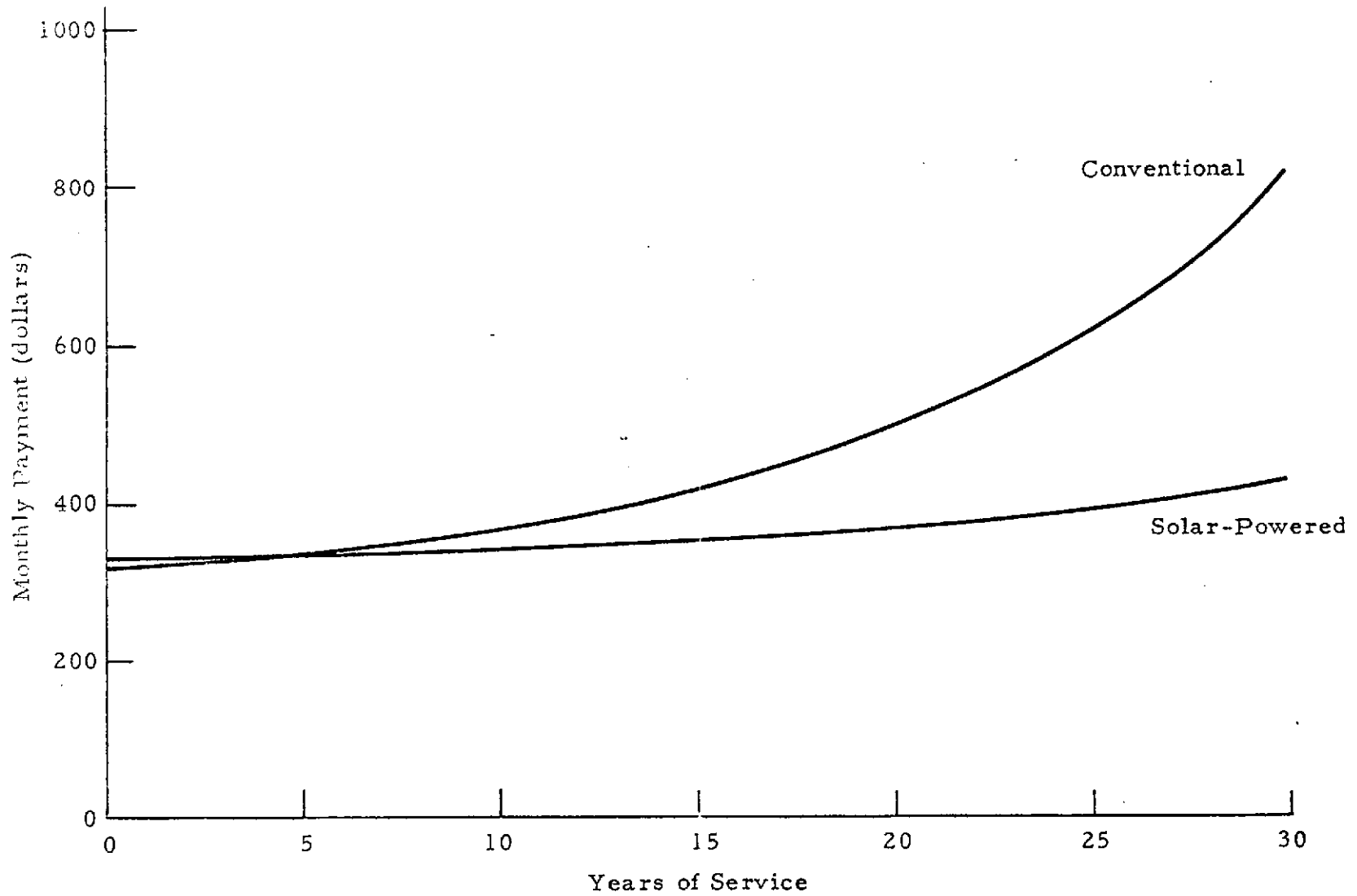


Fig. 39 - Comparison of Solar-Powered vs Conventional Heating and Cooling with a 10% Yearly Increase in Energy Cost

rate increase of 10% for the cost of energy is assumed for Fig. 39. The conclusion to be reached from the curves of Fig.39 can be stated simply. Initially, the solar-powered system will not cost much more per month to own and operate than a conventional system; and, over the lifetime of each system, great savings will be experienced by the owner of the solar-powered system.

Maintenance and repair costs are excluded from the costs of both systems in Fig.39. This should not affect the comparison very much, since such costs should be similar and offsetting. The conventional system will require compressor replacement every few years, while the solar system has no compressor. However, some occasional collector repairs might be required for the solar system.

Figure 40 presents one last cost comparison for the two systems. The costs presented here are the integrated costs over the years for the two systems. The long-term, life-cycle cost savings for the solar system are great. One further point (again suggested by Peter McCrary) is that this money saved by the solar system could be invested to draw interest, thereby multiplying the long-term, life-cycle cost savings.

In summary, a properly designed, mass-produced solar-powered residential heating and cooling system could be close to competitive with conventional systems at today's utility rates, and the projected savings in both monthly payment and total life-cycle cost will be large for the solar-powered system.

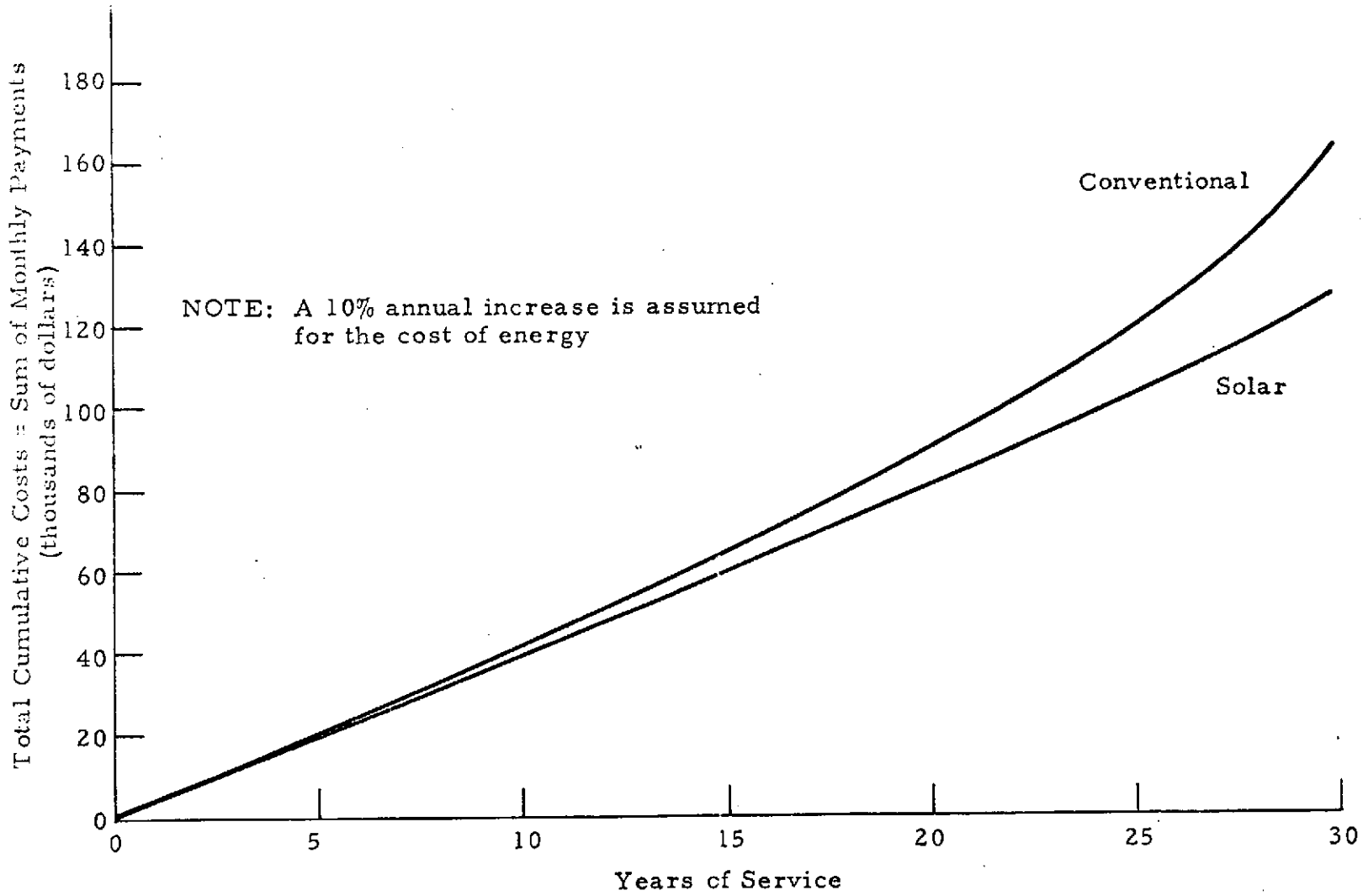


Fig. 40 - Comparison of Total Cumulative Costs for the Solar-Powered and Conventional Heating and Cooling Systems

Section 8

A BRIEF REVIEW OF ALTERNATIVE SOLAR
COOLING CONCEPTS

Although only absorption cycle cooling has been considered in the current study, other investigators are currently involved in the development of numerous solar-cooling concepts. A brief review of these concepts was conducted during this study, based primarily upon the information presented at the NSF Solar Cooling Workshop held in Los Angeles from 6 February to 8 February 1974.

Current and proposed cooling systems can be lumped into five basic categories:

- Absorption cycle systems (Refs. 2 through 6)
- Rankine cycle systems (Refs. 7 through 11)
- Desiccant systems (Refs. 12 through 14)
- Vuilleumier (VM) cycle systems (Ref. 15), and
- Night sky radiation/evaporative cooling systems (Ref. 16).

In the absorption cycle area, several efforts are underway to utilize Arkla Industries' three-ton lithium bromide/water system in solar-powered installations. These efforts include the MSFC effort, of course, and also the following two efforts:

- Colorado State University's Solar-Heated and Cooled Laboratory (Dr. George Löff)
- Honeywell Corporation's Solar-Powered Mobile Research Laboratory (Dr. Roger Schmidt).

Another absorption cycle system is being fabricated at the University of Florida (Dr. Erich Farber) which will utilize ammonia and water as the

fluid combination. Several analytical programs are underway at laboratories and universities around the country.

In the Rankine cycle area, Barber-Nichols Company is fabricating a two-fluid Rankine cycle/vapor compression cycle air conditioner which will also be put in Honeywell's Mobile Research Laboratory. Several other studies of Rankine cycle systems are underway at United Aircraft Corporation, Thermo-electron Corporation, and other facilities.

In the desiccant system area, the MEC cycle developed at the Institute of Gas Technology (William Rush) is being evaluated analytically and empirically. Other desiccant systems are being studied at MIT and elsewhere.

RCA has proposed the use of the heat-driven, Stirling-type VM cycle. This cycle has received much attention in the cryogenic cooler area and appears promising for solar applications after further development.

Sky Therm (Harold Hay) has demonstrated natural cooling (although not actually solar in nature) by nocturnal radiation and evaporative cooling using roof ponds. He also advocates the use of high heat capacity building materials to dampen ambient temperature variations. However, the sky radiation/evaporative cooling system holds very little promise in areas outside the Southwest, since clear night skies and dry night air are essential for the process.

After reviewing these different solar cooling systems, the absorption system still appears superior to the others in terms of state of development, coefficient of performance, running power requirement, safety, dependability and universal usability for the present state of the art of flat plate solar collectors. However, if collectors are developed which are capable of high efficiency operation at high temperatures (300°F and above), some of the other systems will become superior to the absorption cycle for space cooling.

Section 9
MISCELLANEOUS SMALL STUDIES

During the past 15 months, several small rush item tasks have been addressed by Lockheed-Huntsville to aid MSFC in the development of the solar-powered demonstration facility. Although most of these tasks required only minor manpower expenditures and were reported informally over the phone or at weekly meetings, a few were considered worthy of documentation and are presented in the following paragraphs.

9.1 EFFECT OF BLOWER SPEED ON HEATING COIL PERFORMANCE

A study was conducted to determine the thermal effects of blower speed on heating coil performance. An overall heat transfer coefficient (UA) of 2000 Btu/hr-°F was assumed for the coil unit, and an inlet air temperature of 70°F was also assumed. The results are shown in Fig. 41. Note that substantial increases in heat transfer are possible with higher air flows, and that lower outlet air temperatures are achieved with the higher air flow also. Thus, higher blower speeds are desirable from a thermal viewpoint. However, more electrical power is required for higher blower speeds.

9.2 TRANSIENT THERMAL ANALYSIS OF WATER LINES

NASA-MSFC designers were concerned about overnight freezing of water in the transfer lines which would be exposed to the ambient environment. A simple calculation was made to determine the time required for water remaining in insulated pipes exposed to an ambient temperature of 0°F to cool down from 100°F to 32°F. The model consisted of a cylinder of water with a diameter of 1 inch surrounded by 3 inches of insulation. Figure 42 shows the problem geometry and results. The time required to reach freezing temperature is about 34 hours. Since the average ambient temperature in Huntsville during a 34-hour period is much higher than 0°F, no problems from freezing insulated water lines are anticipated.

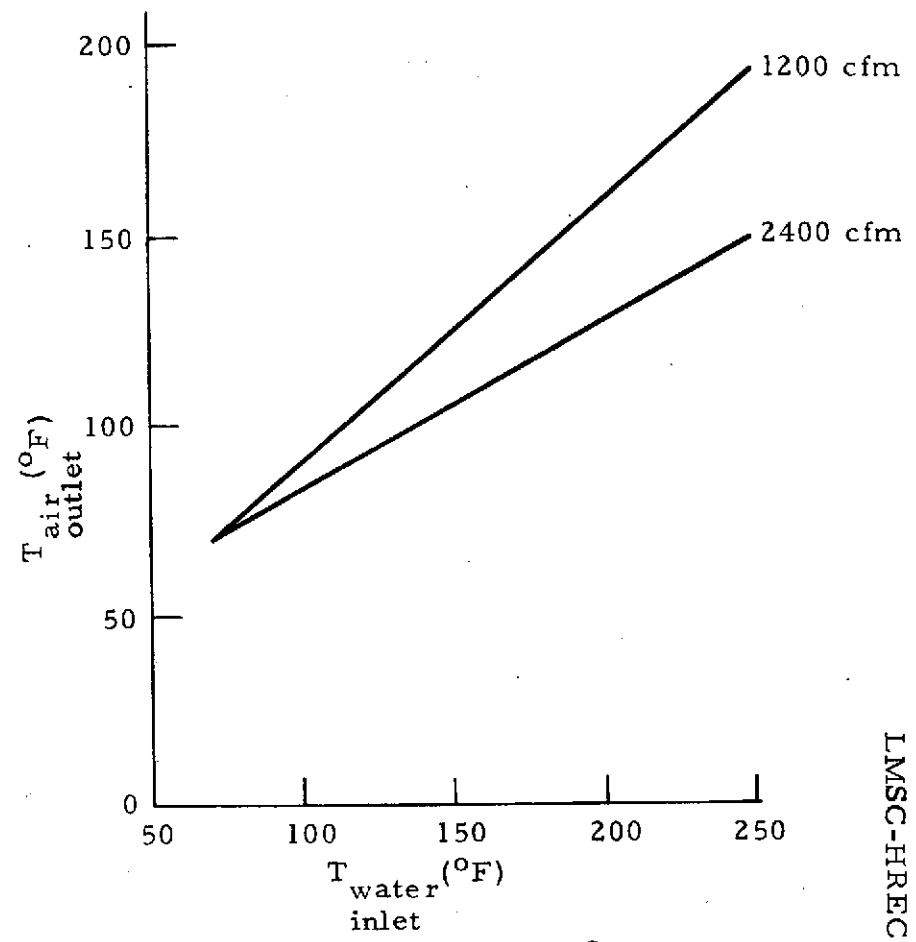
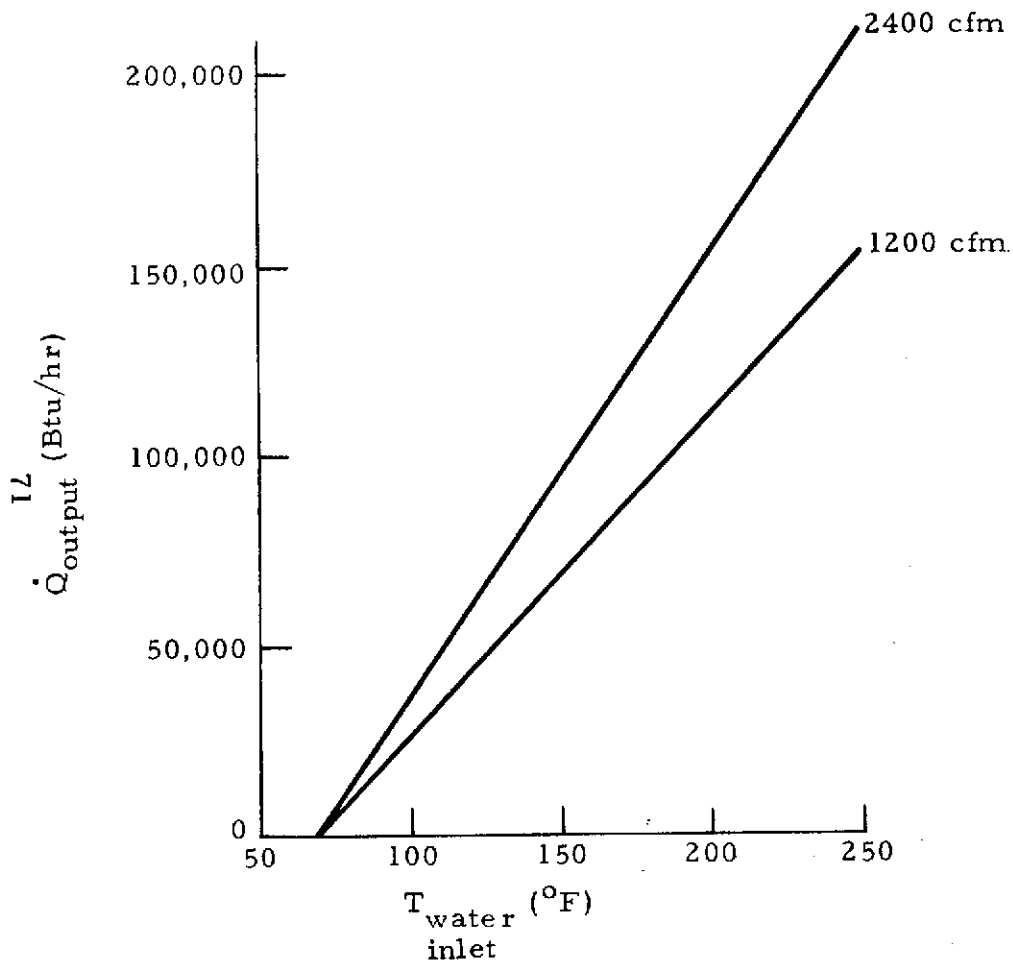


Fig.41 - Effect of Blower Speed on Heating Coil Performance (UA = 2000 Btu/hr °F)

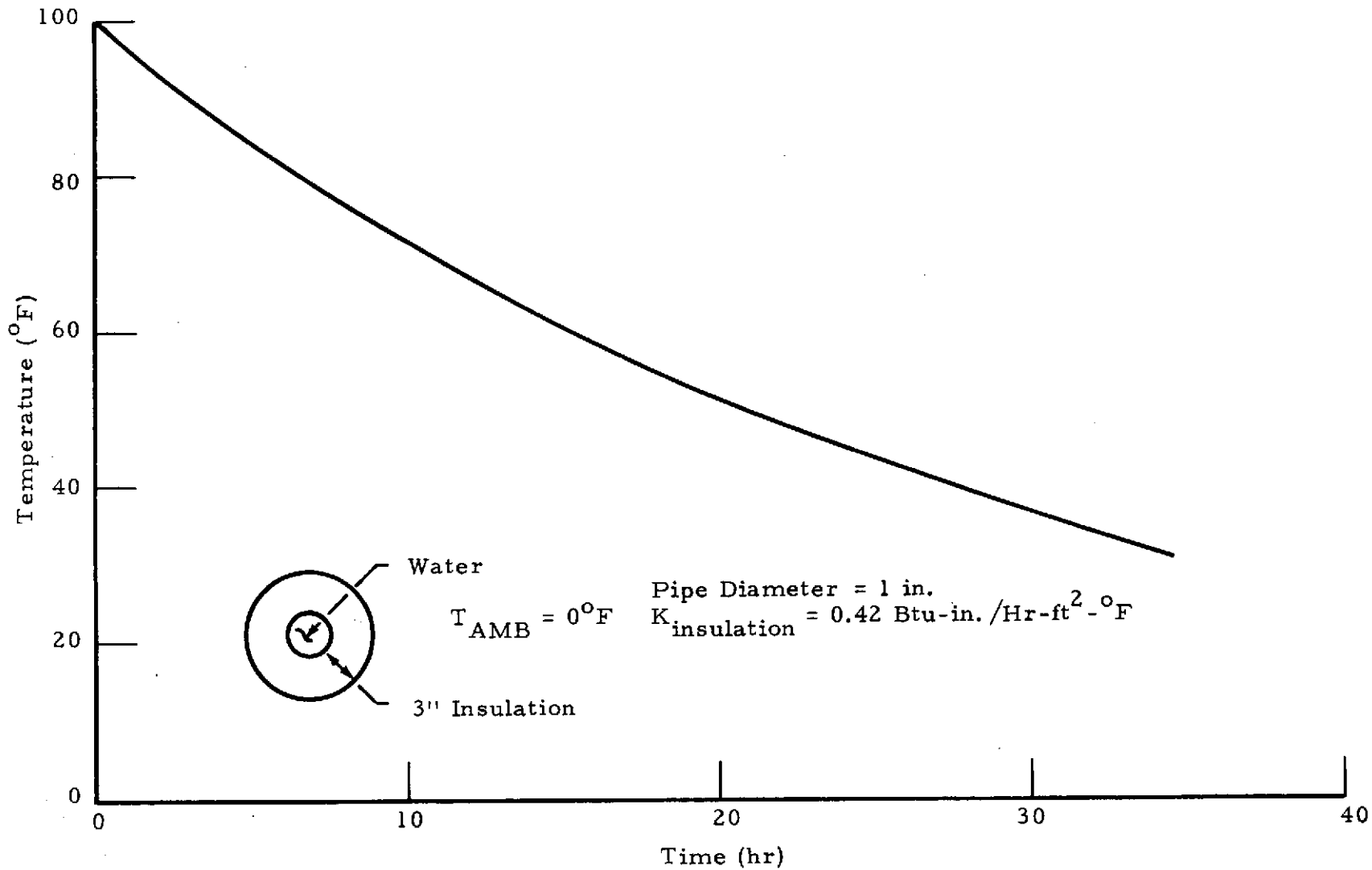


Fig.42 - Temperature of Water in Insulated Pipe as a Function of Time

Section 10
CONCLUSIONS

The following conclusions are drawn, based upon the results of contractual studies of the past three years.

- The utilization of solar energy for space heating, air conditioning, and hot water heating is technically feasible with properly applied current technology. Although most of the contractual studies have been centered upon a system located in Huntsville, Alabama, other Lockheed studies indicate the same technical feasibility for most other areas of the country.
- Solar-powered space heating, air conditioning, and hot water heating systems will be economically competitive with conventional systems when they become mass-produced, commercially available commodities. The additional capital investment required for a solar-powered system will be more than offset by the large reduction in operating cost. As energy costs continue to skyrocket, the economic attractiveness of solar-powered systems will increase exponentially.
- Widespread adoption of the solar-powered system will result in a number of beneficial impacts, including:
 1. Future energy shortages will be partially alleviated.
 2. Since sunshine is pollution-free, a significant reduction in the pollution byproducts of conventional energy usage and production will be achieved.
 3. By partially displacing the need for fossil fuels, natural resources will be preserved.
 4. Environmental protection will be favorably impacted by reducing the need for strip mining, offshore oil drilling, nuclear waste storage, etc.
 5. When the full life-cycle costs are evaluated, the citizen-owner of the solar-powered system will reap significant economic rewards, since solar energy is free.

6. The nation's quest for energy independence will be well served, since no foreign nation controls the flow of sunshine to the United States.
- At the present time, the best solar heating and cooling system design should include:
 1. A double-glazed solar energy collector with an integral tube-in-sheet absorber plate coated with a selective black surface (with high α_s and low ϵ_{ir})
 2. A sensible heat storage system with water as the storage medium (The same water should be used as the energy transport fluid to and from the collector and output units.)
 3. An absorption cycle cooling system, and
 4. An auxiliary heat source that utilizes storable fuel (fuel oil, propane, etc.) rather than natural gas or electricity. This will prevent peak, simultaneous drains on the conventional utilities by solar-powered installations, whenever several days of cloudy weather occur.
 - The use of computerized simulations of solar system performance is essential to compare different system designs, to properly size collector and storage, and to generate near-optimum designs.

Section 11
RECOMMENDATIONS

Based upon the results of all efforts to date, the following recommendations are made.

- Research and development activities to achieve more efficient and less costly solar system components should be actively pursued. Better collectors, cooling units, and energy storage units should be developed to expedite solar energy utilization by improving system economy.
- Generalized total system simulation computer programs should be developed to allow analytical studies of solar-powered systems for various buildings in various regions of the nation. Lockheed-Huntsville is considering the extension of the computer program discussed in Section 5 to provide one such generalized program.
- Detailed analytical studies of solar heating and cooling systems for numerous types of buildings in numerous locations around the country should be conducted. Studies such as the one documented in this report provide the data required for prototype design and economic evaluation.
- More projects to demonstrate solar heating and cooling for different building types in different geographical locations should be initiated. These projects should be well instrumented to allow precise determination of performance characteristics for technical and economic evaluation.
- As more experience is gained in the solar heating and cooling field and as prediction techniques are refined, the arduous task of preparing design manuals, handbooks, and related materials required by architects, building engineers, and contractors should be initiated. Widespread utilization of solar energy for heating and cooling will never become a reality until the design and construction of such systems can be done in a standardized "cookbook" fashion.

Section 12
REFERENCES

1. O'Neill, Mark J., A.J. McDanal and W.H. Sims, "The Development of a Residential Heating and Cooling System Using NASA-Derived Technology," LMSC-HREC D306275, Lockheed Missiles & Space Company, Huntsville, Ala., November 1972.
2. Löff, George (Colorado State University), "The NSF/Colorado State University Solar Heated and Cooled House."*
3. Beckman, William (University of Wisconsin), "The Lithium Bromide Systems Used in Solar Applications."*
4. Anderson, Philip (Arkla Industries), "Current Lithium Bromide Hardware as Used in Solar Applications."*
5. Farber, Erich (University of Florida), "Ammonia and Other Absorption Systems Used in Solar Applications."*
6. Allen, Redfield (University of Maryland), "Solar Absorption Systems."*
7. Burris, William (Garrett Corporation), "Solar Rankine Cycle Powered Cooling Systems."*
8. Curran, Henry (Hittman Associates), "Solar Rankine Cycle Powered Cooling Systems."*
9. Davis, Jerry (TECO), "Solar Rankine Powered Cooling Systems."*
10. Biancardi, Frank (United Aircraft), "A Solar Rankine System."*
11. Barber, Robert (Barber Nichols), "Solar Organic Rankine Cycle Powered Three Ton Cooling System."*
12. Rush, William (Institute of Gas Technology), "Solar Desiccant Systems."*
13. Lunde, Peter J. (The Center of Environment and Man), "Solar Desiccant System Analysis and Materials."*
14. Wellesley-Miller, Sean (Massachusetts Institute of Technology), "Solar Desiccant System Configurations."*

* Paper presented at the NSF Solar Cooling Workshop, 6-8 February 1974, Los Angeles, Calif. (Proceedings to be published).

15. Shelpuk, Benjamin (R.C.A), "A Solar Vuilleumier System."*
16. Hay, Harold R. (Sky Therm Processes and Engineering), "How to Stop Cooling Loads Before They Start."*

* Paper presented at the NSF Solar Cooling Workshop, 6-8 February 1974, Los Angeles, Calif. (Proceedings to be published).

Section 13

BIBLIOGRAPHY

"Applied Solar Energy Research," Association for Applied Solar Energy, Phoenix, Ariz., 1959.

Buchberg, H., and J. R. Roulet, "Simulation and Optimization of Solar Collection and Storage for House Heating," Solar Energy, Vol. 12, No. 1, 1968.

Butz, L., S. A. Klein, W. A. Beckman and J. A. Duffie, "Digital Simulation of Solar Heating and Cooling Systems," International Solar Energy Society - U. S. Section-Annual Meeting, 3-4 October 1973, NASA-Lewis Research Center, Cleveland, Ohio.

Close, D. J., "A Design Approach for Solar Processes," Solar Energy, Vol. 11, No. 2, 1967.

Cunnington, G. R., and E. R. Streed, "Experimental Performance of a Honeycomb Covered Flat-Plate Solar Collector," paper presented at International Solar Energy Society Annual Meeting, NASA-Lewis Research Center, Cleveland, Ohio, 3-4 October 1973.

DeGraff, J. G. A., and E. F. M. Van Der Held, "The Relation Between the Heat Transfer and the Convection Phenomena in Enclosed Plane Air Layers," Appl. Sci. Res., Section A, Vol. 3, 1952, p. 393.

Duffie, John, "Modeling of Solar Heating and Air Conditioning," Solar Heating and Cooling for Buildings Workshop, 21-23 March 1973, Washington, D. C.

Duffie, John A., and William A. Beckman, "Modeling of Solar Heating and Air Conditioning," Semi-Annual Progress Report to the National Science Foundation for Grant NSF/RANN/SE/GI34029, 31 January 1974, University of Wisconsin-Madison, Madison, Wisc.

Duffie, J. A., and G.O.G. Löf, "Solar Energy, Economics and Engineering Research at the University of Wisconsin," Can. J. Chem. Eng., April 1959, p. 77.

Farber, E. A. et al., "University of Florida Solar Air-Conditioning System," Solar Energy, Vol. 10, No. 2, 1966, pp. 91-95.

Hale, D. V., M. J. Hoover and M. J. O'Neill, "Phase Change Materials Handbook," NASA CR-61363, Lockheed Missiles & Space Company, Huntsville, Ala., September 1971.

Hottel, H. C. and B. B. Woertz, "The Performance of Flat-Plate Solar-Heat Collectors," Trans. ASME, February 1942.

"Introduction to the Utilization of Solar Energy," Edited by A. M. Zarem and Duane D. Erway, McGraw-Hill, New York, 1963.

Löf, G.O.G. et al., "Residential Heating with Solar-Heated Air - The Colorado Solar House," ASHRAE J., October 1963, pp. 77-86.

Löf, G.O.G., and R. A. Tybout, "Cost of House Heating with Solar Energy," Solar Energy, Vol. 14, 1973.

Low Temperature Engineering Application of Solar Energy, Richard C. Jordan, Editor, American Society of Heating, Refrigerating, and Air-Conditioning Engineers, Inc., New York, 1967.

Klein, S. A., J. A. Duffie and W. A. Beckman, "Transient Considerations of Flat-Plate Solar Collectors," ASME Paper No. 73-WA/Sol-1, Winter Annual Meeting, 11-15 November 1973, Detroit, Michigan.

Sheridan, N. R. et al., "Study of Solar Processes by Analog Computer," Solar Energy, Vol. 11, No. 2, 1967.

Solar Energy, the Journal of Solar Energy Science and Engineering, published quarterly by Association for Applied Solar Energy, Phoenix, Ariz.

Telkes, M., and E. Raymond, "Storing Solar Heat in Chemicals: A Report on the Dover House," Heating and Ventilating, November 1949, p. 80.

Thomason, Harry E., "Experience with Solar Houses," Solar Energy, Vol. 10, No. 1, 1966, pp. 17-22.

Whillier, A., "Solar Energy Collection and Its Utilization for House Heating," Sc.D. thesis, Department of Mechanical Engineering, MIT, Cambridge, Mass., 1953.

Yellott, John I., "Utilization of Sun and Sky Radiation for Heating and Cooling of Buildings," ASHRAE J., December 1973, pp. 31-42.

Appendix
SOLAR COLLECTOR MODEL

The solar collector model treats all of the following energy exchanges, as shown in Fig.43:

- Solar radiation energy exchanges, including transmission, absorption, and reflection of this short wavelength radiation. Also, the sun-earth astronomy is included to determine the time-dependent incidence angle of direct solar radiation for any collector orientation. Diffuse solar radiation is also treated by the model.
- Infrared radiation energy exchanges, including emission, absorption, reflection, and transmission (through non-opaque transparent covers like Tedlar) of this long wavelength radiation.
- Natural convection between parallel surfaces inside the collector.
- Forced and-or natural convection between the outer transparent cover and the ambient atmosphere.
- Conduction losses through the backside insulation.

The model solves the transient energy transfer problem numerically to yield the temperature of the collector components and the energy transfer rates between collector components as functions of time, as shown in Fig. 44. Some of the design variables which can be handled with the model include the following:

- | | |
|--|---|
| 1. Latitude | 12. Transparent cover infrared emittance |
| 2. Solar constant variation | 13. Transparent cover infrared transmittance |
| 3. Day of year | 14. Transparent cover thickness |
| 4. Ambient temperature variation | 15. Collector tilt angle from horizontal |
| 5. Average collector temperature | 16. Absorber plate infrared emittance |
| 6. Number of transparent covers | 17. Absorber plate solar absorptance |
| 7. Ratio of diffuse to total radiation | 18. Absorber plate thickness |
| 8. Wind speed variation | 19. Absorber plate material |
| 9. Pertinent collector dimension | 20. Spacing between absorber plate and bottom transparent cover |
| 10. Transparent cover index of refraction | 21. Spacing between transparent covers |
| 11. Transparent cover extinction coefficient | 22. Insulation thermal conductivity |
| | 23. Fluid flow heat transfer. |

Thus, the collector model allows a great deal of flexibility in collector design and represents a more accurate model than the steady-state solution used by other investigators in simulation studies.

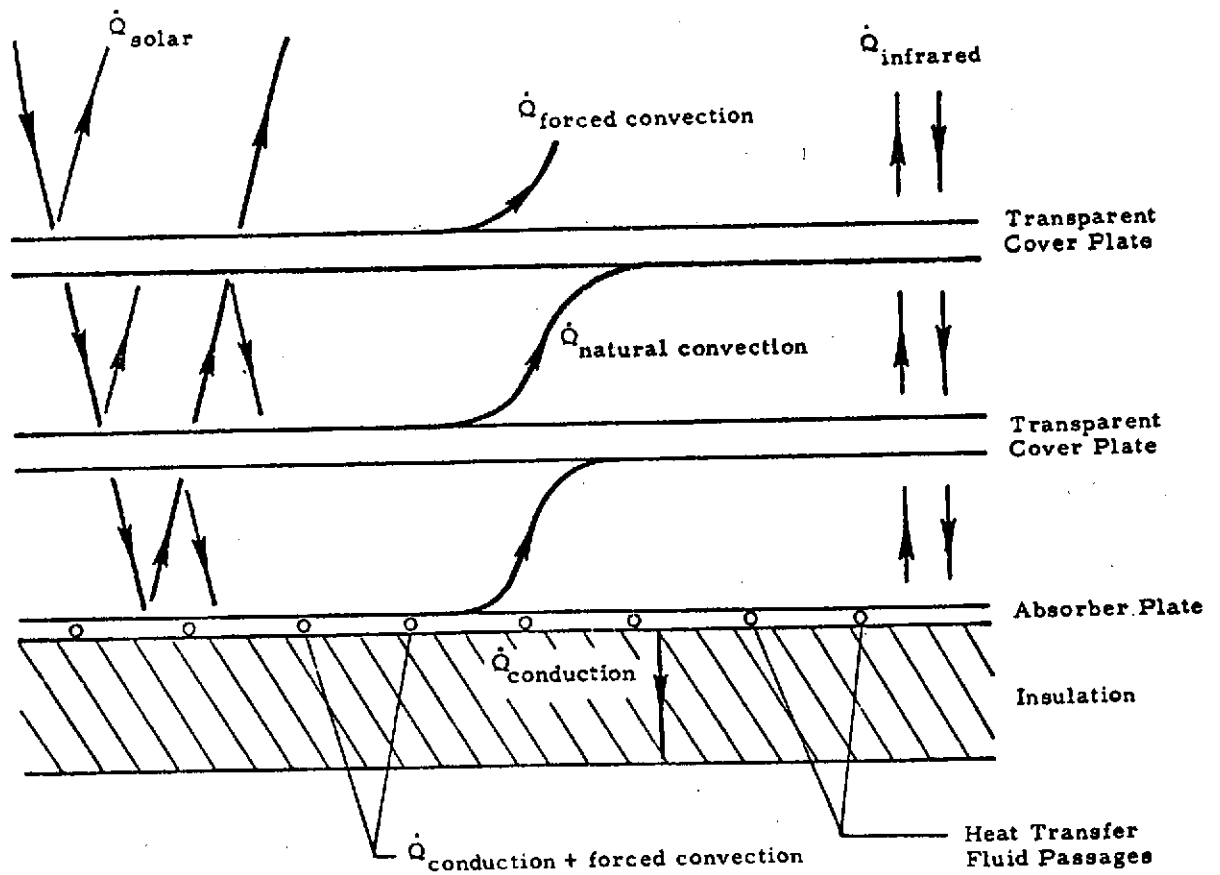


Fig.43 - Energy Exchange Mechanisms in Flat-Plate Solar Collector

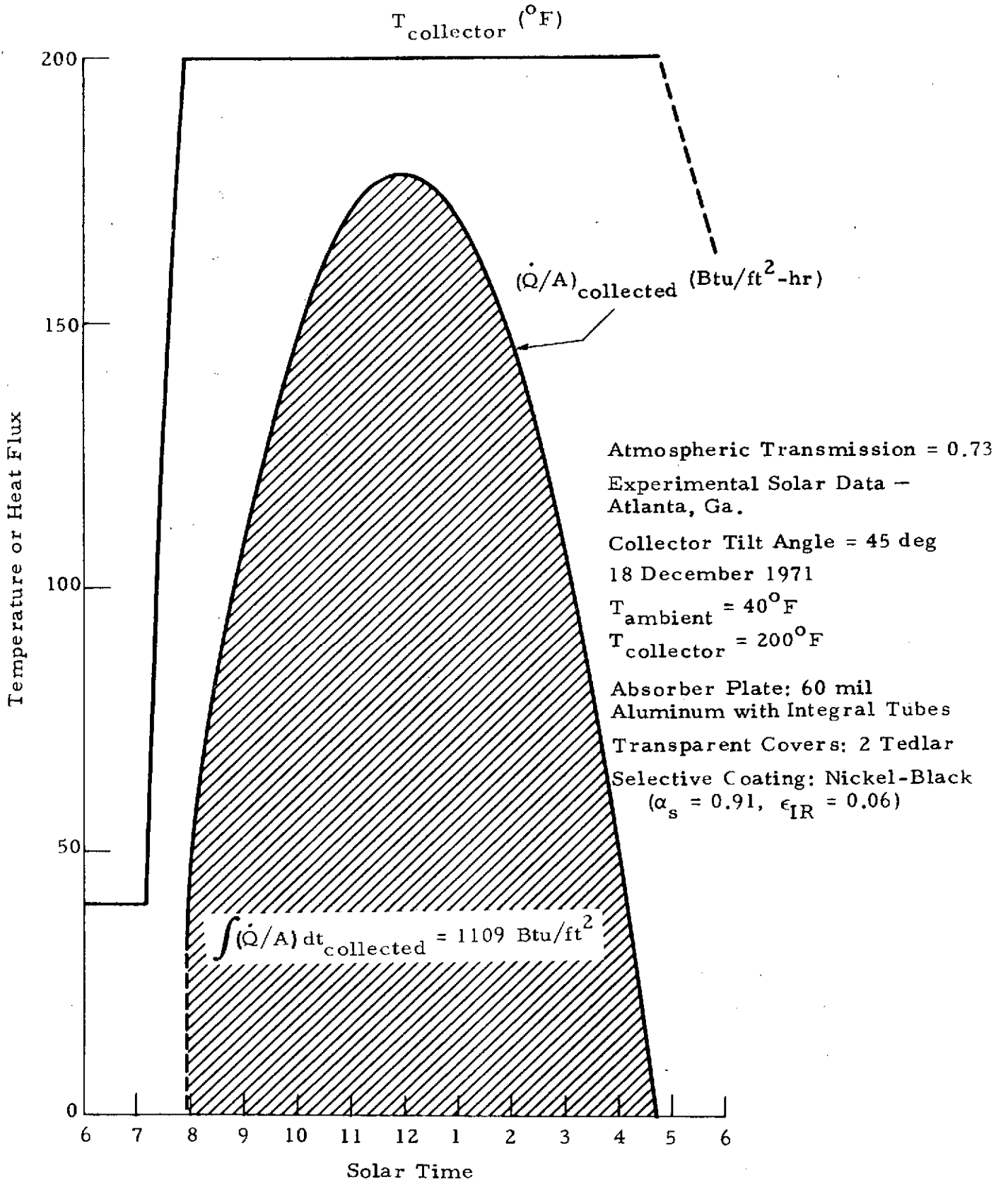


Fig. 44 - Daily Transient Solar Collector Performance